2015

Remote Quantification of Stack Emissions from Marine Vessels in the South Coast Air Basin

FINAL REPORT

Chalmers University

FluxSense Inc.

29 August 2017

Date: 2017-05-21

Title: Remote Quantification of Stack Emissions from Marine Vessels in the South Coast Air Basin

Authors: Johan Mellqvist[1,2,3] Jörg Beecken[1], and Johan Ekholm[1]

[1]Chalmers University of Technology, Hörsalsvägen 11, SE-41296 Göteborg, Sweden
[2]FluxSense AB, Hörsalsvägen 11, SE-41296 Göteborg, Sweden
[3]FluxSense Inc., 113 W G Street # 757, San Diego, CA 92101

E-mail: johan.mellqvist@chalmers.se

[Cover: Picture taken at the Port of Los Angeles.]

Acronyms, Definitions and Units

Acronyms used in this report

BC	Black Carbon, here defined as the sum of light absorbing particles
CPC	Condensation Particle Counter
ECA	Emission Control Area (ratified thru IMO)
DOAS	Differential Optical Absorption Spectroscopy
DWT	Deadweight
EEPS	Emission Exhaust Particle Sizer
EF	Mass specific emission factor, (g emission per kg fuel)
ER	Emission rate, (g emission per hour)
FSC	Fuel Sulfur Content
GMD	Geometrical mean diameter of particles
GT	Gross tonnage
IMO	International Maritime Organization
Marpol	International Convention for the Prevention of Pollution from Ships
MEPC	Marine Environment Protection Committee (part of IMO)
MEng	Main engine type
OGV	Ocean Going Vessels
OPS	Optical Particle Sizer
PoLA	Port of Los Angeles
PoLB	Port of Long Beach
PM05	Fine and ultrafine particulate matter below 500 nm in size.
PM2.5	Particulate matter below 2500 nm in size
PM10	Particulate matter below 10000 nm in size
PN	Particulate Number
RPM	Revolutions Per Minute (crankshaft)
SFOC	Specific Fuel Oil Consumption (g emission per kWh axial power)
YoB	Year of Built

Definitions

DPM	Diesel Particulate matter. Used by ports in inventories. We assume it is the same as PM1 from diesel exhaust.
NO_x	Nitrogen oxide, consist of nitrogen dioxide (NO_2) and nitrogen monoxide (NO)
SO_2	Sulfur dioxide

Units

Wind direction	degrees w.r.t. North
Wind speed	m/s
Column	mg/m^2
Concentration	mg/m^3
Emission factor	g/kg_{fuel}
Emission rate	kg/h

Unit Conversions

1 kn (knots) = 0.514 m/s
1 kg/h = 52.9 lbs/day

Executive summary

BACKGROUND

Accurate characterization of emissions from ports and industrial sources on a real or near-real time basis is critical for developing effective control strategies to improve regional air quality, promoting compliance, and reducing exposure levels in nearby communities. To improve the understanding of such emissions in the South Coast Air Basin (SCAB), the South Coast Air Quality Management District (SCAQMD) has promoted and sponsored a series of measurement projects to study port and industrial emissions using remote sensing methods. The projects include experimental studies of emissions from the ports, refineries, oil depots, treatment facilities, oil wells, gas stations, fuel islands and barges. In addition, SCAQMD has sponsored technology demonstration and validation studies to assess potential uncertainties of different optical techniques through side-by-side measurements of real sources and controlled source gas releases.
This report presents the results from a five week technology demonstration study at the ports of Los Angeles and port of Long Beach in which new innovative techniques were used to measure of emission factors (in units of g/kg_{fuel}) of SO_2, NO_x and particulate matter (PM) from individual ships. The data represents "snap shot" measurements of multiple ships (tankers, containers, cruise ships, tugs) in various stages of operations, for example at anchor, ships being towed by tug boats, and ships passing the harbor entrances of the two ports. In addition, optical remote sensing methods were applied from the ground, on the water, and from an aircraft to measure actual emission rates (in units of g/s) of nitrogen dioxide (NO_2) from isolated ships as well as from the full harbor area. As part of a parallel study, VOC emissions from fueling of ships were also obtained.

The results from this project improve the understanding of the ship emissions in the harbor, both in terms of their magnitude and variability. Significant resources during the project were allocated to follow ships from the time they leave the dock, through the port, and into open waters in order to measure their emissions in different modes of operation. This study also demonstrated that our measurements can be used to verify ships compliance with low sulfur fuel usage requirements.

METHOD

Stationary and mobile (i.e. on-vessel) measurements of ship specific emission factors (g/kg_{fuel}) and total emission (g/s) were carried out by Chalmers University of Technology and FluxSense Inc. in the ports of Los Angeles and Long Beach from October 8 until November 10, 2015.
During stationary measurements, the equipment was installed in a passenger-size van, which was stationed at the following three locations throughout the ports of Los Angeles and Long Beach:

- Coast Guard Base at the Port of Los Angeles – October 9 through October 14.
- Campus of the South Coast Marine Institute at the Port of Los Angeles – October 26 through November 1.
- Parking lot of the Port of Long Beach Command and Control Center at the entrance of the Port of Long Beach - November 2 through November 10.

During mobile measurements, the equipment was installed on a research vessel (Yellow Fin) operated by the South Coast Marine Institute from which ships were tracked moving in and out of the ports between October 14 and October 26.

In total, the data in PoLA and PoLB correspond to 571 ship plume measurements of 132 individual ships that were identified from the received AIS signals of the ships. Part of the data corresponds to "chase experiments" in which 24 specific ships have been tracked from berth to a few nautical miles outside the harbor entrances, or vice versa.
In-situ "sniffer" techniques were used for measurements of SO_2, NO_x, CO_2 and particulate matter, and optical zenith sky Differential Optical Absorption Spectroscopy (DOAS) was used for measurements of NO_2. Particulate matter was characterized by particulate number, particulate mass, and black carbon (BC). The objective of the "sniffer" measurements was to measure ratios of various pollutants (SO_2, NOx, PM) to CO_2, from which the emission factors, i.e. mass of pollution per kg fuel, could be derived.

The sniffer system is operated by custom software that calculates the sulfur fuel content and NO_x emission factors in real time. It tags the data to individual passing ships by making use of wind measurements and information from the Automatic Identification System (AIS) of the vessels. The instruments and methodologies have been developed by Chalmers University of Technology in Sweden and the technique is used in several places in Europe, from both fixed sites and surveillance aircraft, to monitor whether by-passing ships operate with the allowed fuel sulfur content, with respect to IMO rules and national legislation.

As part of the project a demonstration of airborne remote sensing measurements was carried out in which the total emission of NO_2 from the harbors was obtained. In these measurements the path integrated concentration of NO_2 below the aircraft was retrieved by spectroscopic analysis of visible light observed with a downward viewing telescope. The measurements were done at approx. 600 m in several circles around the harbor area. By combining these measurements with wind information it was possible to obtain the emission of NO_2.

In addition, as part of a parallel project, VOC emissions in the harbors were investigated using the Solar Occultation Flux (SOF) technique. This included for instance studies of emissions from fueling of ships.

RESULTS AND DISCUSSION

Average ship emission rates and factors measured during this study are summarized in Table ES. 1. For comparison, emission factors used in the 2014 inventories at the ports of Los Angeles and Long Beach are also presented. The measured emission factors are normally in units of g/kg_{fuel}, while units of g/kWh are generally used in the inventories. Therefore measured emission factors (in units of g/kg_{fuel}) were multiplied with the fuel oil consumption factor of 0.2 kg_{fuel}/kWh in order to convert them into units of g/kWh.

The average and median ship NO_2 emission rates, obtained with optical sky measurements, were 4 and 9 kg/h, respectively. Assuming that 20 % of the NO_x is in the form of NO_2, the corresponding average and median ship NO_x emission rates are 20 and 45 kg/h, respectively.

Airborne remote sensing measurements conducted around noon time on the weekend of November 8 indicated that 345 kg/h of NO_x were emitted from the harbor areas. However, these measurements represent only a 20 minute snap-shot of the emissions occurring. This value is almost ½ of the two ports' reported annual average value of 628 kg/h, excluding transit emissions of the ocean going vessels, and a possible indicator that inventories overestimate ports' NOx emissions. Reduced activities over the weekend can explain this discrepancy.

Longer-term measurements are required to better characterize actual port emissions.

Figures ES. 1 and ES. 2 examine NO_x and BC emission factors (in g/kg_{fuel}) versus ship speed, illustrating that the observed emission factors varies within a factor of 2 and that the emissions increase with ship speed. The speed dependence is actually contrary to what is applied in the inventories. The observed emission factors in this study are also 20-30 % lower than published in the literature. The fact that this study focused primarily on maneuvering at lower speeds can explain this discrepancy.
SO_2 emission factors of most of the sampled ships were below the 0.4 g/kWh assumed in the inventories. However, one ship was measured on two separate occasions to have an emission factor of 6-8 g/kWh, corresponding to the usage of high fuel sulfur content (2 %). According to the California Air Resources Board this ship has a special permit to operate on fuel with high sulfur fuel content since it is equipped with a steam turbine engine.

The measured median and average values for PM2.5 emission factors were 0.122 g/kWh and 0.208 g/kWh, respectively. 55-70 % of the particulate mass appears to be in particles that are smaller than 0.5 µm in diameter. The variability of the observed emission factors is within a factor of 2 and, on average, the emissions are the highest at slow speeds and decrease as vessel's speed increases. The average measured PM2.5 emission factors are comparable to the 0.26 g/kWh used in the PoLA 2014 emission inventory.

The observed PM2.5 emission factors measured in this study are lower than the ones obtained in other studies. Part of the reason may be that the ships in the previous studies were running on higher FSC (1 %) which in turn caused higher particle emissions. However, it should be noted that the PM2.5 measurements are associated with relatively large measurement uncertainties of >30%, due to the type of instruments utilized.

The observed emission factor for black carbon particles (BC) corresponds to a median value of 0.098 g/kWh and an average value of 0.15 g/kWh. A large fraction of the measured PM2.5 mass (70-80 %) hence appears to consist of BC. The observed emission factors of BC versus ship speed, Figure ES. 2, varies within a factor of 2 and they show high and variable values for speeds between 0 and 4 knots which then decrease at higher ship speed. Here in particular the 75^{th} percentile shows a distinct maximum at speeds between 2 to 4 knots. i.e. during maneuvering phase. The pattern for the PM05 measurements is rather similar. The high observed BC emission factor at low speeds is probably caused by intensive work by the tugs, but it could also be caused by incomplete combustion of the main ships at low load. The apparent high BC fraction in the PM2.5 is somewhat surprising since in general, the organic particle matter is believed to be the dominant particle form in ship exhaust. However, most of the measurements in this study were carried out for ships that were maneuvering and therefore the BC emissions could be higher here, possibly with the organic particles being deposited on the BC. There are also measurement uncertainties for the PM2.5 instruments with regard to BC that needs further consideration, as mentioned above.

Table ES. 1. Summary of the observed emission factor data for individual ships. The data were calculated by assuming a specific fuel oil consumption of 0.2 kg_{fuel}/kWh. The emission inventory corresponds to the official

2014 emission inventory by PoLA and PoLB. The data corresponds to a 50/50 mixture of low and medium speed diesel ships following the Tier 1 standard (1999-2011) and load dependence has been neglected.

Emission Factors	Unit	Avg	Standard deviation	Median	25th percent	75th percentile	Emission inventory
EF_{NOx}	g/kWh	8.10	4.16	7.25	4.98	10.53	14
EF_{SO2}	g/kWh	0.05	0.60	0	-0.05	0.03	0.41
$EF_{PN(5-1000\ nm)}$	10^{15}/kWh	1.20	1.34	0.95	0.45	1.71	NA
$EF_{PM05\ (5.6-560\ nm)}$	g/kWh	0.115	0.168	0.083	0.047	0.136	
$EF_{PM1\ (5.6-1117\ nm)}$	g/kWh	0.130		0.091	0.05	0.152	
$EF_{PM2.5\ (5.6-2500\ nm)}$	g/kWh	0.208		0.122	0.062	0.242	0.26
$EF_{BC\ 5-1000\ nm)}$	g/kWh	0.150	0.261	0.098	0.050	0.177	

The observed emission factors for particle number have a median value of $0.95 \cdot 10^{15}$ particles/kWh and an average value of $1.2 \cdot 10^{15}$ particles/kWh and this is in agreement with several other port studies. However, care should be taken when comparing particle number since in contrast to particulate mass it is not a conserved number since particles coagulate downwind the plume. The observed emission factor of PN are the highest values for the slowest speeds.

The VOC emission measurements from various activities in the harbor showed emission rates that varied between 4 and 27 kg/h, with a total of 69 kg/h. The activities included oil extraction at fuel islands, ship fueling and ship venting. Compared to other VOC sources in the SCAB (Mellqvist 2016b, Mellqvist 2016c) these emissions are moderate in size.

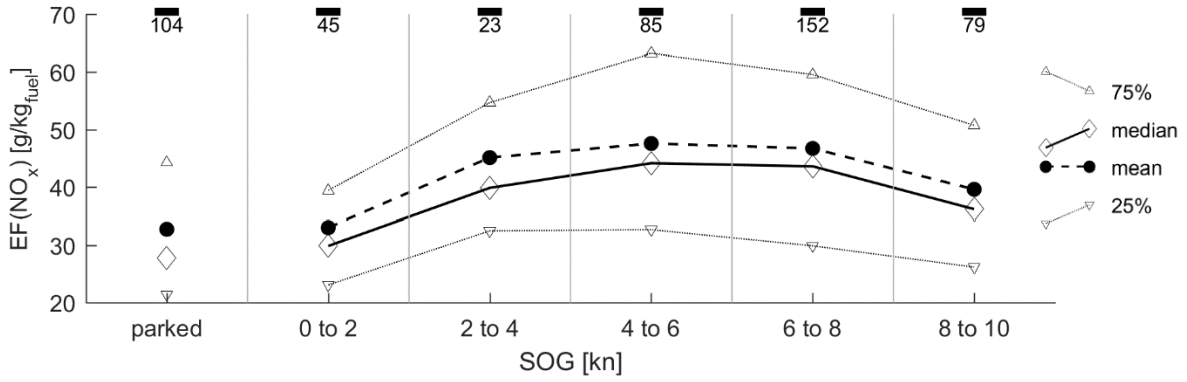

Figure ES. 1. Emission factor of NO_x over vessel speed, i.e. load.

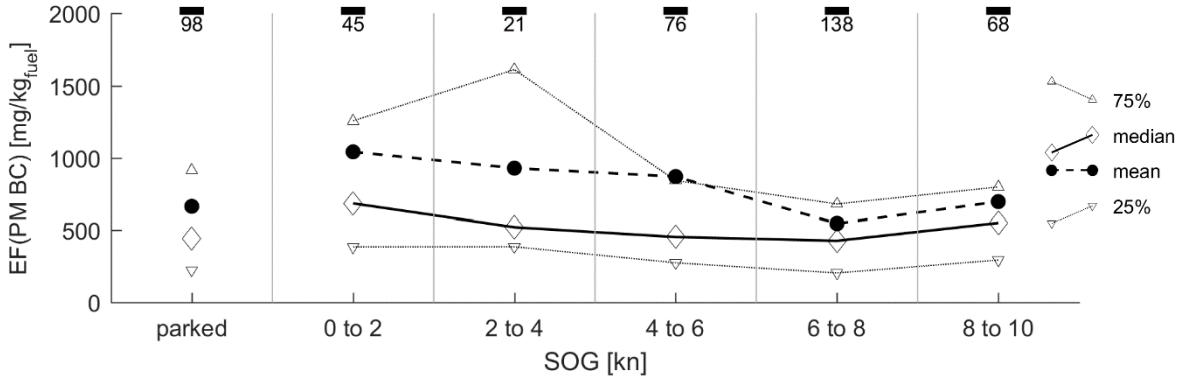

Figure ES. 2. Emission of BC particles over vessel speed, i.e. load.

CONCLUSION AND OUTLOOK

The new IMO rules forces ships to use new fuels and abatement techniques. This will result also in changing emission factors for SO_2 and NO_x but potentially also for particles. The measurements conducted within the Ports of Los Angeles and Long Beach demonstrates the capability of the remote measurements for autonomous compliance monitoring. In this study the data indicate that the compliance rate with respect to using the allowed fuel sulfur content is very good with about 99 %, this is similar to results that we see in our current sulfur compliance monitoring measurements in the Baltic Sea. But it should be noted that the sulfur may have been under predicted in this study due to wall artifacts affecting the SO_2 measurements in the PM10 sampler used as the common inlet.

The observed NO_x emission factors during this study were below those that have been assumed in earlier inventory studies. We found that both the NO_x emission factors for individual ships and the net emission rate of the whole harbor area of PoLA and PoLB shows lower values. It hence seems that the NO_x emission for the ports of LA and LB may be overestimated.
The magnitude of the measured particle emissions agree reasonably well with the assumed values of the inventory, even considering the variability. In general the BC, PM2.5 and PN emissions are highest at low speeds during which intensive maneuvering is carried out, corresponding to transient combustion conditions. It should be noted that tugs contribute significantly to the presented statistics since most ships are assisted by these vessels when operating in the harbor.

The results in this study give an improved understanding of the magnitude and variability of the actual emission factors in different modes of operation, providing better input to air quality modelling in the Los Angeles basin.

Table of Contents

List of Figures

List of Tables

1 Introduction and Background

The combustion of residual fuels by shipping gives rise to emissions of sulfur dioxide (SO_2), and particulate matter (PM), the latter includes primary soot particles, and secondary inorganic sulfate particles formed as a result of atmospheric oxidation of sulfur dioxide and secondary organic particles from the lubrication oil. Nitrogen oxides (NO_x) are also emitted when fuels are burned, as a result of oxidizing atmospheric N_2, and to a lesser extent the nitrogen content of the fuel.

Secondary PM from, as well as primary PM, SO_2 and NO_x, has impacts on human health in coastal areas terms of effects on mortality and on morbidity (illness, including exacerbation of asthma, incidence of bronchitis and heart failure). Modeling (Corbett 2007) indicates that smokestack emissions from international shipping kill up to 64,000 people a year at a cost to society of more than US$330 billion per year. NO_x emissions also contribute to the formation of photochemical smog (ground level ozone), which can harm human health and vegetation and cause nitrification on the sea, the latter of particular concern for sensitive waters such as Baltic sea and inland lakes. In addition to causing health impacts from particle formation the SO_2 emissions contribute significantly to acidification in coastal areas damaging built environment and sensitive ecosystems (EMEP, 2002).

The average sulfur content of marine heavy fuel oil worldwide is currently 2.7 %, or 27,000 parts per million (ppm), compared to 2,000 ppm maximum for heating oil, and a limit of 10 ppm for automotive petrol and diesel. However new rules have been ratified within the IMO Marpol Annex VI, and further implemented in national environmental legislation, which have reduced the fuel sulfur content (FSC) dramatically (0.1 %) in certain areas, such as northern Europe and the coastline of the US from 2015 and onward. In California such rules for reduced FSC in ocean going vessels have been implemented since 2008 to the 24 nautical mile zone but since 2015 the geographical area has been extended to 200 nautical miles through the new IMO rules. In addition, the NO_x emissions will be lowered since ships built after 1 Jan 2016 are required to emit 90 % less NOx by applying abatement technique such as selective catalytic reduction. Even though the new IMO rules have already been implemented there is a lack of real world compliance control of ships and instead all control is carried out by stepping on board the ships while at berth. In Europe several pilot projects are carried out, for instance measuring all ships entering the Baltic Sea from bridges and aircraft. In the US the EPA is still investigating how such compliance control could be carried out.

Accurate characterization of emissions from ports and industrial sources on a real or near-real time basis is critical for developing effective control strategies to improve regional air quality, promoting compliance, and reducing exposure levels in nearby communities. To improve the understanding of such emissions in the South Coast Air Basin (SCAB), the South Coast Air Quality Management District (SCAQMD) has promoted and sponsored a series of measurement projects to study port and industrial emissions using optical remote sensing methods. The projects include experimental studies of emissions from the ports, refineries, oil depots, treatment facilities, oil wells, gas stations, fuel islands and barges (Mellqvist 2016b; 2016c). In addition, SCAQMD has sponsored technology demonstration and validation studies to assess potential uncertainties of different optical techniques through side-by-side measurements of real sources and controlled source gas releases.

This report shows the results from a five week pilot study at the port of LA (PoLA) and port of Long Beach (PoLB) in which new innovative observational methods were demonstrated and

used to measure real world emission factors (g/kg_{fuel}) of SO_2, NO_x and particulates and emission rates of NO_2 from individual ships maneuvering or mooring within the harbor areas. The data have been compared to emission factors applied in emission inventories by the ports. These techniques are also applicable for automatic compliance monitoring of fuel sulfur content (FSC) and this application was demonstrated by carrying out automatic measurements during several weeks at three fixed locations.
In addition and optical method was applied from the ground and from the air to measure actual emission rates (g/s) of nitrogen dioxide (NO_2) from isolated ships as well as from the full harbor area.

2 Instrumentation and method

2.1 Instrumentation

The measurement system used in this project, Table 1, consists of an optical instrument for remote sensing measurements and extractive instruments for sniffer measurements of gases and particles in the exhaust plume of the target ships. This system has been operated elsewhere from both airborne and fixed platforms for compliance monitoring of fuel Sulphur content (Alföldy 2013, Berg, 2012, Balzani et al., 2014, Beecken 2014, Beecken 2015a, Beecken 2015b, Mellqvist 2015). The system is operated by a custom software IGPS real (Identification of Gross-Polluting Ships) which logs all data, including wind and AIS information from ships, and in real time plots ships on a map. It automatically identifies ship plumes and calculates the emission factors, see Figure 1.

Table 1. Overview of the instruments used during the study.

Species	**Measured property**	**Method**	**Response time**	**Detection limit**
CO_2	Mixing ratio	Cavity ring down spectrometer (Picarro).	0.5 s/ 1 s	0.2 ppm
SO_2	Mixing ratio	Fluorescence (Thermo)	30 s/2 s	1 ppb
NO_x	Mixing ratio	Chemiluminiscence (Thermo)	1 s	0.5 ppb
NO_2	Column density/derived flux	Zenith sky DOAS (Andor)	2 s	20 ppb (over 50 m)
PN/ derived PM	Number size dist. 5.6 - 560 nm	Electrostatic mobility in 16 channels. (TSI Engine Exhaust Particle Sizer, EEPS)	0.1 s	n/a
PN/ derived PM	Number size dist. 300 - 10000 nm	Laser scattering. (TSI, Optical Particle Sizer, OPS)	1 s	n/a
PN	Concentration 5 nm - 1 µm	Water based Condensation Particle Counter (TSI CPC)	1 s	n/a
BC	Mass below 1 µm	Aethalometer, 7 wavelengths (370-950nm) dual spot (Magee)	1 s	100 ng/m3
Meteorology	Wind speed and direction	Anemometer	1 s	
Ship info	Position in longitude, latitude, and other navigational info	AIS	2 s	
VOC	Column density/derived flux	Solar Occultation Flux	2 s	

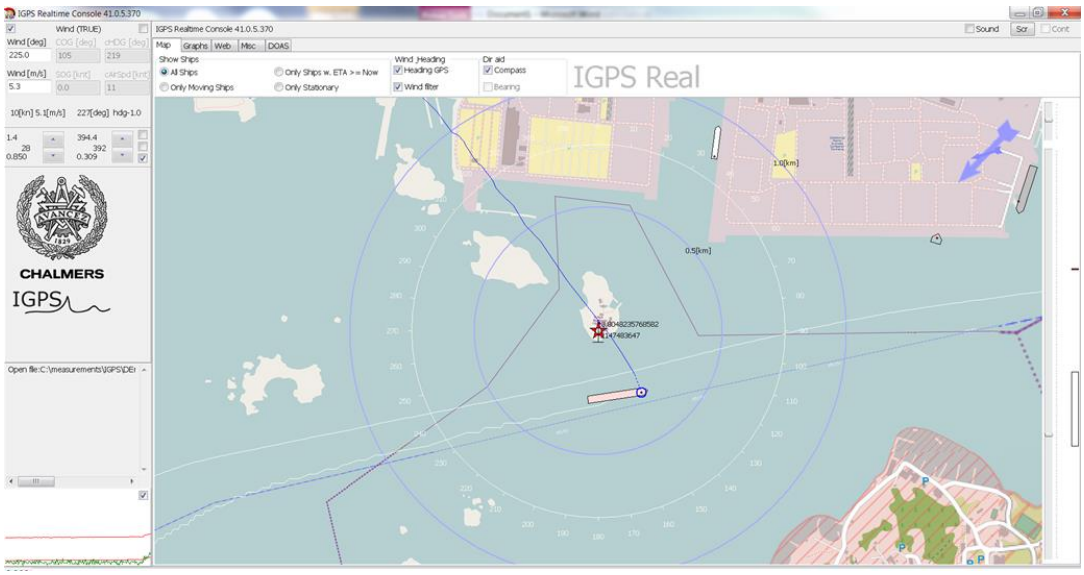

Figure 1. A screen dump from the software *IGPS real* which shows the measured data and which calculates the position of the ship plumes. When the station, red star, is hit by a ship plume the program automatically calculates the FSC and various emission factors and also identifies from which ship the plume originates from.

The gas instruments are based on the following physical principles: UV fluorescence for SO_2, chemiluminiscence for NO_x and cavity ring down spectroscopy for CO_2. Two particle instruments are measuring the number size distribution of the particles between 5.6 nm to 10 µm, i.e. an EEPS measuring between 5.6 to 560 nm and an OPS measuring between 300 nm to 10 µm. The particles below 560 nm are classified by their electric mobility while the larger ones are classified by laser scattering. The size distribution is converted to mass distribution by calculating the mean volume of the particles, assuming a spherical shape, multiplied with an assumed density (unit density, i.e. 1 g per cm^3).
The mass of soot in the ship exhaust plumes is measured by using an aethalometer that utilizes the optical absorption properties of soot collected on a filter in 7 wavelength channels (370-950nm) for detection of particles smaller than 1 µm in size. The instrument uses two spots and in this way it reduces filter loading effects which generally is a problem with this technique. In this study we have used the wavelength 850 nm to obtain the soot, i.e. black carbon.
The extractive techniques for gases are available as commercial state of the art instruments and they are being used worldwide as reference methods for air quality measurements. In our measurement system we have modified these instruments to obtain a fast response, smaller weight, smaller form factor and field robustness. The optical method is based on the same hardware and data analysis as being used in satellite measurements. The application of carrying out ship emission measurements is unique for this project, however.
A remote sensing instrument, Solar Occultation Flux (SOF) was to measure columns of VOCs to investigate emissions from ship fueling and other oil and gas related activities in the harbor. This system has been explained in detail two parallel project reports (Mellqvist 2016b; 2016c) and it will not be further described here.

2.2 Measurement quality

The gas sniffer measurements were calibrated against gas standards and a gas blender provided by SCAQMD, with typical mixing accuracy 1 %. The estimated uncertainty in the emission factors for gas species it is about 20-25 % (Beecken 2015a, Alföldy, 2013), obtained from validation measurements and analysis of the measurement precision.

In more detail the SO_2 instrument has a cross-sensitivity to NO (100 ppb NO corresponds to 1.5 ppb SO_2 reading) which is subtracted utilizing the data from the NO_x measurements, assuming that 90 % of the NO_x is in the form NO. This assumption causes an estimated absolute uncertainty in the calculated FSC of about 0.1 %. The median value of all measured SO_2 emission factors was first negative, due to overcompensation of the NO interference effect, and we therefore adjusted all emission factors of SO_2 upwards with 0.02 % in FSC (same as 0.08 g/kWh or 0.4 g/kg_{fuel}) to obtain a median SO_2 emission factor of 0 g/kWh, see result section below.
The particle sensors were not calibrated during this project and we mostly relied upon factory calibration. However, since the CPC is assumed to be the most reliable instrument, the EEPS data were corrected by the ratio of the total particle numbers from the CPC and the EEPS (i.e. 24%). The PM measurements by the EEPS rely on the inherent density and shape of the particles and here we assumed spherical particles with unit density (1 g/cm^3). For BC (i.e. soot) both the density and the shape differs from the assumed one. In a recent study (Furusho-Percot, 2016) it was shown that the values of the EEPS changes by ±30 % when taking into account soot in diesel engine plumes. In other studies similar uncertainties are shown (Burtscher 2005, Park 2003, Park 2004).
An additional uncertainty for the EEPS, CPC and aethalometer is particle losses in the antistatic sampling tubing, which was 7 m long. Note that for the OPS this is not the case since it was used without sampling tubing. Our flow calculations show that the losses for small particles below 1 µm should theoretically be neglible.
The OPS data for particle sizes above 1 µm showed very small number amounts of particles and when converting these numbers to mass, the signal was rather noisy and uncorrelated with the ship plumes. Note that the measured number is multiplied with the cube of the particle radius and the larger particles are therefore heavily weighted when calculating the particulate mass. Due to this noise the coarse particle data was omitted and only the channels bellow particle sized of 2.5 µm were used together with EEPS data to obtain PM1 and PM2.5 data. Here the PM2.5 was noisier than the PM1 data. In addition, during the first period (Oct 8- Oct 20) of the campaign, during which most chase experiments were carried out, the OPS instrument was malfunctioning and then we only had data for particles with size smaller than 500 nm. However, in a similar study (Beecken 2015b) in Sankt Petersburg it was estimated that the particles below 300 nm contribute to 70% of the total particle mass in fresh ship plumes and, if this is the case for this study, it means that we should have captured a large fraction of the particle mass in the PM05 measurement.
In addition, the OPS is based on scattering properties of particles in the near infrared region with an assumed refractive index of the particles. Since the refractive index of soot differs significantly from standard particles used to calibrate the OPS there is a potential uncertainty in the PM measurements of soot; this requires further investigation. As discussed above particle measurement methods are often biased and when combining several instruments, as we have done in this study, this adds uncertainty to the measurements.

An additional measurement uncertainty lies in the fact that the flue gas stacks of the ships are elevated and the flue gas from the ship may therefore not reach down to the ground. In such a case only the emissions from the tugboats would be measured. However the experience is that there is a turbulent wake downwind of the ship that causes the emissions to swirl down on the ground, especially if the measurements are carried out at some distance. It is therefore estimated that most of the measurements represents emissions from both the main ship engine and the accompanying tugboat. Note also that the main objective of this study was to measure the actual combined emission factor from tugboat and ships, since this represents the actual emissions affecting the harbor.

Another remark is that since the plume passes our sniffer sensor rather quickly, within 20-30 s, it is easy to distinguish between the emission plume of the ship and the background concentration. However an important quality criteria is that the baseline does not change too much before and after the plume has passed and that only one ship (including tugboats) is present in the nearest upwind sector.

2.3 Calculation of observed emission factors from sniffer measurements

One objective with the ship emissions measurements is to obtain mass specific emission factors (and fuel sulfur content) for different gas and particulate species. In Eq. 1 below is described how to calculate observed emission factors for various gases, X, based on the assumption that the CO_2 emission is directly related to the amount of combusted fuel and that ratio of the pollutant and the carbon in the fuel is conserved from the fuel/combustion to the emission plume. It is also assumed that the carbon fraction of the fuel is 87%. For particles number the emission factor is obtained through Eq. 2. More details can be found in Beecken et al (2014). This approach is consistent with the on board method described in the MEPC guidelines 184(59) and it has been used in several studies (Alföldy, 2013, Balzani 2014).

$$\mathrm{EF(X)}_{(\mathrm{g\cdot kg_{fuel}^{-1}})} = \frac{\mathrm{M(X)}\cdot\sum(\mathrm{X_{ppb}})}{\mathrm{M(C)}\cdot\sum(\mathrm{CO_{2,ppm}})/0.87} \quad (1)$$

$$\mathrm{EF}\left(\mathrm{PN}_{(\#\cdot\mathrm{kg_{fuel}^{-1}})}\right) = \frac{\sum\left[\mathrm{PN}_{(\#\cdot\mathrm{m^{-3}})}\right]}{\sum\left[\mathrm{CO}_{2,(\mathrm{kg\cdot m^{-3}})}\right]}\cdot \mathrm{EF(CO_2)} \quad (2)$$

An example of a plume measurements conducted 300 meters downwind of a ship in PoLA is shown in Figure 2. Each peak corresponds to plumes from single ships, and the ratio of the specific species versus CO_2 yields the observed emission factors according to Eq. 1 and Eq. 2. In reality the area of the concentrations above baseline for each peak is used to calculate these ratios, instead of the actual concentration values to compensate for different instrumental time responses.

In order to ensure the quality of the calculations, the measured results for each species in each plume have to fulfill according requirements. All plumes for all species were separately examined for their significance during the first step of the evaluation. Later, a necessary requirement was that the CO_2 peak is significantly above the ambient CO_2 level. See Figure 16 for an example of a peak and reference regions. If the 90th percentile of the CO_2 value during the plume measurement was less than twice the standard deviation of the ambient CO_2, the whole plume was omitted in further emission factor calculations. Also unreasonably negative results during plume occasions have been interpreted as not measured for the respective species.

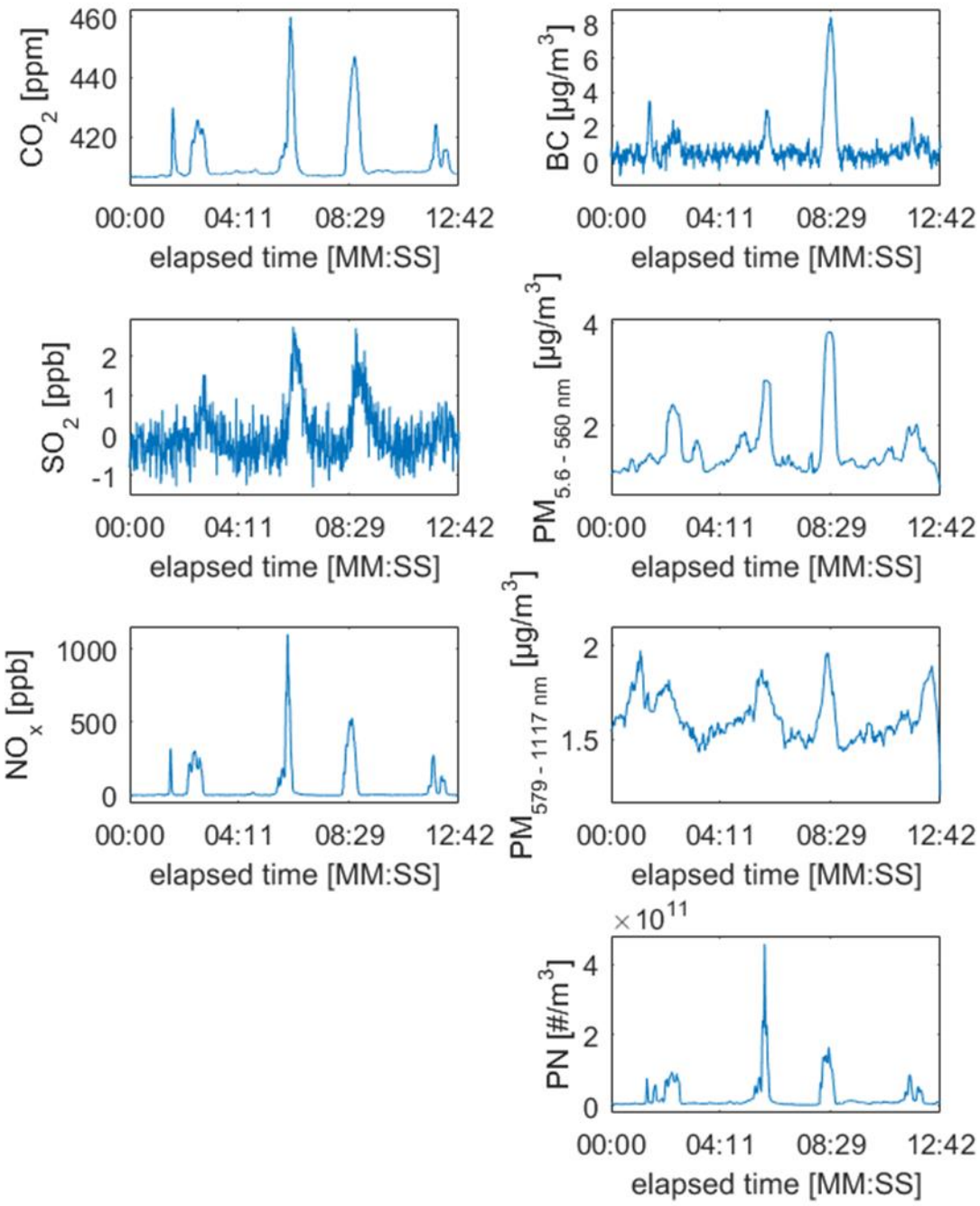

Figure 2. Here an example of plume measurements several 100 meters downwind of a ship is shown. Each peak corresponds to a single ship measurement.

2.4 Optical measurements

The optical measurements used here are based on measuring sky spectra at 420-470 nm with a grating spectrometer connected to a telescope using a liquid light guide. The used instrument

was a UV/visible spectrograph (Andor Shamrock SR–163i) connected with a UV enhanced CCD camera (Andor Newton 920BU). The focal length of the spectrograph is 163 mm, see Figure 3.
From the visible spectra it is possible to derive the path integrated concentration of NO_2 along the light path using known absorption features (cross sections) of NO_2. Here we have used NO_2 cross section from Vandaele et al (1999). The analysis method is denoted the DOAS technique (Differential Optical Absorption Spectroscopy) (Platt 2008) and this is widely applied within the research community and in several commercial air quality instruments.
To account for spectral artifacts and drift the spectral line shape of the instruments was measured on a daily basis. Spectral artifacts were also checked with a gas calibration cell, see photo in Figure 3. The uncertainty of the path integrated concentration is typically within 5 %, which considerably smaller than the uncertainty due to radiative transfer and wind which is important for the flux estimation, see section 3.
In this study we have collected the sky spectra in two modes, i.e. by pointing a telescope connected to a spectrometer either towards zenith in ground based fixed mode and mobile measurements, or downward for airborne measurement. An example spectrum is shown in Figure 4 when measuring in the plume of the oil tanker TAQAH.

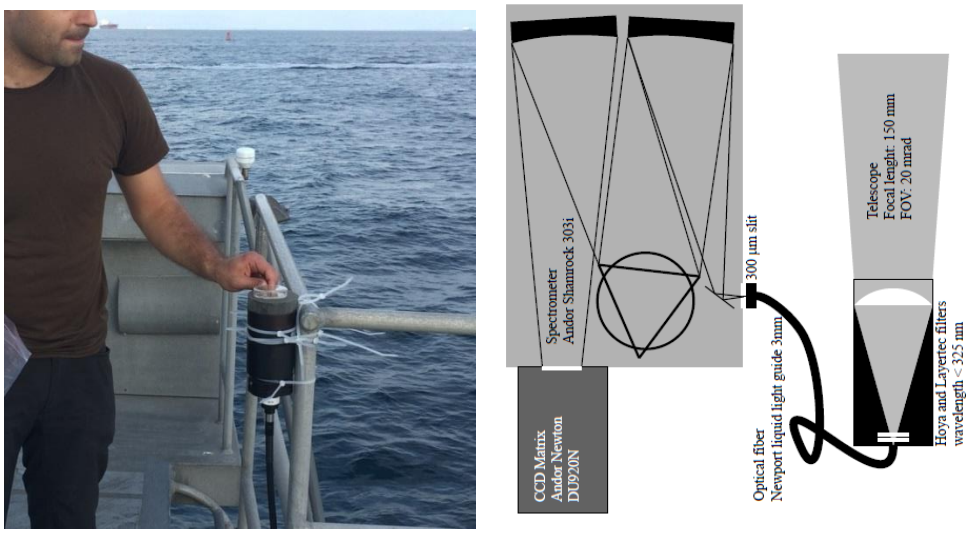

Figure 3. Upward looking optical system. Here an upward looking telescope is connected an optical fiber which transmits light into a UV/visible spectrometer measuring wavelengths between 420-470 nm.

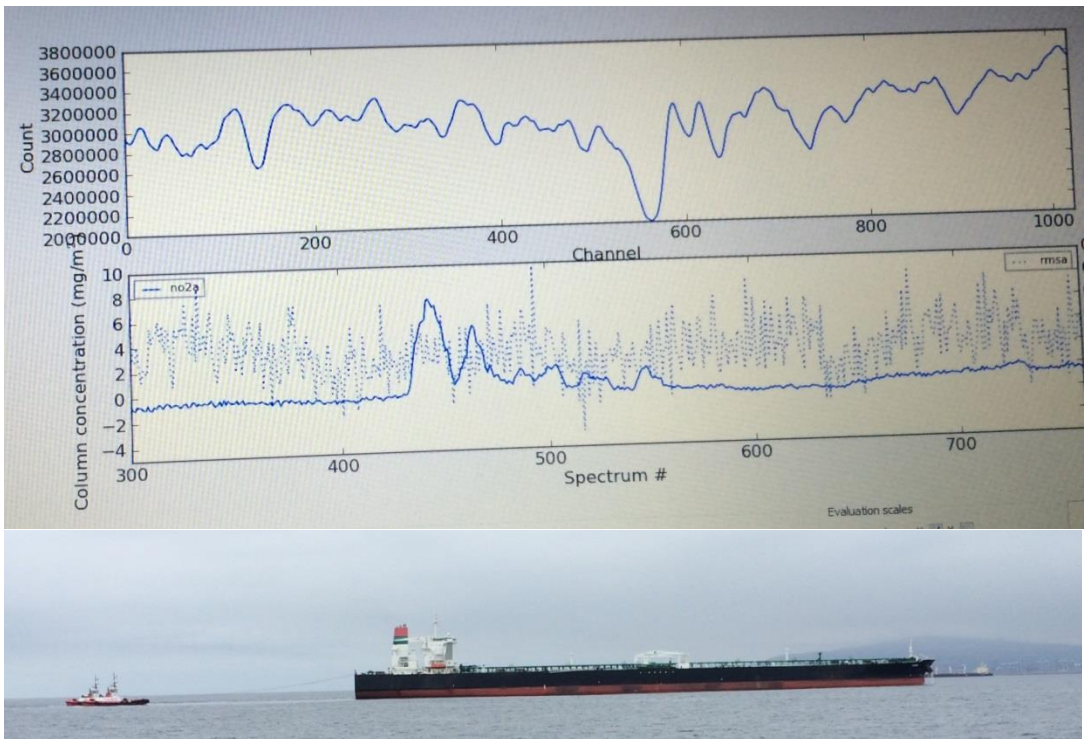

Figure 4. A screen shot of the DOAS computer when measuring while the plume from the oil tanker TAQAH, lower panel. The measurement was taken 500 m distance while the plume drifts across the telescopes field of view. The collected spectrum is shown in the upper panels and the derived column density of NO_2 is shown in the lower one.

In the ground based application the instrument is deployed downwind of passing ships, which ideally should move orthogonally to the wind direction, and the wind drives the plume across the telescope's field of view. In such a way a profile of the path integrated concentration along a cross section of the plume can be retrieved. If measurements are performed from a moving platform the plume may also be traversed by moving across it. In this study both ways described above have been utilized.

To obtain the gas flux from the ships in g/s the path integrated concentration summed over the cross section of the plume needs to be multiplied with the apparent wind speed and wind direction of the plume. This is the wind one feels while being on the deck of a ship and this is obtained as the superposition of the true ambient wind and the ships motion, see Figure 5. Thus, it is important to know not only the wind direction and speed, but also the ship's navigational data, as well as the speed and direction of the measurement platform. With this information the apparent wind can be calculated, see Berg 2012, Beecken 2015b, and Balzani 2013.

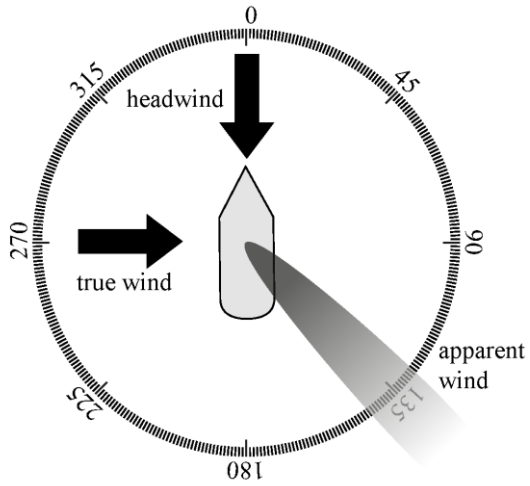

Figure 5. The apparent wind is the superposition of the true wind and the headwind due to the ship's motion, The gas plume from a ship will appear to move in this direction. This wind is used to calculate the gas flux from ships, see Berg et al. (2012).

In an airborne campaign, the NO_2 net emission in g/s of the combined harbor areas of PoLA and PoLB and an adjacent industrial area was measured with a downward looking configuration. The area of interest was twice fully encircled in a box-like pattern. As such the incoming flux of NO_2 could be subtracted from the outgoing flux and as such a net flux of NO_2 could be calculated.

In the airborne application the telescope is pointed downwards with a certain angle to gather the skylight that is reflected and/or scattered at the ground surface. In other projects we have done such measurements to obtain SO_2 and NO_2 emissions from individual ships Berg (2012), but in this project the objective was instead to measure large scale gas fluxes from multiple ships and other activities in the harbor, as illustrated in Figure 6. The light that reaches the telescope has traversed through the plume twice; first when heading towards the ground surface, second after reflection on the latter, heading upwards towards the telescope. The optical measurements are first corrected for the slant observation angle and then the gas flux is obtained by multiplying with the orthogonal wind speed, in a similar manner as done in the two projects in the SCAQMD study (Mellqvist 2106b; 2016c) and elsewhere (Mellqvist 2010a).

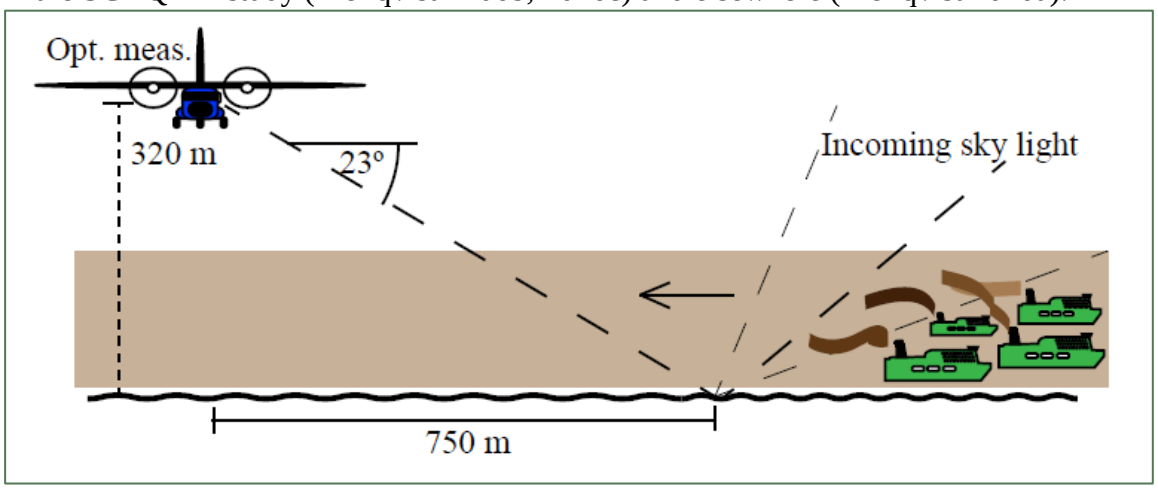

Figure 6. An illustration of the airborne optical measurement. It is assumed that the sky light is reflected in a specular fashion on the surface. The objective here is to measure the gas flux which is the product of the wind and the path integrated concentration along the flight transect.

3 Measurements

Stationary and mobile (i.e. on-vessel) measurements of ship specific emission factors (g/kg_{fuel}) and total emission (g/s) were carried out in the port of Los Angeles and Long Beach from October 8 until November 10, 2015.
The measurements were first carried out from a van, Figure 8, for 5 days at the Coast Guard site at the Port of Los Angeles, PoLA_1 site, Figure 7.
The equipment was then moved to the research vessel Yellow Fin, Figure 9 to Figure 12, operated by the South Coast Marine Institute. From this mobile platform chase studies were carried out of individual ships to measure their emissions at different modes of operation, Figure 13. In Figure 7 the GPS-track of the ship during one of the campaign days is shown, showing the typical area of the measurements.
The mobile measurements were succeeded by stationary, land-based measurements from the van at the South Coast Marine Institute from October 27 to November 1, PoLA_2, Figure 7, and at the ground of the Port of Long Beach Command and Control Center at the entrance of the Port of Long Beach between November 2 and November 10, PoLB Figure 7.
In addition to the activities in the port an airborne study was carried out on November 8 to investigate the total emissions of NO_x from the port. The optical instrument described in section 2.4 were installed in a Piper PA 28 aircraft and were used to measure the atmospheric columns of NO_2 below (and above) the aircraft in a box around the port and industrial area, Figure 14.

Figure 7. Fixed ship emission measurement sites in Port of Los Angeles and Long beach, respectively, shown by stars, together with a GPS track of the measurement vessel, Yellow Fin for one of the campaign days.

Figure 8. Fixed measurements at the port of Los Angeles site 1 site at the coast guard facility

Figure 9. The research vessel Yellow Fin, used for chase studies.

Figure 10. The measurement setup inside the Yellow Fin is shown in the upper picture while the gas and particle inlet system is shown in the lower picture on the right-hand side. Here a particulate matter inlet, typically for PM10 measurements, is here connected to 7 m Teflon tubing for the gas analysis and antistatic tubing for the particle analysis. On the right-hand side in the lower picture is shown a sonic wind meter. On the lower right-hand side in the picture is shown the OPS measuring the fine/coarse particles between 300 nm to 10 µm. Only a short 15 cm tubing was used here.

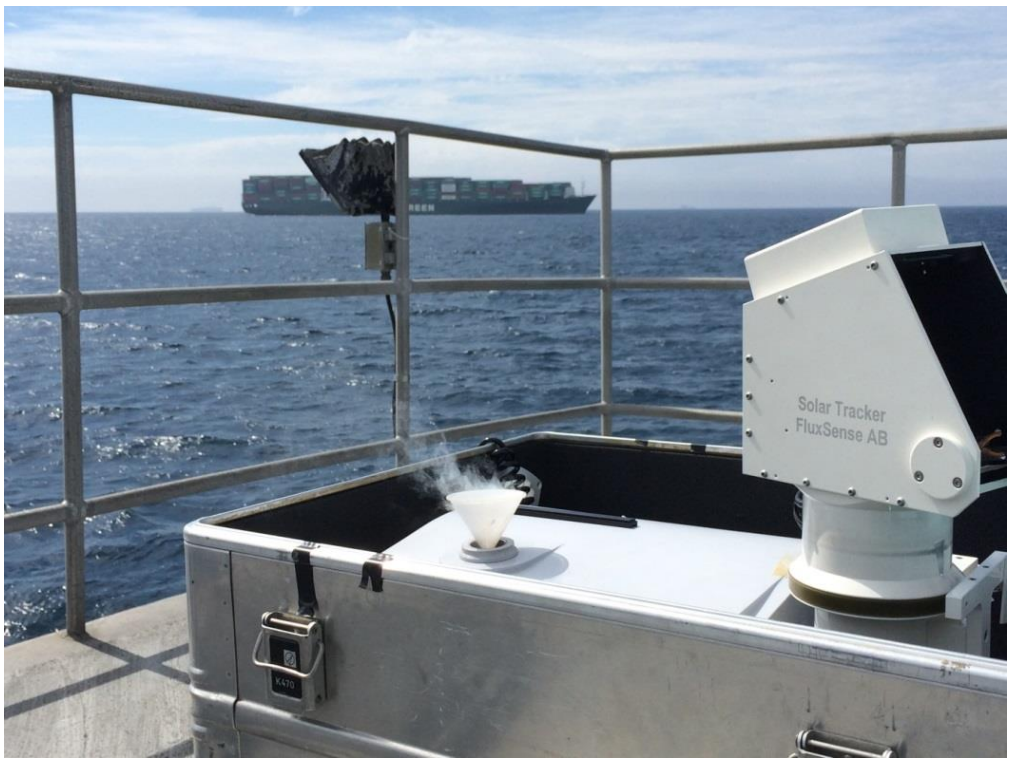

Figure 11. A Solar Occultation Flux instrument used to measure VOC emissions from shipping and port activities on board the research vessel Yellow Fin.

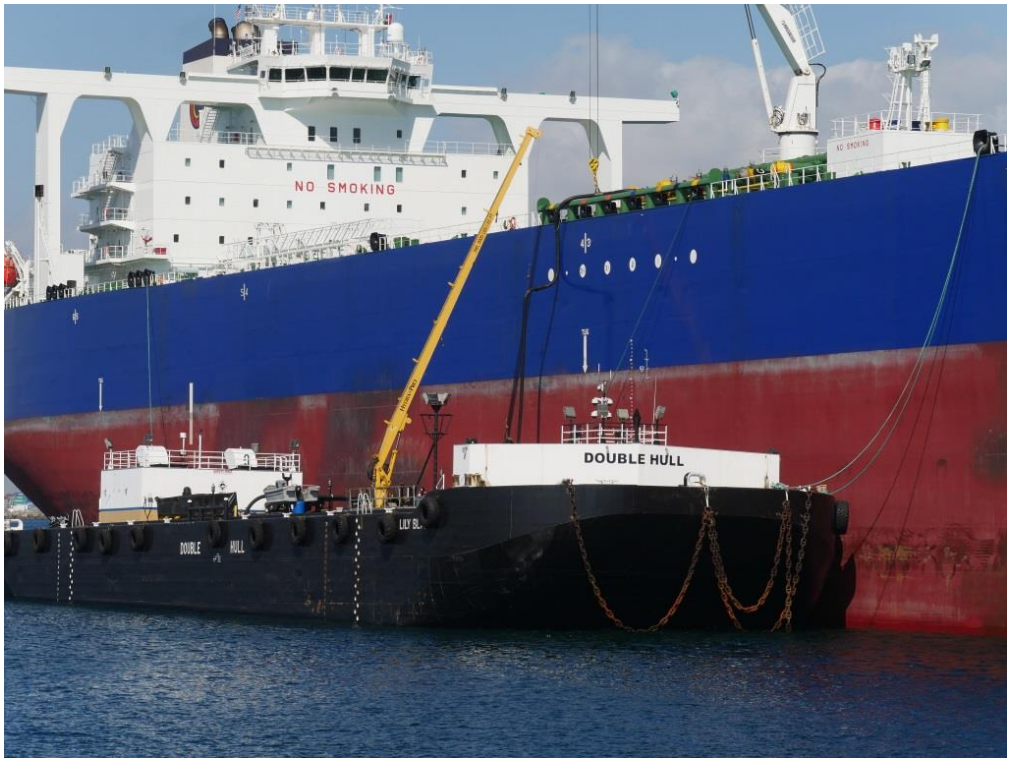

Figure 12. Example of a ship fueling operation in the port of Long Beach during the study measured from the research vessel Yellow fin.

Figure 13. A photo taken from the control bridge of the research vessel Yellow Fin. Here a chase study of the cargo ship NYK DANA was carried out in the port of Los Angeles.

Figure 14. The Piper PA 28 aircraft used for large scale optical measurements. The optical equipment is shown in the bottom left picture while the telescope setup is shown.

4 Results

During a 5 week campaign 571 ship plumes were measured from 132 individual ships that were identified via AIS. Another 100 distinct plumes were measured but for these it was not possible to identify the vessel/source and they have therefore been omitted.

4.1 Chase studies

Twenty-four chase studies were carried out during the project from the measurement vessel Yellow Fin. In these we obtained emissions (EF and ER) by analyzing gas and particle concentrations a few hundred meters downwind in the ship plumes, while the ships were running in different modes of operation. In Figure 13 and Figure 15 one such study is shown of the ship NYK Diana from start of the engines until it was operated at 10 knots in open sea. The ship is shown with different colors depending on the time (UTC) it was measured. In addition the location of the measurements is shown with a red circle while a black dot indicates the presence of tug boats. The wind direction is indicated by the arrow which points towards the wind (SSW wind). Noteworthy is that many ships were accompanied by tugs and these vessels therefore stand for a significant part of the emissions at the harbor.

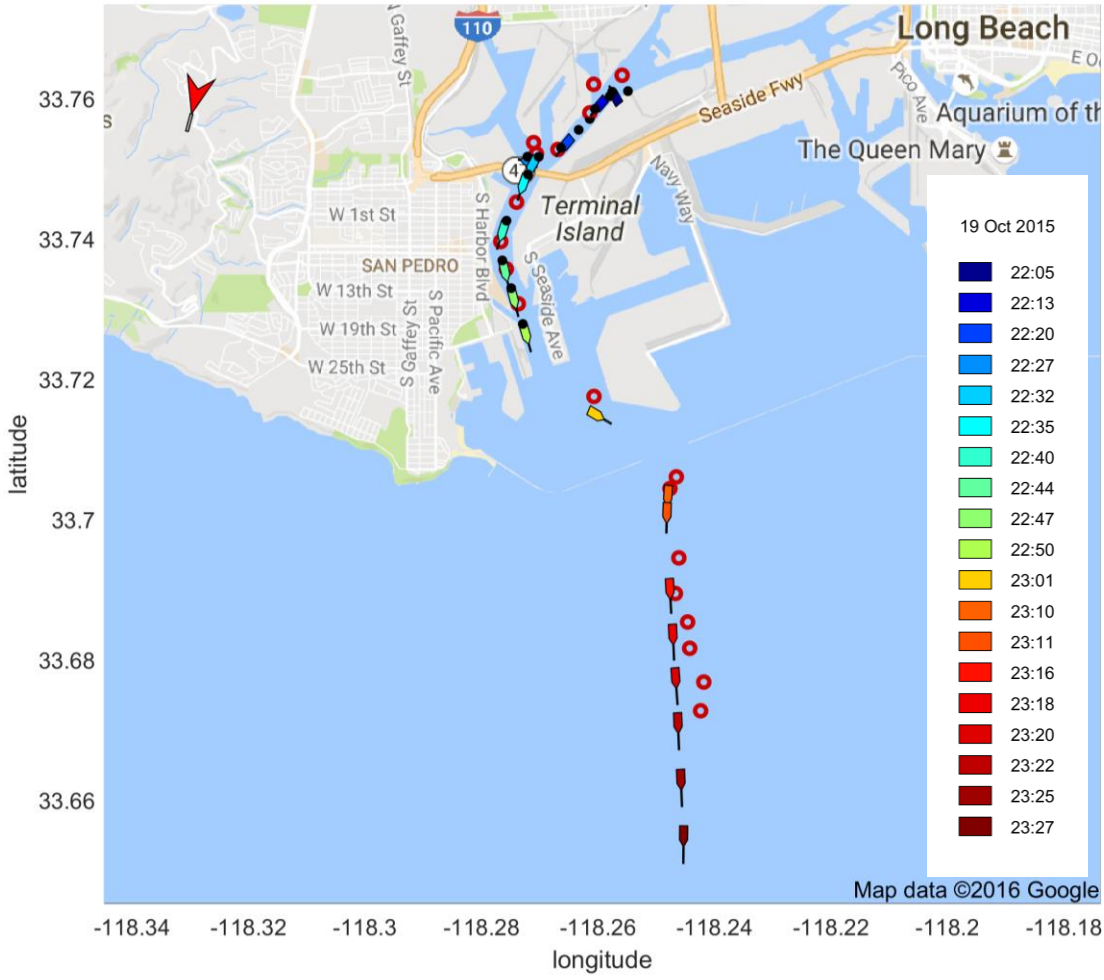

Figure 15. An illustration of a chase-study in Port of Los Angeles of the cargo vessel NYK DIANA (MMSI: 372319000, cargo) on October 19 from the research vessel Yellow Fin.

In Figure 16 the various concentration measurement data for NYK Diana are shown for the measurement situation shown in Figure 17 at 22:32 (UTC), i.e. close in time to passing under the bridge on Seaside fairway, Figure 17. Here the ship was accompanied by two tugs, i.e. Robert Franco (MMSI 367569830 and Lela Franco (MMSI 367678850).
In Figure 18, the observed emission factors for NO_x, BC, PM05 and PN are shown versus speed of the ship. In the figures the black circles indicate measurements during which the ships were accompanied by tugboats with the color coding corresponding to the time of the measurements according to the legend in Figure 15. The reason for plotting data in this manner in is to investigate whether the observed emission factors depend on the engine load. Ship engines in general have load dependent characteristics and one often assumes that NO_x increases with load, since it is caused by high temperature while particle emissions are highest at low load due to incomplete combustion. However, in the real data the situation appears to be more complex, especially during the maneuvering phase.
It can be seen for this particular ship that the observed emission factor of NO_x and mass and number of fine/ultrafine particles below 560 nm increased with speed. For BC there was no clear correlation.
The absolute emission rate of NO_2, is shown in Figure 19. Ideally it should increase with speed but since the ship and accompanying tugs are maneuvering and since we are measuring NO_2 and not NO_x the emission pattern gets more complicated. Our interpretation is that the high NO_2 emissions in the beginning of the chase study are caused by strong maneuvering of the tugs.

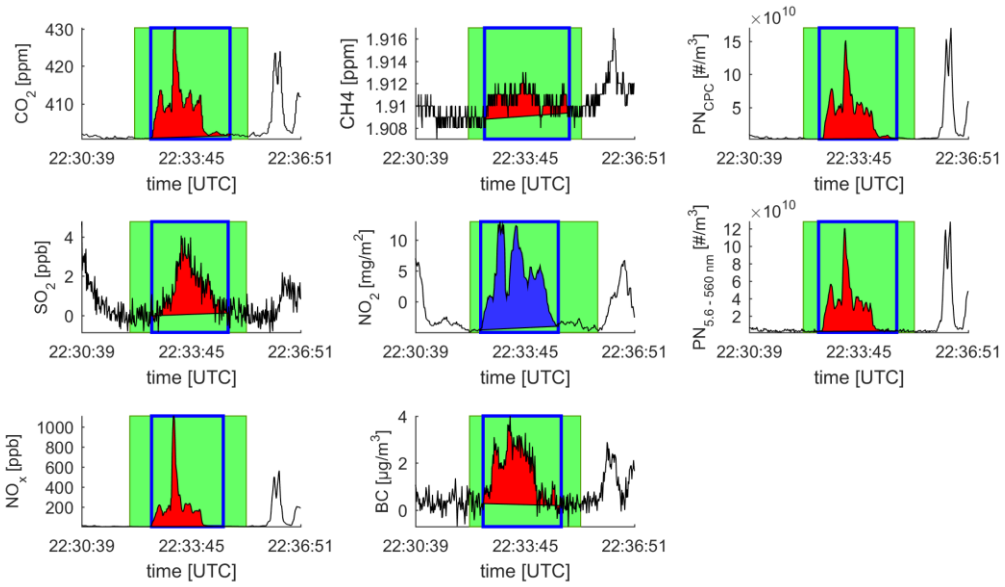

Figure 16. The measurement data for the NYK DIANA plume measured on 19 October 2015 at 22:32. The figures from top left to bottom right correspond to CO_2, CH_4, PN measured with CPC, SO_2, NO_2 vertical column (blue), PN measured with EEPS, NO_x, BC measured at 880 nm. Red shaded area: excess contribution of species due to emission for calculation of observed emission factor; blue shaded area: excess contribution due to emission of NO_2 measured by DOAS for calculation of emission rate; green shaded area inside blue frame: values accounted as plume; green shaded area outside blue frame: values accounted for baseline retrieval.

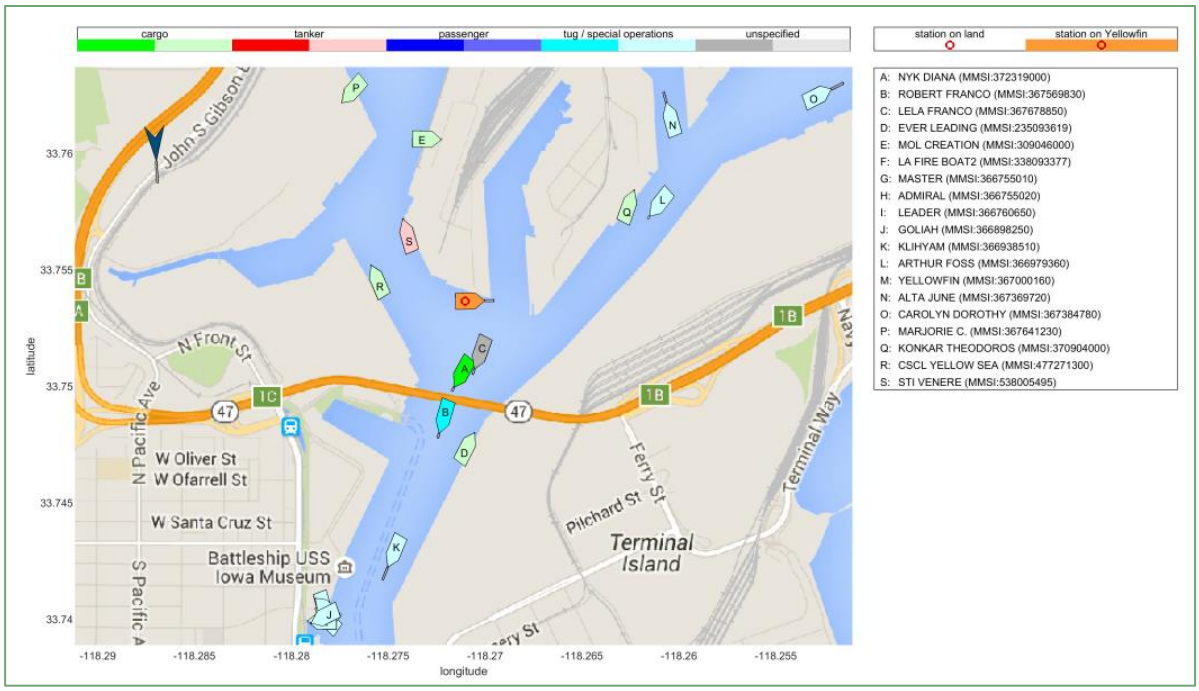

Figure 17. Locations of ships when measuring NYK DIANA at 22:32. Note that the measurements vessel Yellow Fin is marked in orange with a red circle inside.

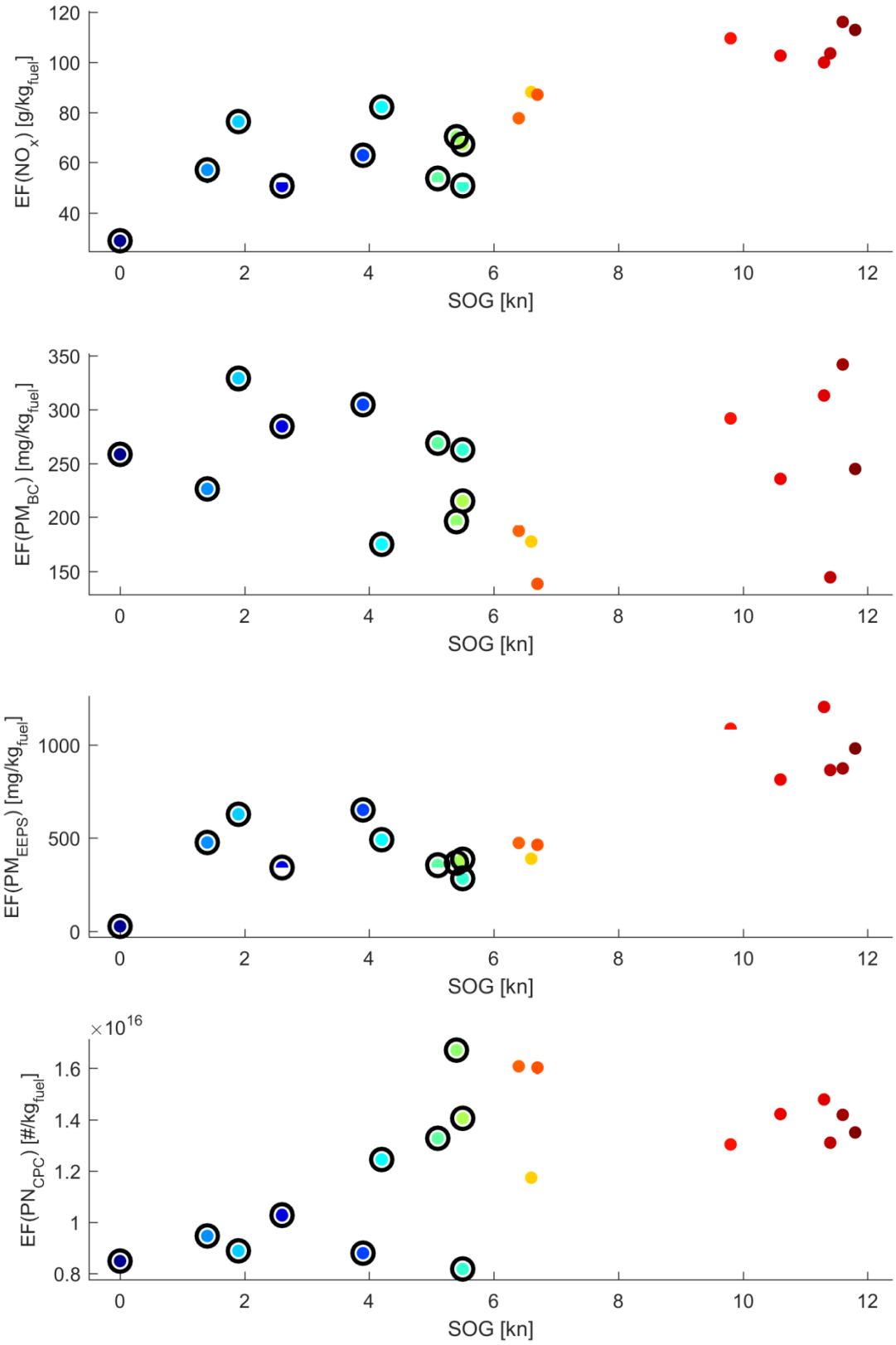

Figure 18. Specific emissions factors for NYK DIANA versus speed, when leaving port of Los Angeles. Different colors correspond to different times as shown in the legend in Figure 15. Here PM_{EEPS} corresponds to partcilate matter in the size range 5 to 560 nm, i.e. PM05.

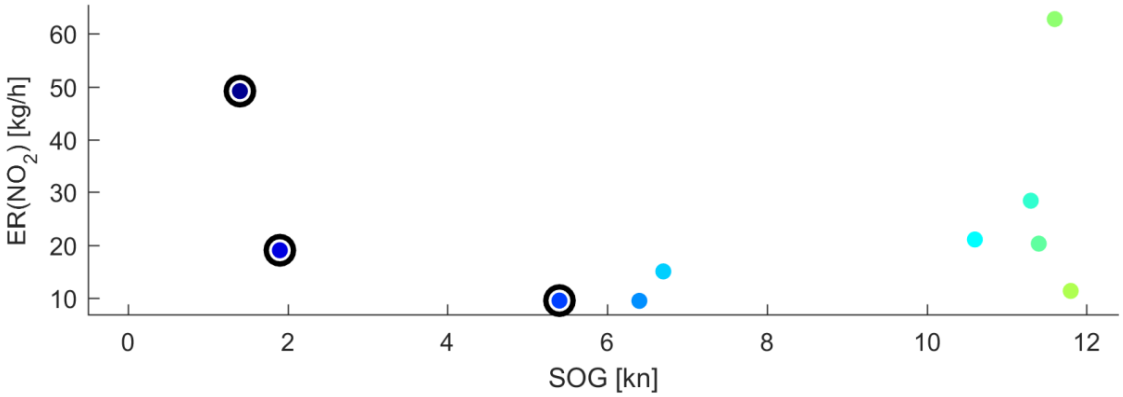

Figure 19. Here the emission rate of NO_2 is shown for some of the cases in Figure 15. Different colors correspond to different times as shown in the legend in Figure 15.

In Table 2 the main chase studies are summarized with observed emission factor values shown as average values with their associated standard deviations. Detailed plots of these chase studies can be found in appendix I. In the table we also show the typical emission values that are applied in the port emission inventories. In these the particle mass emission factor is given as DPM (Diesel Particulate Matter), which typically consist of particles with sizes below 2500 nm (PM2.5) with the major fraction in the fine size range below 500 nm. For comparison reasons we have converted the inventory values from g/kWh to g/kg fuel, assuming a specific fuel oil consumption (SFOC) of 200 g fuel/kWh for all ships without any load dependence applied. The SFOC is typically 160-170 g fuel per kwh for slow speed two stroke engines and 200-220 g fuel per kwh for medium speed engines when tested new, but these number gets higher when the ships get older. The assumption of constant SFOC hence causes an estimated 20 % possible bias in the comparison between the measurements and the inventory emission factors. The load dependence applied in the port inventory studies (PoLA, 2015) vary for different types of ship engine, differentiating between 3 types of 2 stroke engines, i.e. MAN engines being equipped with either (a) conventional or (b) slide valves and (c) non MAN engines. The load dependence in these inventories is strongest at very low loads (0-20%) with a maximum enhancement factor of 2-4 for NO_x and 0.5-7 for PM for different engine types. In all cases the load dependence for the emission factors is negative for NO_x while for PM it is positive for MAN engines and negative for all other engines.

From Table 2 it can be deduced seen that the observed NO_x emission factors on average varied within 50 % in different modes of maneuvering, i.e. when comparing the 98th percentile compared to average. The average NO_x emission was 50 % lower than the ones used in the port inventories (PoLA 2015).

For SO_2 all of the ships, with the exception of one, were below the 2 g SO_2/kg fuel assumed in the inventories for the ships, see section 4.4 for further discussion on this.

For both PM05 and BC, respectively, the observed emission factors on average varied within a factor of 2 (100%) in different modes of maneuvering (98th percentile compared to average).

The average PM05 values were approximately 50 % lower than the inventory values. For PM2.5 there was only 5 chase studies with valid measurements from the combined OPS and EEPS. The PM2.5 was within ±50 % of the inventory value and 65 % of the mass was below particle sizes of 0.5 µm with 83 % of the mass corresponding to soot. The BC fraction was surprisingly high compared to other studies which show that PM emissions from ships running on marine gasoil are dominated by organic particles with 2-3 times more organic particles than soot

(Beecken 2015b). However, most of the measurements in this study were carried out for ships that were maneuvering and therefore the amount of soot emissions could be higher here, possibly with the organic particles being deposited on the BC. There is also uncertainty in the PM2.5 measurements of soot by the OPS instrument which needs further consideration, see section 2.

In Figure 18 and appendix I the observed emission factors have been plotted versus ship speed to investigate their variability in different modes of operation. Several parameters play a role in these measurements, for instance maneuvering, influence of tugboat activity, ship engine type and load and it is therefore not always easy to see distinct trends in the individual data. Note that general trends are discussed in section 4.3.

The observed NO_x emission factors appears to increase with ship speed, as shown in Figure 18 for NYK Diana and quite of few the others ships in appendix I. The variability is a factor of 2-3 from the maneuvering phase to running at constant speed at 10 knots outside the harbor. Note that that these trends are contradictory to the load adjustment factors used in the ship models which predicts decreasing emission factors versus load.

For particles the trends are variable. The observed BC and PN emission factors show little correlation with speed while PM05 in several cases increase with speed, as shown for NYK Diana, Figure 18. This is consistent with the load characteristics in the port inventories for PM.

Table 2. Here the main chase studies carried out are summarized. The average value and the standard deviation of the observed emission factors are shown together with the typical inventory data used by the ports. Each chase study is shown in detail in the appendix.

Ship name	**MMSI**	**Ship type**	**Speed Range [knots]**	**Species**	**$EF_{measured}$ [g/kg]**	**EF PoLA * [g/kg]**	**ER*** /GMD [kg/h]**
AQUA LEGEND	636015176	Tanker with 2 tugs Engine type: 2 stroke MAN engine	0-5.9	SO_2 NO_x PN PM1 *BC* *PM05*	<2 31.3±8.5 $(3.1±2)\cdot10^{16}$ NA *0.98±0.95* *0.50±0.45*	2.05 70 1.300	 ER_{NO2}: 6±9 kg/h ER_{NOx}: 22-56 kg/h GMD: 46±16 nm
MILLENIUM MAVERICK	366998840	Tug	8.4-10.6	SO_2 NO_x PN PM1 *BC* *PM05*	<2 37±21 $(1.4±1.1)\cdot10^{16}$ NA *0.35±0.14* *0.19±0.24*	2.05 70 1.300	 NA [kg/h] GMD: 33±5 nm
SWAN ARROW	311682000	Cargo and pilot vessel 4 stroke Daihatus engine	7.8-9.6	SO_2 NO_x PN PM1 *BC* *PM05*	<2 41±14 $(0.8±0.6)\cdot10^{16}$ NA *0.40±0.23* *0.79±0.43*	2.05 70 1.300	 ER_{NO2}: 1±1.2 kg/h ER_{NOx}: 4-100 kg/h GMD: 52±22 nm
CMA CGM GEMINI	235078078	Cargo and 1 tug 2 stroke MAN engine	0.9-8.6	SO_2 NO_x PN PM1 *BC* *PM05*	<2 46±17 $(1.0±0.6)\cdot10^{16}$ NA *0.60±0.6* *0.66±0.21*	2.05 70 1.300	 ER_{NO2}: 27±22 kg/h ER_{NOx}: 110-270 kg/h GMD: 41±4 nm
GERD MAERSK	220415000	Cargo and 2 tugs 2 stroke Sulzer engine	0.5-4.3	SO_2 NO_x PN PM1 *BC* *PM05*	<2 37±7 $(0.9±0.2)\cdot10^{16}$ NA *0.40±0.23* *0.94±0.3*	2.05 70 1.300	ER_{NO2}: 78±12 kg/h ER_{NOx}: 300-780 kg/h GMD:38±10 nm
GULF STREAM	309038000	Tanker and 2 tugs	5.2-7.6	SO_2 NO_x PN	<2 30±15 $(0.2±0.01)\cdot10^{16}$	2.05 70	ER_{NO2}:1.6±2 kg/h ER_{NOx}: 6-15 kg/h

		2 stroke B&W engine		PM1 *BC* *PM05*	NA *0.66±0.64* *0.39±0.36*	 1.300	GMD: 50±6 nm
NORD GAINER	219290000	Tanker 2 stroke Man engine	0-9.6	SO_2 NO_x PN PM1 *BC* *PM05*	<2 25±10 $(0.97±0.2)·10^{16}$ NA *1.25±0.50* *0.78±0.*25	2.05 70 1.300	ER_{NO2}:6±9 kg/h ER_{NOx}: 24-60 kg/h GMD: 29±7 nm
NORD GOODWILL	219011000	Tanker and 1 tug 2 stroke MAN engine	0-0.1	SO_2 NO_x PN PM1 *BC* *PM05*	<2 25±5 $(1.0±0.25)·10^{16}$ NA *1.12±0.51* *0.58±0.*24	2.05 70 1.300	ER_{NO2}:3±2 kg/h ER_{NOx}: 12-30 kg/h GMD: 29±3 nm
TAQAH	538004833	Tanker and 2-4 tugs 2 stroke Wärtsilä engine	0-7.8	SO_2 NO_x PN PM1 *BC* *PM05*	<2 29±4 $(0.25±0.06)·10^{16}$ NA *0.68±0.49* *0.37±0.13*	2.05 70 1.300	ER_{NO2}:9±8 kg/h ER_{NOx}: 35-90 kg/h GMD:42±10 nm
KALAMAS	636014807	Tanker and 2 tugs 2 stroke MAN engine	4.6-6	SO_2 NO_x PN PM1 *BC* *PM05*	<2 49±21 $(0.8±0.9)·10^{16}$ NA *0.70±0.45* *0.94±0.81*	2.05 70 1.300	ER_{NO2}:13±15 kg/h ER_{NOx}: 50-130 kg/h GMD:45±5 nm
MOLLY MANX	235105197	Cargo and pilot boat 2 stroke MAN engine	0-7.8	SO_2 NO_x PN PM1 *BC* *PM05*	<2 39±10 $(0.62±0.47)·10^{16}$ NA *1.4±1.26* *0.77±0.395*	2.05 70 1.300	ER_{NO2}:69±90 kg/h ER_{NOx}: 279-690 kg/h GMD:45±25 nm
CAROLYN DOROTHY	367384780	Tug Towing/waiting/stopped Hybrid propulsion engine powered by 4 stroke Cummins engine	0.2-0.5	SO_2 NO_x PN PM1 *BC* *PM05*	<2 43±9 $(0.5±0.15)·10^{16}$ NA *0.77±0.44* *0.43±0.36*	2.05 70 1.300	ER_{NO2}:13±15 kg/h ER_{NOx}: 50-130 kg/h GMD: 39±12 nm
EVER LEADING	235093619	Cargo & 3 tugs 2 stroke MAN engine	0.6-7.4	SO_2 NO_x PN PM1 *BC* *PM05*	<2 61±2 $(0.8±0.33)·10^{16}$ NA *0.58±0.58* *0.82±0.44*	2.05 70 1.300	*ER_{NO2}:45±61 kg/h* *ER_{NOx}:* 180-450 kg/h GMD:*46±7 nm*
NYK DIANA	372319000	Cargo with partly 3 tugs 2 stroke MAN engine	0-12	SO_2 NO_x PN PM1 *BC* *PM05*	<2 78±24 $(1.25±0.27)·10^{16}$ NA *0.24±0.06* *0.59±0.31*	2.05 70 1.300	*ER_{NO2}:30±20 kg/h* *ER_{NOx}:* 120-300 kg/h GMD: *33±5 nm*
LELA FRANCO *(chase 1)*	367678850	Tug 4 stroke Caterpillar engine	3.5-10.6	SO_2 NO_x PN PM1 *BC* *PM05*	<2 30±7 $(0.50±0.48)·10^{16}$ NA *0.9±0.3* *0.50±0.24*	2.05 70 1.300	*ER_{NO2}:* *1±0.8 [kg/h]* *ER_{NOx}:* 4-10 kg/h GMD: *55±17 nm*
LELA FRANCO *(chase 2)*	367678850	Tug 4 stroke Caterpillar engine	6.4-7.4	SO_2 NO_x PN PM1 *BC*	<2 25±6 $(7.2±1.7)·10^{14}$ *NA* *0.65±0.16*	2.05 70	*ER_{NO2}:3.7±3 kg/h* *ER_{NOx}:* 1537 kg/h GMD: *46±4 nm*

				PM05	*0.39±0.10*	1.300	
VICKI_ANN	367006790	Cargo	5.5 -6.4	SO_2 NO_x PN *BC* *PM05* PM1 PM2.5	<2 23±0.1 (0.50±0.48)·10^{16} *0.53±0.14* *0.36±0.06* *0.43±0.07* *0.6±0.07*	2.05 70 1.300	*ER_{NO2}: NA* *ER_{NOx}: NA* GMD: *66±4 nm*
OOCL LONG BEACH	477316000	Cargo and partly 2 tugs 2 stroke B&W engine	6.4-9.6	SO_2 NO_x PN *BC* *PM05* PM1 PM2.5	<2 55±7 (0.46±0.14)·10^{16} *0.92±0.1* *0.55±0.19* *0.65±0.017* *0.77±0.017*	2.05 70 1.300	*ER_{NO2}:46±31 kg/h* *ER_{NOx}:* 180-460 kg/h GMD: *42±10 nm*
CARNIVAL IMAGINATION	309933000	Passenger 4 stroke Sulzer engine	0-10	SO_2 NO_x PN *BC* *PM05* PM1 PM2.5	<2 41±12 (1.2±2.0)·10^{16} *0.27±0.25* *0.24±0.19* *0.307±0.25* *0.677±0.11*	2.05 70 1.300	*ER_{NO2}:17±28 kg/h* *ER_{NOx}:* 70-170 kg/h GMD: *26±17 nm*
ARTHUR FOSS	366979360	Tug 4 Stroke EMD (Electro-Motive),	5.6-7	SO_2 NO_x PN PM1 *BC* *PM05*	<2 33±14 (0.7±0.27)·10^{16} NA *0.47* *0.83±0.37*	2.05 70 1.300	*ER_{NO2}:NA* *ER_{NOx}:NA* GMD: *44±10 nm*
CHICAGO BRIDGE	352018000	Cargo and 1 tug 2 stroke MAN engine	0.1-10	SO_2 NO_x PN *BC* *PM05* PM1 PM2.5	<2 31±9 (0.50±0.10)·10^{16} *1.7±0.44* *1.0±0.35* *1.2±0.41* *1.3±0.56*	2.05 70 1.300	*ER_{NO2}:43±61 kg/h* *ER_{NOx}:* 170-430 kg/h GMD: *43±8 nm*
STELLAR LILAC	370731000	Tanker and 1 tug 2 stroke MAN engine	8.6-10	SO_2 NO_x PN *BC* *PM05* PM1 PM2.5	<2 60±21 (0.70±0.30)·10^{16} *0.76±0.20* *1.5±0.60* *1.7±0.69* *1.9±1.7*	2.05 70 1.300	*ER_{NO2}:43±61 kg/h* *ER_{NOx}:* 170-430 kg/h GMD: *60±2 nm*
CHEMICAL AQUARIUS	477211400	Tanker and & tug 2 stroke MAN engine	0.1-1	SO_2 NO_x PN PM1 *BC* *PM05*	<2 32±15 (0.36±0.10)·10^{16} *NA* *0.88±0.54* *0.46±0.37*	2.05 70 1.300	*ER_{NO2}:0.7±0.3 kg/h* *ER_{NOx}:* 3-7 kg/h GMD: *70±73 nm*
HYUNDAI NEW YORK	566999000	Cargo partly tug 2 stroke MAN engine	3.8-5.4	SO_2 NO_x PN PM1 *BC* *PM05*	<2 60±7 (0.97±1)·10^{16} *NA* *0.47±0.05* *1.0±0.27*	2.05 70 1.300	*ER_{NO2}:3.8±4 kg/h* *ER_{NOx}:* 15-40 kg/h GMD: *46±4 nm*
HORIZON NAVIGATOR	366792000	Cargo Electric steam turbine Westing-house engine,	5.6-9	SO_2 NO_x PN PM1 *BC,* *PM05*	39±2.7 11.7±5 (1±0.35)·10^{16} NA 0.083±0.044 1.27±0.20	2.05 70 1.300	25±13kg/h

*here we have converted g/kWh to g/kg fuel assuming a SFOC of 200 g/kWh. No speed /load dependence in the PoLA inventory data. ** The measured PM10 and DPM in the environmental reporting are assumed to be the same thing. *** ER of NO_2 is measured and the NO_x is derived assuming that the NO_2/NO_x ratio is 10-25% (Alföldy 2013, Cooper 2003).

4.2 Overall results of ship emissions

In Figure 20 the overall emissions for various species are shown as frequency distributions, i.e. number of measured ship plumes for different ship categories binned into different emission intervals. In Table 3 the statistics for the same data is shown. The data corresponds to emission plumes that come from both single vessels and vessels accompanied by tugs (multiple). For multiple ships the indicated ship type corresponds to the largest ship that contributed to the plume. Since the measurements were conducted mostly inside the harbor area, most plumes of cargo and tanker vessels were measured either when these vessels were moving together with tugs or were anchored or moored respectively. The presented results for harbor crafts correspond mostly to plumes from single ships. The measurements of passenger ships are dominated by the repeated measurements of the mooring cruise ship Carnival Imagination when it was preparing to leave. In appendix 2 the corresponding plots for plumes only from single vessels is shown, having a similar appearance as the one in Figure 20.

The observed emission factors of PM05 is mainly distributed between 0.1 and 0.8 g/kg$_{fuel}$ (median 0.43 g/kg$_{fuel}$) for all types of ships, with a tendency of cargo and tanker vessels to the upper end and passenger vessels and harbor craft on the lower end. For PM1 and PM2.5, obtained by combining the EEPS and OPS data for part of the measurement days, the corresponding median values are 0.46 and 0.61 g/kg$_{fuel}$, respectively and the variability is within a factor of 2. The particle emissions can be compared to the emission inventory results (PoLA 2014) of 1.3 g/kg$_{fuel.}$ It hence appears that the particle emissions are somewhat low when comparing to the median values; on the other hand when comparing to the average value there is better agreement with measurement and inventory.
The mass of the emitted BC is mostly below 0.8 g/kg$_{fuel}$ for all types (median 0.43 g/kg$_{fuel}$). A peak in the distributions can be found between 0.2 and 0.3 g/kg$_{fuel}$. It hence appears that BC corresponds to 70% of the particles, see discussion in section 4.1 w.r.t. the chase studies.
While the distributions for particle masses for particles below 560 nm and BC indicate clear peaks, this cannot be seen from the distribution of the particle numbers measured with a CPC from 5 nm to 1 µm. Particle number, in contrast to particulate mass, is on the other hand not a conserved number since particles coagulate downwind the plume. The observed emission factor of PN was mostly below $1.2 \cdot 10^{16}$particles/kg$_{fuel}$ (median $0.47 \cdot 10^{16}$particles/kg$_{fuel}$). A clear tendency can be seen for harbor craft toward lower emissions below $0.6 \cdot 10^{16}$ particles/kg$_{fuel}$ and cargo vessels toward higher emissions above $0.4 \cdot 10^{16}$particles/kg$_{fuel}$.
The NO_x emission factors vary between 15 and 90 g/kg$_{fuel}$ (median 36 g/kg$_{fuel}$) There is a clear tendency for harbor craft and tanker vessels towards lower emissions, both peaking around 25 g/kg$_{fuel}$. The emission of NO_x of cargo vessels on the other hand seems to be more evenly spread above 30 g/kg$_{fuel}$. The NO_x emissions can be compared to the emission inventory results (PoLA 2014) of 70 g/kg$_{fuel}$-

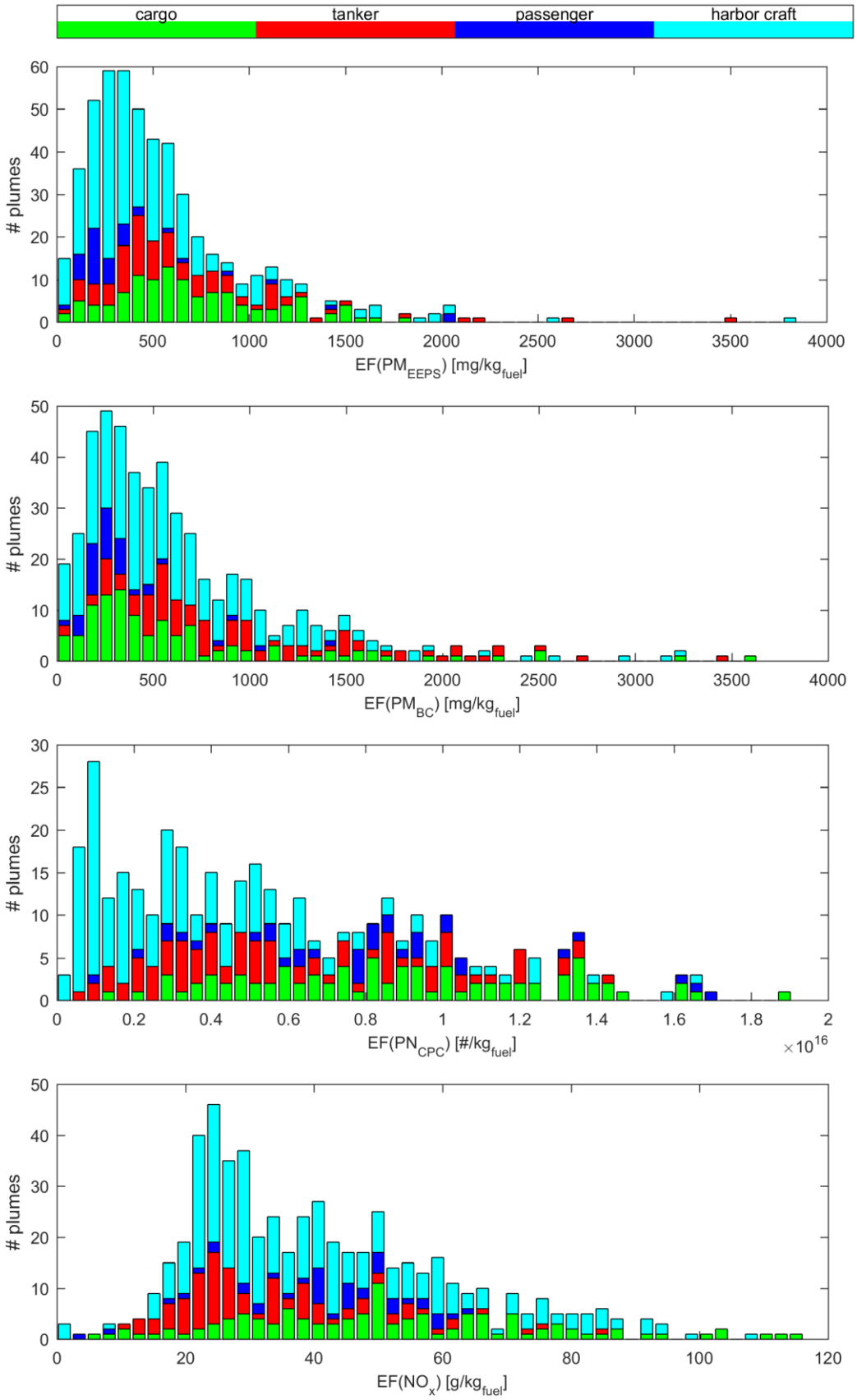

Figure 20. Frequency distributions for particulate matter and NO_x emissions from all measurements. The results for particulate matter are shown as particulate mass between 5.6 to 560 nm, as measured by EEPS, and BC and particle number between 5 nm to 1 µm, as measured by CPC. The colors indicate the main ship types.

Table 3. The measurement data were obtained assuming a specific fuel oil consumption of 0.2 kg_{fuel}/kWh. The emission inventory corresponds to the official 2014 emission inventory by PoLA and PoLB. The data corresponds to a 50/50 mixture of low and medium speed diesel ships following the Tier 1 standard (1999-2011) and load dependence has been neglected.

Parameter	**Unit**	Average	Standard deviation	**Median**	**25th percent**	**75th percentile**	**Emission inventory**
EF_{NOx}	g/kg_{fuel}	40.5	20.8	36.3	24.9	52.6	70
EF_{SO2}	g/kg_{fuel}	0.25	3	**0**	-0.23	0.16	2
$EF_{PN(5-1000\ nm)}$	$10^{16}/kg_{fuel}$	0.6	0.67	0.47	0.23	0.86	
$EF_{BC(5-1000\ nm)}$	g/kg_{fuel}	0.75	1.305	0.49	0.25	0.89	
$EF_{PM(5.6-560\ nm)}$	g/kg_{fuel}	0.575	0.84	0.42	0.23	0.68	
***EF*$_{PM1}$ ***	**g/kg_{fuel}**	**0.65**		**0.46**	**0.25**	**0.76**	1.3
EF*$_{PM2.5}$	**g/kg_{fuel}**	**1.04**		**0.61**	**0.31**	**1,21**	

* Only part of the data was used for PM1 and PM2.5. The data was obtained by combining EEPS and OPS data.

4.3 Emissions versus load/speed

4.3.1 Overall and separated by ship type

In this section we show the emission data as a function of ship speed, in a similar manner as for the chase studies in section 4.1 but for the whole data set, instead of individual ships. Measurements from both the fixed and mobile measurements are included here. The emission factors of PM05, PN and NO_x are shown in Figure 21 to Figure 24, binned by the ship speed. In Figure 25 the emission rate of NO_2, is shown. Ships with a speed of less than 0.11 knots are assumed to be parked and these emissions are therefore binned separately. The figures are separated in three parts: the upper part show emission results of all ships with average median and 25^{th} and 75^{th} percentile value, the middle part shows the same data but separated into each ship category shown in different colors, averages (full line) and the lower part shows data only for plumes corresponding to single ships separated into different ship categories.
In Figure 21 the statistics of the observed emission factors of PM05 for fine and ultrafine particles are shown. The upper graph shows that parked ships have a median emission factor of 300 mg/kg_{fuel}. When the ships run at speeds between 2 and 4 knots the median emission factor increases to 600 mg/kg_{fuel}, probably during intensive maneuvering phase and then it decreases to 400 mg/kg_{fuel} when the ships are running at steady state of 6 to 8 knots. Most of the observed PM05 emission factors (25^{th} to 75^{th} percentile) vary within a factor of 2.
The observed emission factors of BC, Figure 22, show a similar pattern as for PM05, with increasing values for speeds between 0 and 4 knots which then decrease. Here in particular the 75^{th} percentile shows a distinct maximum at speeds between 2 to 4 knots, i.e. during maneuvering phase.
The observed emission factors of particulate number in Figure 23 are rather constant for ships running at speeds up to 6 knots and then they decrease by approximately a factor of 2. However, as discussed in the previous section, the particulate number is not necessarily conserved, since particles may coagulate in the plume and the lower emission factors for higher speeds may be caused by somewhat longer observational distance to the ships. The plot in Figure 23 is strongly influenced by harbor craft. But as vessels of this kind stand for the vessel major traffic in the PoLA and PoLB, this plot is representative for the emissions in the harbor.
The statistics of the emission factors of NO_x versus ship speeds is shown in Figure 24. The median emission from parked ships is around 28 g/kg_{fuel}. The emission factor increases to about 45 g/kg_{fuel} at 6 knots and then it decreases to 35 g/kg_{fuel} for higher speeds.
In Figure 25 the overall NO_2 emission measurements using zenith sky DOAS are shown. As already discussed in the chase section the total NO_2 emission should increase with speed but since the ship and accompanying tugs are maneuvering and since we are measuring NO_2 and not NO_x the emission pattern gets more complicated. Our interpretation is that the peak in NO_2 emissions at low speeds is caused by strong maneuvering of the tugs.

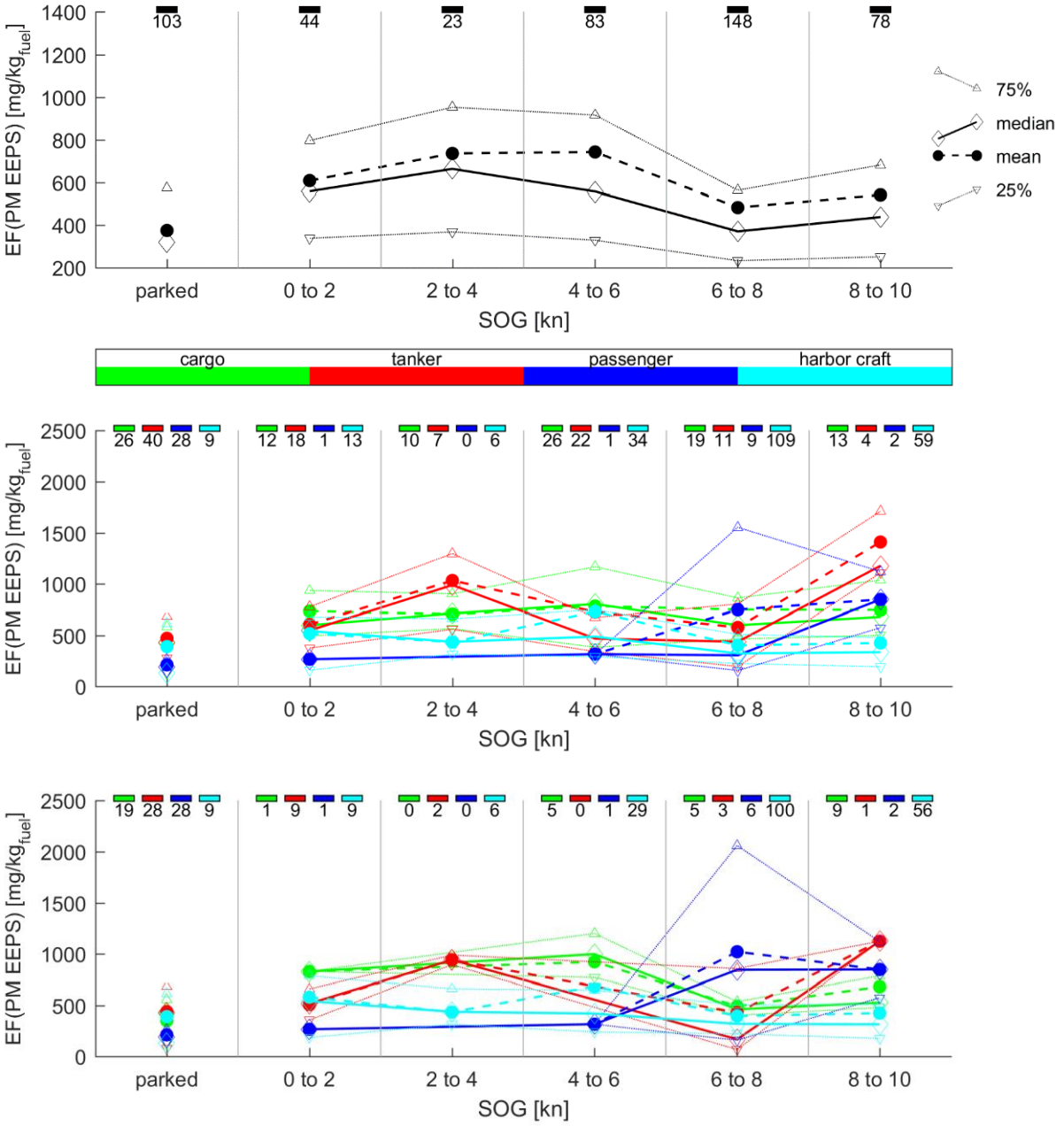

Figure 21. Emission of particulate mass for particles between 5.6 and 560 nm over vessel speed, i.e. load. In the upper plot, the emission of all types is shown for all plume measurements. The same is shown separated by the type of main contributing ship in the middle plot. In the lower plot, only plumes that can be connected to a single contributing vessel are accounted for.

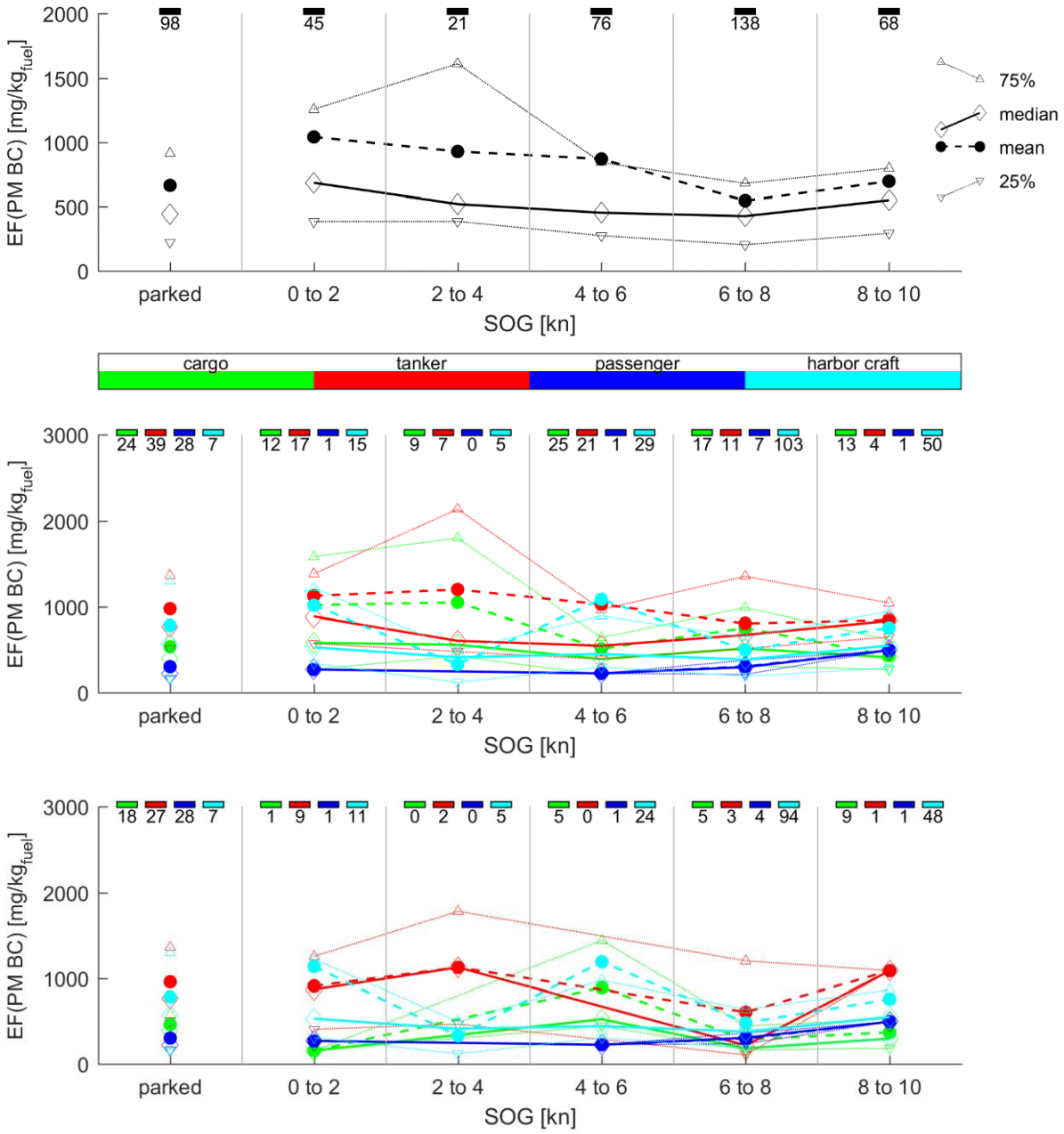

Figure 22. Emission of particulate mass for BC particles over vessel speed, i.e. load. In the upper plot, the emission of all types is shown for all plume measurements. The same is shown separated by the type of main contributing ship in the middle plot. In the lower plot, only plumes that can be connected to a single contributing vessel are accounted for.

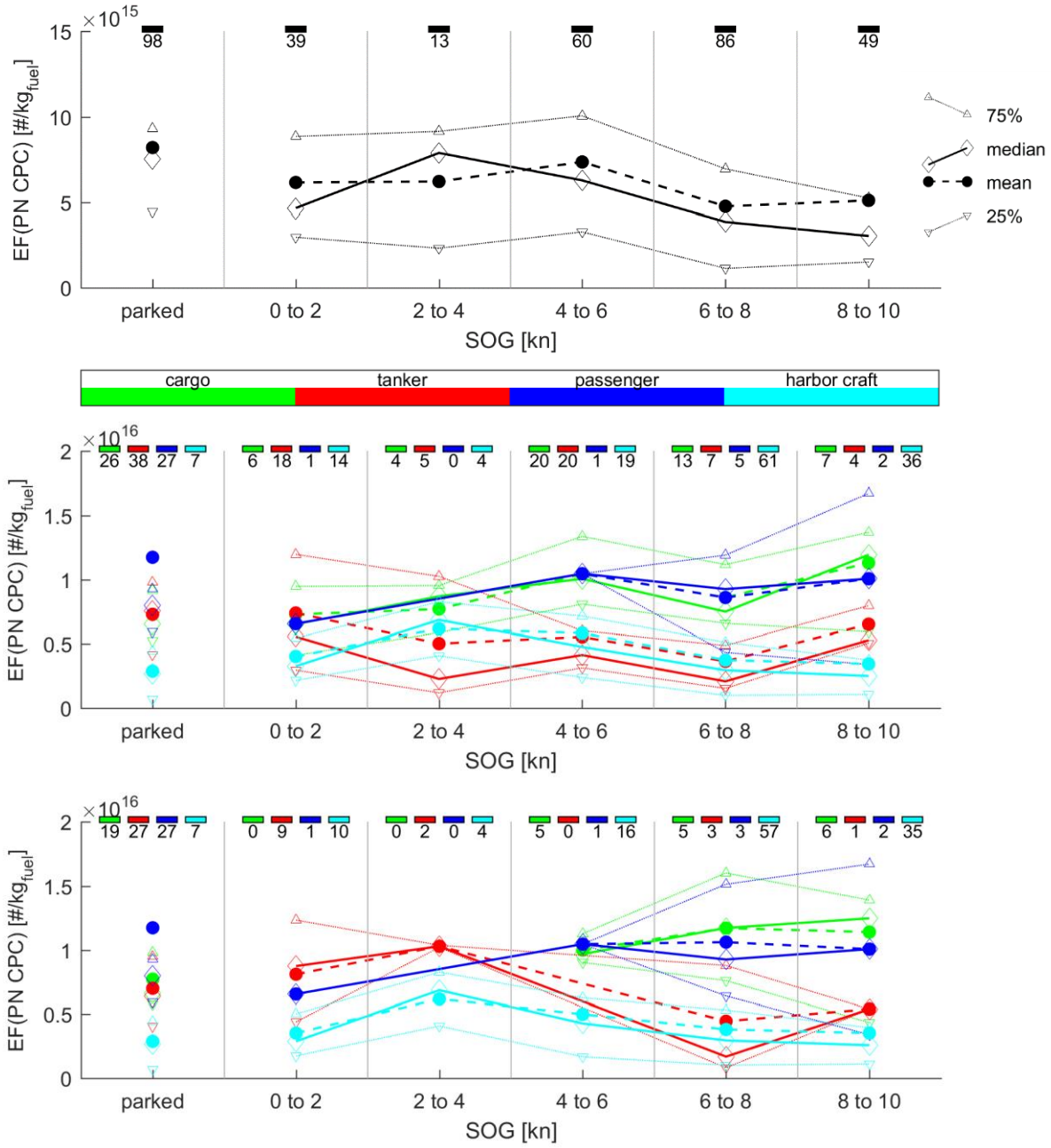

Figure 23. Emission of particulate number for particles between 5 nm and 1 µm over vessel speed, i.e. load. In the upper plot, the emission of all types is shown for all plume measurements. The same is shown separated by the type of main contributing ship in the middle plot. In the lower plot, only plumes that can be connected to a single contributing vessel are accounted for.

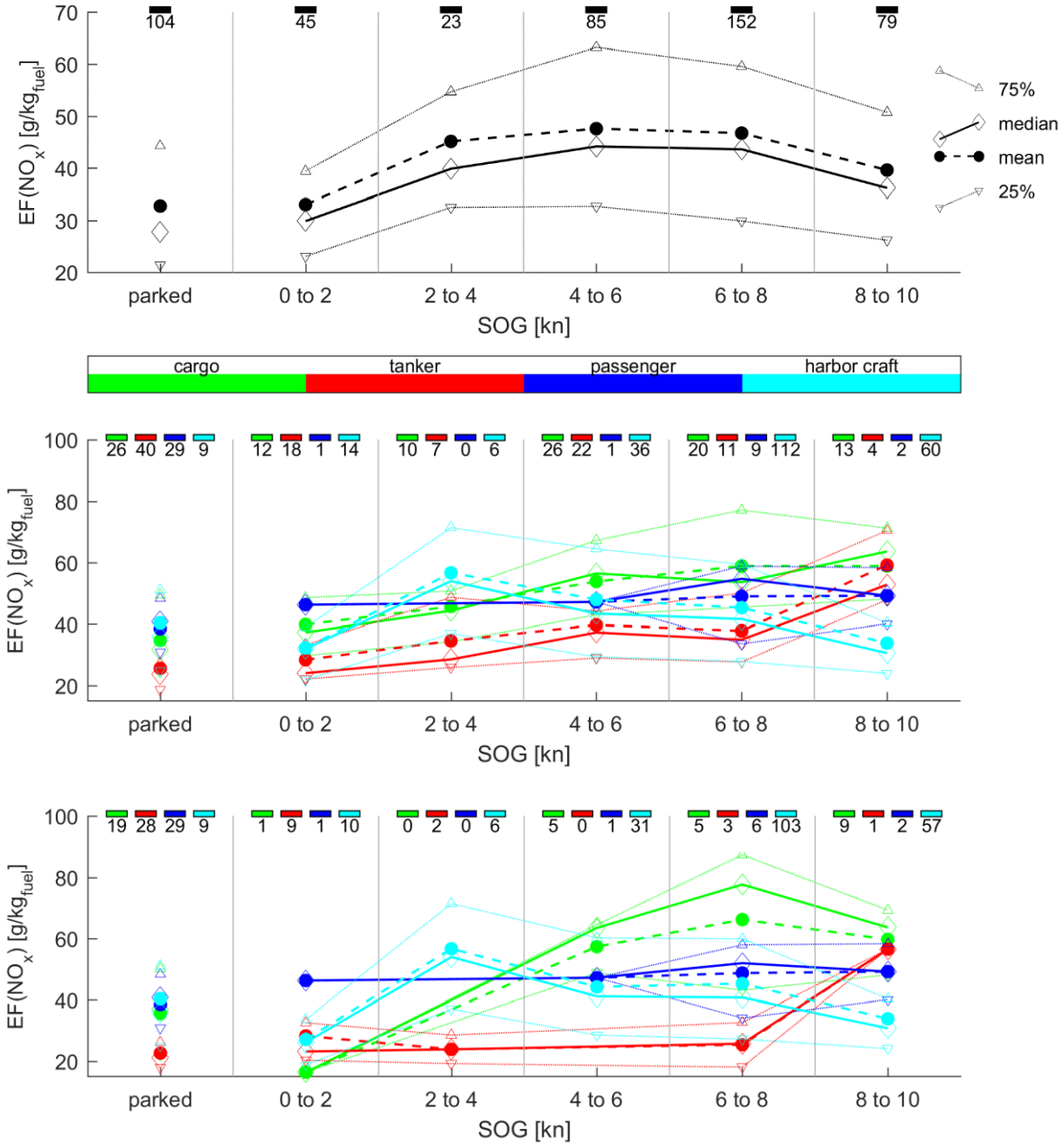

Figure 24. Emission of NO_x over vessel speed, i.e. load. In the upper plot, the emission of all types is shown for all plume measurements. The same is shown separated by the type of main contributing ship in the middle plot. In the lower plot, only plumes that can be connected to a single contributing vessel are accounted for.

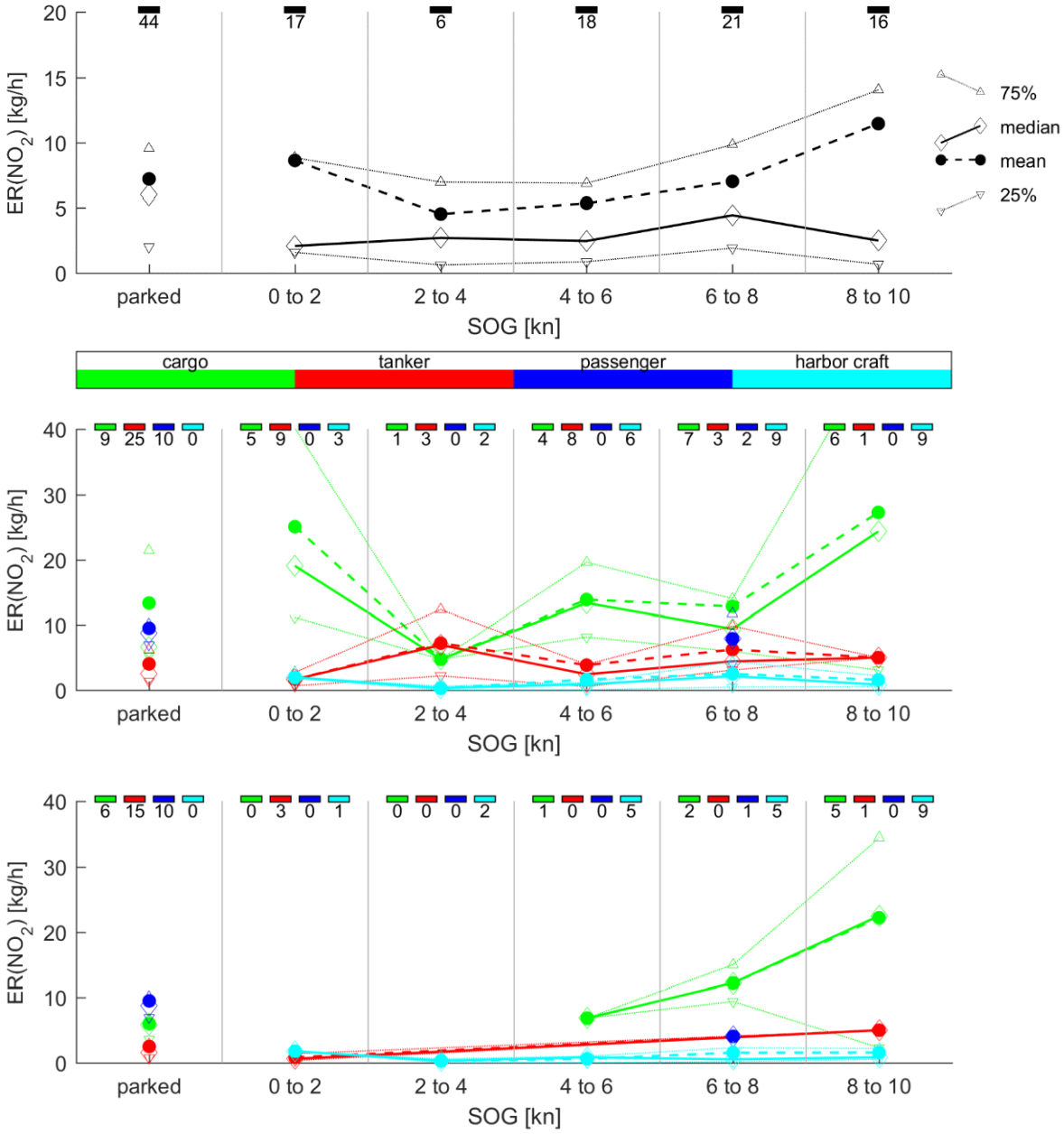

Figure 25. Emission of NO_2 over vessel speed, i.e. load. In the upper plot, the emission of all types is shown for all plume measurements. The same is shown separated by the type of main contributing ship in the middle plot. In the lower plot, only plumes that can be connected to a single contributing vessel are accounted for.

4.3.2 Multiple measurements of specific ships

The pilot boats VEGA and POLARIS were measured frequently at variable speeds between 5 to 25 knots. The results for BC, particle number for sizes between 5.6 and 560 nm, and NO_x is presented in Figure 26 and Figure 27. While for speeds below 10 knots a significant trend can barely be recognized, the emission factors indicate increasing values for BC mass in both cases by about a factor of 2 for speeds between 20 and 25 knots. A contrary behavior can be seen for the number of fine and ultrafine particles and also NO_x in the case of pilot boat VEGA, Figure 26 which decrease by about the same factor.

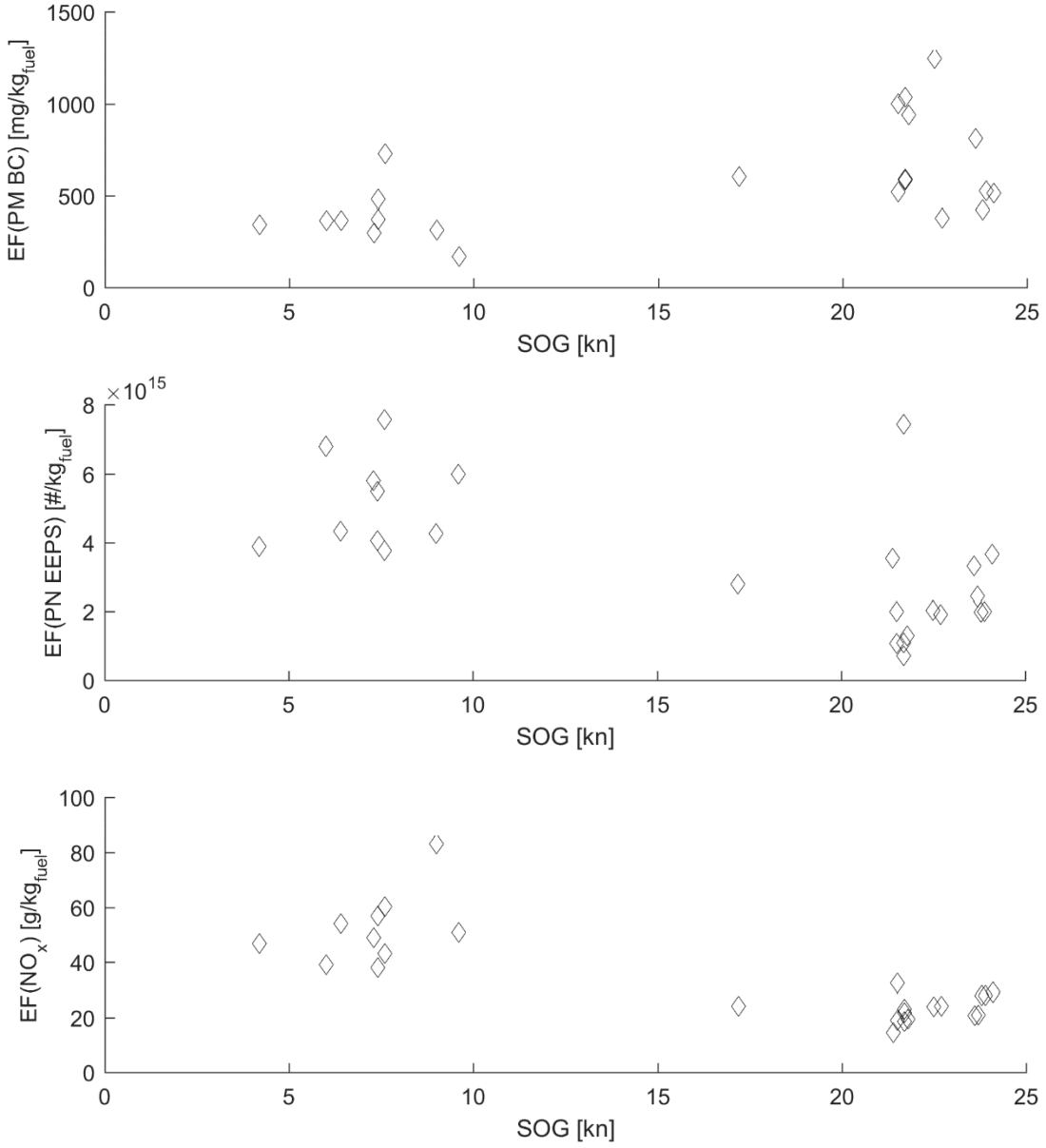

Figure 26. Emissions of BC, particle number between 5.6 and 560 nm, and NO_x from pilot boat VEGA at different speeds and occasions.

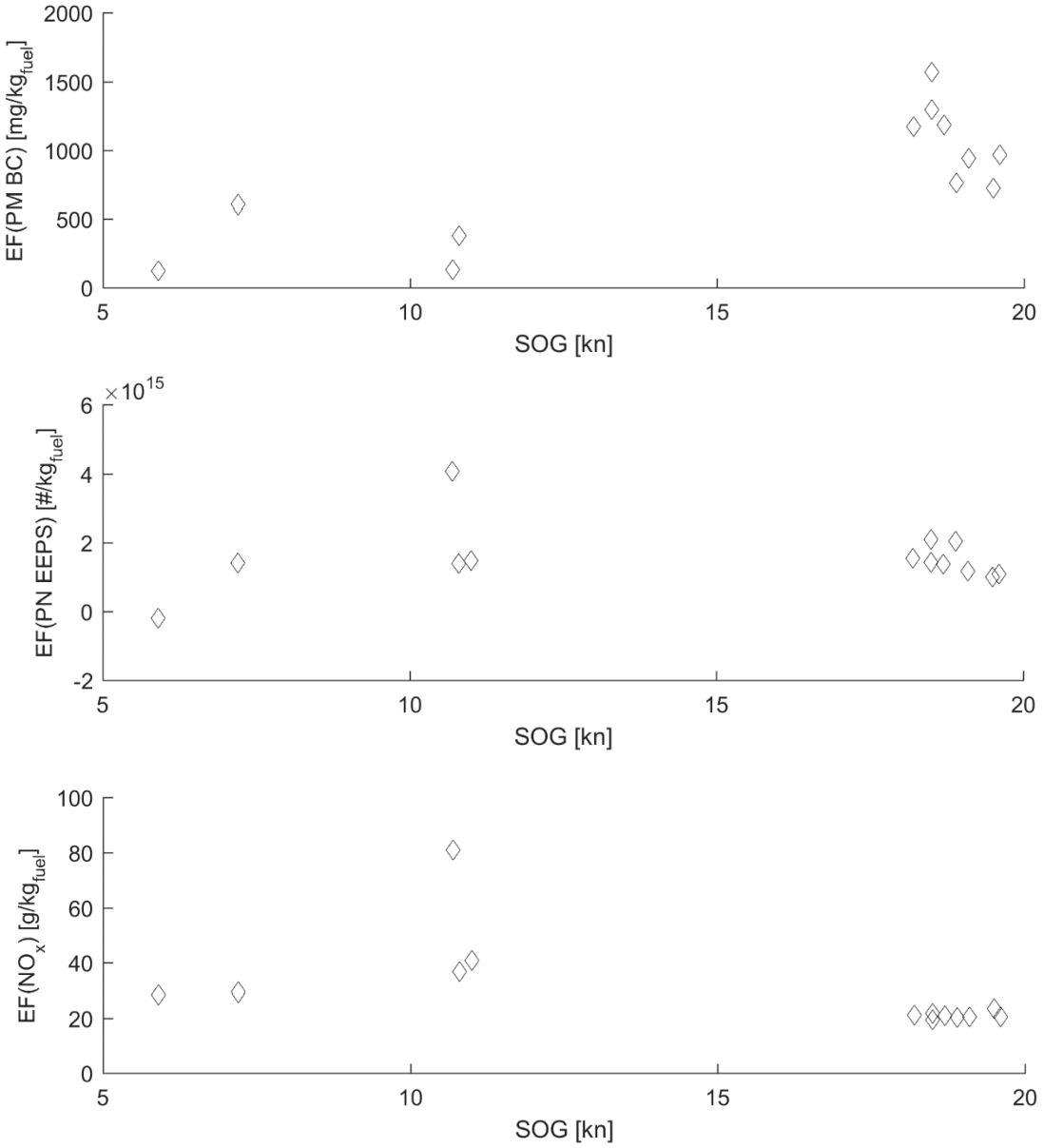

Figure 27. Emissions of BC, particle number between 5.6 and 560 nm, and NO_x from pilot boat POLARIS at different speeds and occasions.

4.4 Compliance monitoring of fuel sulfur content

In Figure 28 and Figure 29 the time series during the campaign of FSC measurements is shown for 571 emission plumes corresponding to 132 individual ships. A zoomed in version of the data is shown in Figure 29. Eight measurements, out of the 571 plumes, corresponding to 4 individual ships were above the FSC limit; this corresponds to a compliance rate of at least 98.5 %. The average FSC and standard deviation, excluding the 8 highest points, is (-0.002±0.017) %, and we believe that this standard deviation mainly reflects the noise in the data.
The compliance rate with regard to the new IMO MARPOL Annex VI rules requiring the usage of fuel with a maximum of 0.1 % FSC was hence very good during the campaign and it appears that the CARB regulation, being in place since 2008, has been rather effective.
The high values on 16 October and 29 October correspond to the same ship, i.e. Horizon Navigator, Figure 30. On the first occasion the ship was measured from the research vessel, while on the second one it was measured automatically at the fixed site PoLA_2. The fact that the measurement system can target the same ship twice as a gross polluter is a nice illustration of the system's suitability for automatic compliance monitoring.
Data from the measurements on 16 October is shown Figure 31. Here the SO_2 concentration (in ppb) is 6 times higher than the one of CO_2 (in ppm), thus indicating a ship with more than 1.5 % FSC according to Eq. 1. The Horizon Navigator is a cargo carrier with a turbo electric steam turbine engine for its main propulsion and apparently it is exempt from the regulation (*personal comm., A. Barber, CARB, April 2015*).
One potential problem with the performed SO_2 measurements during this campaign is the fact that a PM10 sampler made of aluminum was used as a combined particle and gas inlet, Figure 32. We have recently found out that similar inlets may cause underestimation in measured SO_2 concentrations presumably due to wall effects; consequently this may have caused a negative bias in the derived FSC level of the sampled ships, especially for ships running with intermediate levels of FSC (0.3 - 0.5 %).

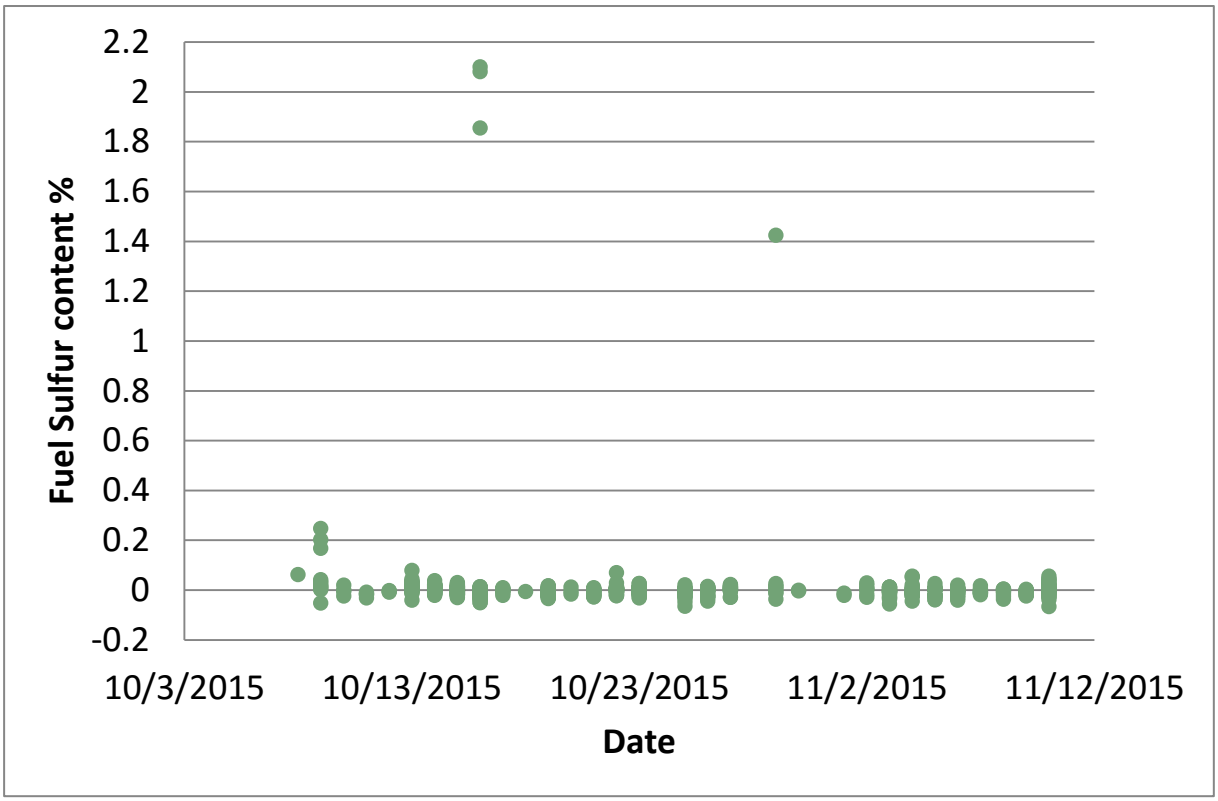

Figure 28. The FSCof ships measured during the campaign. Many of these measurements were carried out through automatic operation of the instruments at fixed sites

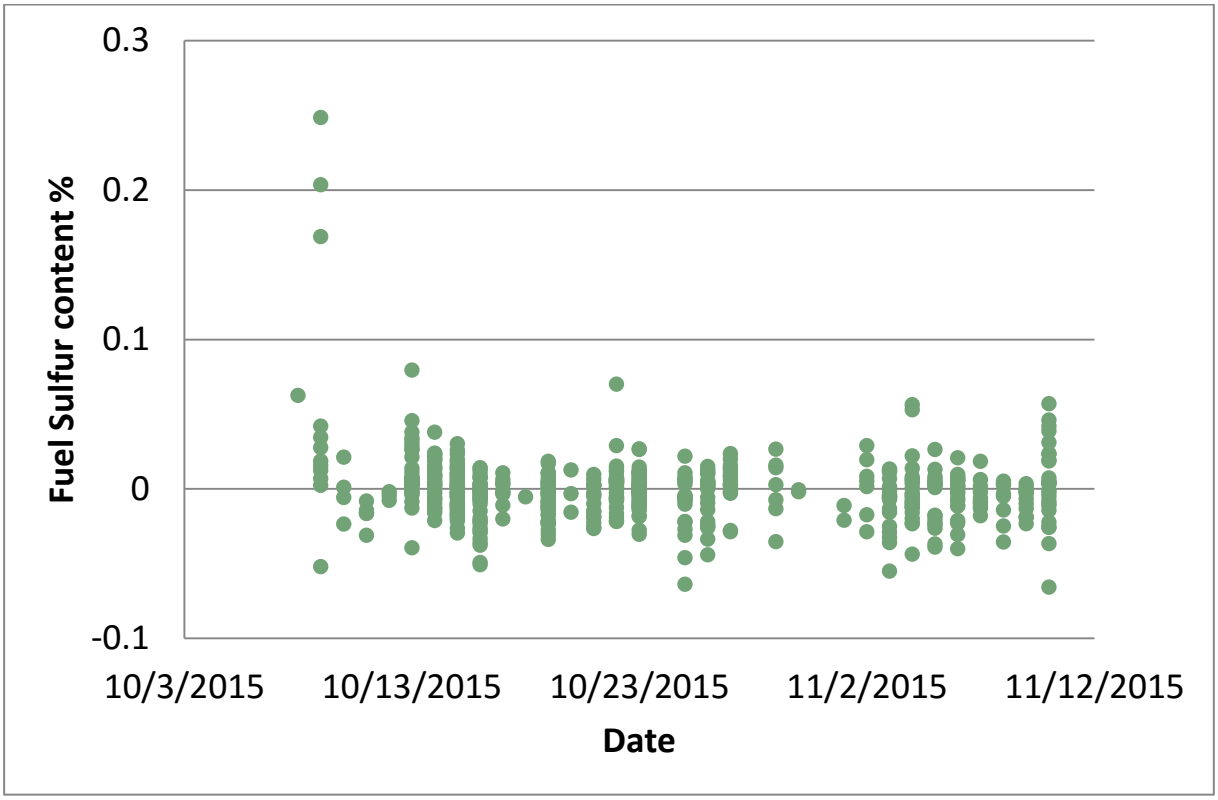

Figure 29. The FSC of ships measured during the campaign (zoomed in). Many of these measurements were carried out through automatic operation of the instruments at fixed sites.

Figure 30. HORIZON NAVIGATOR, showing a FSC of about 2 %.

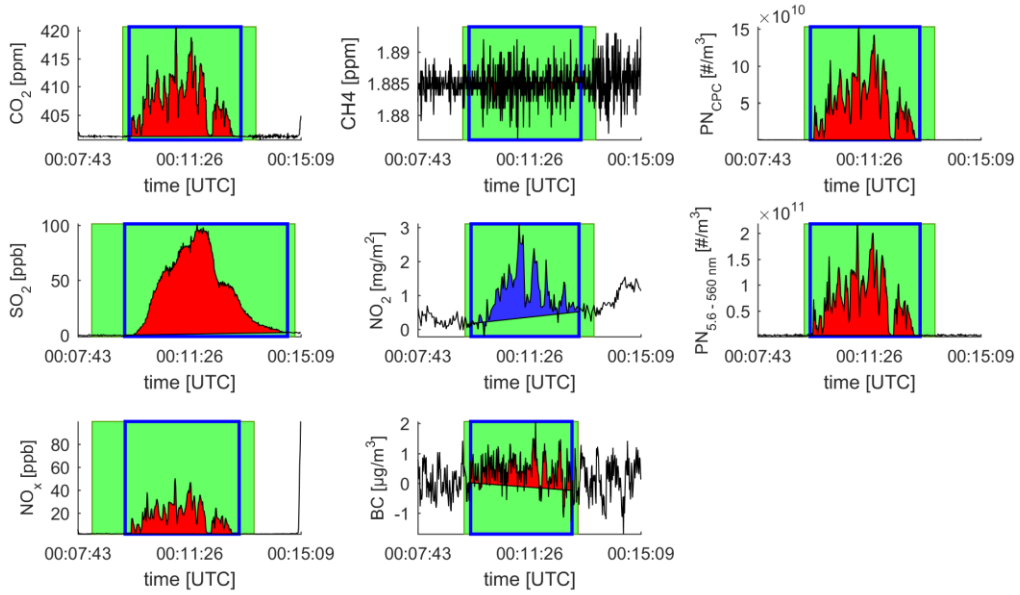

Figure 31. The measured data for the HORIZON NAVIGATOR on 16 October 2015 at 00:09 UTC, corresponding to 2 % FSC. Red shaded area: excess contribution of species due to emission for calculation of emission factor; blue shaded area: excess contribution due to emission of NO_2 measured by DOAS for calculation of emission rate; green shaded area inside blue frame: values accounted as plume; green shaded area outside blue frame: values accounted for baseline retrieval.

Figure 32. The PM 10 inlet used for gas and particulate sampling. The inlet is made of aluminium and it has been found out later that some of the SO_2 might be adsorbed on its surface.

4.5 Offshore alkene measurements of Fuel Islands and Fuel Barges

VOC emissions from seven different offshore sites and events were observed during the survey. The measurements were carried out with the Solar Occultation Flux method, which is an optical remote sensing technique based on mobile solar infrared measurements (Mellqvist 2010b). This method is described in a parallel report, see Mellqvist (2016c). The alkane emissions varied from 4 kg/h (Fuel Island Grissom) to 27 kg/h (ship venting), as seen in Table 4. In total, 69 kg/h were observed from these sources based on 21 measurements.

Table 4. Summary of offshore alkane SOF-measurements.

Source Offshore	Day [yymmdd]	Timespan (Local Time) [hhmmss-hhmmss]	No. of Meas	Emission Average±SD [kg/h]	Wind Speed Min-Max [m/s]	Wind Dir Min-Max [deg]
Fuel Island White	151013	131421 -132323	2	6.7±2.0	2.3-3.3	218-224
Fuel Island White	151015*	143335 -143511	1	4.5	4.0	232
Fuel Island Freeman	151013*	125038 -125311	1	8.6	3.3	187
Fuel Island Freeman	151015*	142832 -143049	1	7.9	5.4	232
Fuel Island Chaffee	151013*	130322 -130526	1	6.9	1.7	221
Fuel Island Chaffee	151015*	141358 -141609	1	16	5.6	239
Fuel Island Grissom	151015*	144825 -145121	1	4.0	3.4	222
Fuel Barges Port LA	151015	132908 -134256	2	8.1±6.7	4.5-6.6	204-244
Fuel Barges Port LA	151026	122818 -161745	4	5.8±3.3	2.7-5.5	243-345
Ship Venting	151026	121948 -122550	2	27±1.2	5.7-6.3	213-229
Ship Fueling	151026	131407 -161745	4	5.2±2.8	2.7-5.1	213-345

4.6 Optical Airborne Flux measurements of NO_x from harbor and the industrial area

Airborne optical measurements of NO_2 which were conducted in a box pattern around the port area are shown in Figure 33 with the color of the flight track indicating the measured slant columns (path integrated concentration). The flights were conducted in clockwise direction on November 8, between 1:45 PM to 2:03 PM local time. The median wind was 4.2 m/s from 210 degrees obtained from measurements at the Command and Control Center of the Port of Long Beach. Two box measurements were carried out with the aircraft, with very similar measured slant columns.

In Figure 34 the corresponding derived gas flux from the data in Figure 33 is shown. The net fluxes for the industrial area (area 1) and the port area (area 2) are 733 kg/h and 311 kg/h, respectively. In a parallel project (Mellqvist, 2016b) it was found that 154 kg/h of NO_2 were emitted from industrial activity in area 1 and 35 kg/h in area 2 (port area). The rest of the emissions are probably due to mobile sources in area 1 (i.e. 579 kg/h) and both mobile and shipping sources in area 2 (i.e. 276 kg/h). Studies in Texas show that the NO_2/NO_x ratio is typically 80 % at steady state conditions (Rivera, 2010). If one assumes this is the case also in California the port activities at PoLA and PoLB hence emit 345 kg/h of NO_x.

This can be compared to the average NO_x emissions values reported by the two port authorities (PoLA 2014; PoLB 2014) of 1772 kg/h for all sources in the South Coast air basin and 628 kg/h for all sources but with transit of ocean going vessels removed. The latter includes harbor craft, cargo handling, locomotives, heavy duty vehicles and OGVs in maneuvering and hoteling mode.

The measured emissions from area 2 include much less emissions from ocean going vessels than in the port inventories since the latter includes pollution from ships up to 60 nautical miles away from shore. Since the measurements were performed on a Sunday the work activity in the harbor were apparently lower than on normal working days and there was also fewer ships moving and entering the harbor. According to the AIS data there were 23 cargo ships, 7 tankers and 2 cruise ships in the harbor and only two of them were moving with 1.5 knots. In addition there were 41 harbor craft, and out them 8 tugs and two smaller express ferries were in movement. See Table 5 for activity during the different days.

In summary, the emissions of 345 kg/h of NO_x that were estimated from the harbor areas were considerably smaller than the estimated amount of 628 kg/h in the port inventories when excluding the transit emissions of ocean going vessels. This may be due to lower general activity in the harbor area.

Table 5. The ships within the PoLA and PoLB during the time of airborne measurements on Sunday, 8 November and other weekdays at the same daytime period. The numbers in parentheses shows ships that were moving faster than 0.3 m/s.

	cargo	**tanker**	**passenger**	**harbor craft**
Mo Nov 2	23(1)	5(2)	0(0)	52(12)
Tue Nov 3	18(3)	9(3)	0(0)	51(12)
Wed Nov 4	18(3)	9(0)	0(0)	50(18)
Thu Nov 5	19(1)	9(0)	0(0)	52(13)
Fri Nov 6	28(1)	8(0)	0(0)	54(0)
Sun Nov 8	23(1)	7(1)	2(0)	46(11)

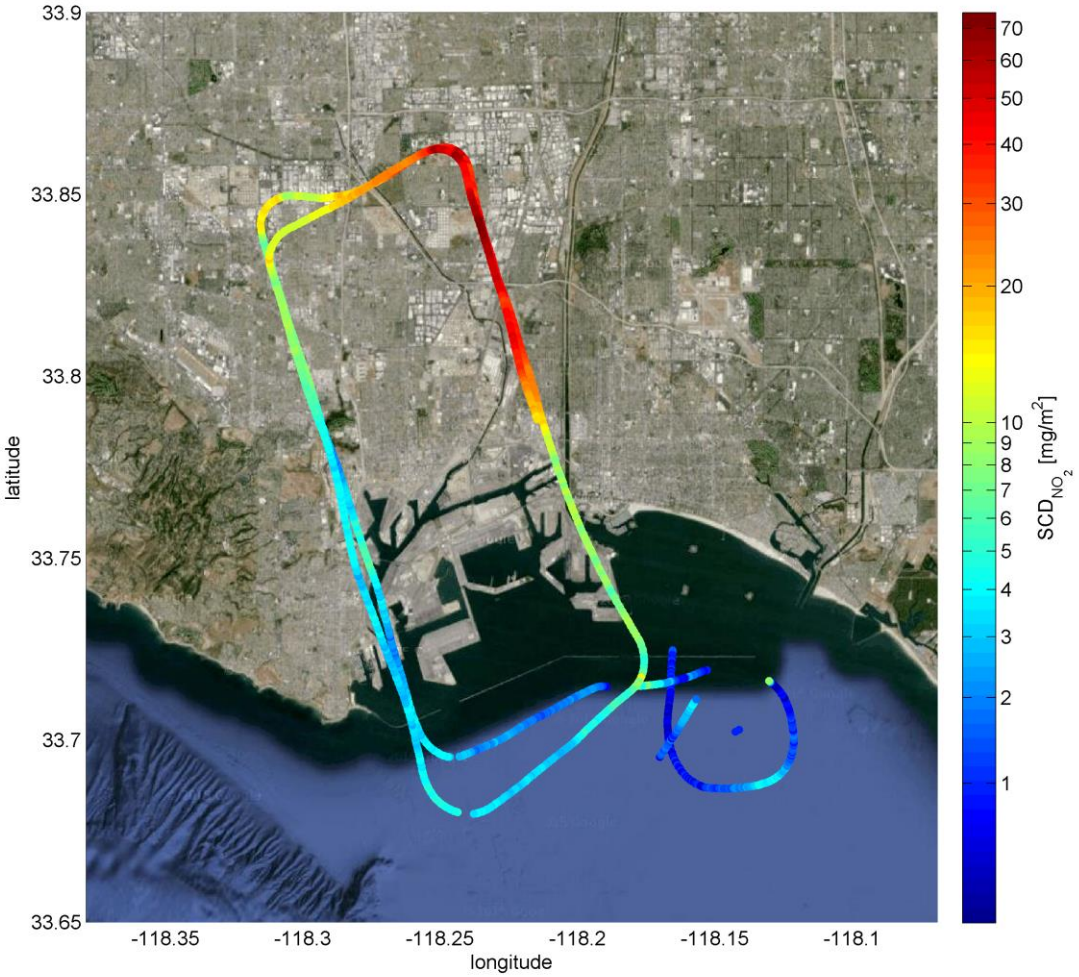

Figure 33. Slant column measurements of NO_2 obtained by optical airborne measurements.

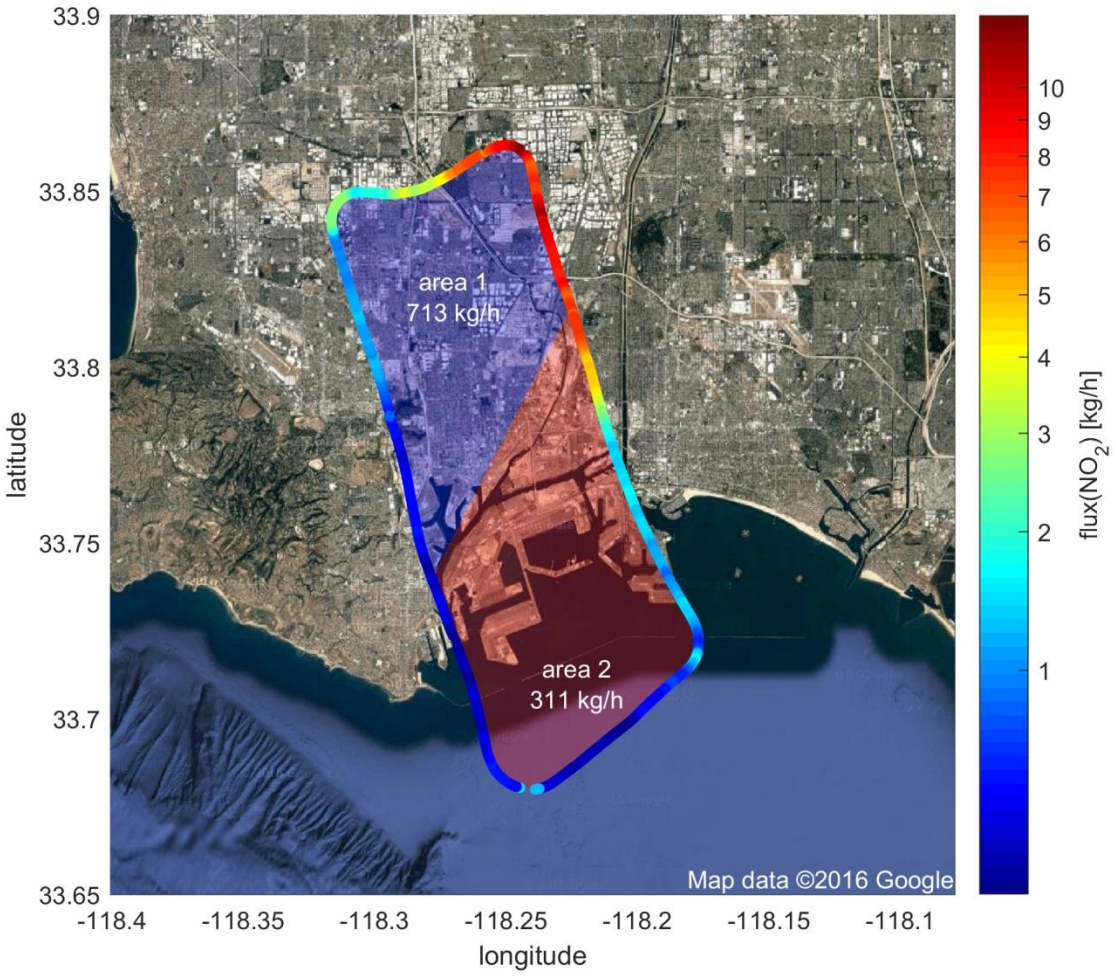

Figure 34. Map showing the flight track during one full circle of the box pattern flight on 8 November, conducted between 1:45 PM to 2:03 PM. The color of the flight track indicates the measured flux. The net fluxes for the industrial area and the port area are 713 kg/h and 311 kg/h, respectively.

5 Discussion

In Table 6 the emission factor data found in this study, given as median values and 25th and 75th percentile values, are compared to other measurement studies carried out close to harbors or ship channels. For NO_x it can be observed that the median emission factor of 36.4 g/kg_{fuel} (average 40.5 g/kg_{fuel}) appear to be smaller than emission factors measured in other studies. One reason for this is the fact that in the present study most measurements correspond to ships that were maneuvering inside or in the vicinity of the harbor (transient combustion conditions), while in the comparative studies the ships were moving at more constant and higher speed. The difference in NO_x emission between the various studies is consistent with the general findings in this study that the emission factors increase with speed, e.g. Figure 18 and Figure 24. In addition, when comparing the measured data against inventories, the measured emission factors are considerably lower than the inventory data (70 g/kg_{fuel}) and they have opposite load dependence. It hence seems that the NO_x emission from the harbors of SCAB is over-predicted in the inventories. This is consistent with the results of the airborne remote sensing measurements in section 4.6 showing 50 % less NO_x emission than the inventory one. The emission factor of SO_2 between the different studies in Table 6 reflects the difference in the FSC of the ships. The currently allowed sulfur content in the harbor areas of PoLA and PoLB is 0.1 % which corresponds to an emission factor of SO_2 of 2 g/kg_{fuel}.

Table 6. Emission factor data from this study compared to several other studies in ship channels and harbors.

Reference (platform)	**EF(NO_x) g/kg_{fuel}**	**EF(SO_2) g/kg_{fuel}**	**EF(PM) g/kg_{fuel}**	**EF(BC) g/kg_{fuel}**	**EF(PN) $10^{16}/kg_{fuel}$**	**No of Plumes / Ships**	**Location (Year)**
This study median (25^{th}|75^{th} percentile)	**36.3** (24.9|52.6)	**0** (-0.23|0.16)	**PM05**: 0.42 (0.23|0.68) **PM1**:0.46 (0.25|0.76) **PM2.5**: 0.61 (0.31|1.21)	**0.49** (0.25|0.89)	**0.47** (0.23|0.86)	574/137	SCAB harbors (2015)
Lack (2008)				0.85 ± 0.76		100/96	Gulf of Mexico
Williams (2009) (ship-borne)	66.4 ± 9.1	13.2 ± 10.4				>200/--	Near harbor (2006)
Jonsson (2011) (land-based)			2.05 ± 0.11[a]		2.55 ± 0.11[a]	734/--	Harbor (2010)
Alföldy (2013) (land-based)	53.7	6[e] 14 … 18[f]			0.8[e] 1.8[f]	497/--	Harbor (2009)
Pirjola (2013) (land-based)	25 - 100	2.5 … 17	1.0 … 4.9[c]		0.32 … 2.26[d]	11/--	Harbor & Ship channel (2010/2011)
Beecken (2014) (airborne)	66.6 ± 23.4	18.8 ± 6.5	2.8 ± 1.6[a]		1.8 ± 1.3[a]	--/174	Open sea (2011/2012)
Beecken (2015b) (ship- & airborne)	57.7 ± 20.9	11.6 ± 7.3	1.72 ± 1.66[d]		1.6 ± 0.8[a]	466/311	Ship channel to Sankt Petersburg (Neva Bay) (2011/2012)

[a] for particulate matter between 5 and 560 nm (results from EEPS only)
[b] for particulate matter up to 1 µm (combined results from EEPS and OPS)
[c] for particulate matter up to 2.5 µm
[d] for particulate matter up to 10 µm (combined results from EEPS and OPS)
[e] distillate fuel

[f] residual oil

For particulate mass (PM2.5) the observed emission factor with median value 0.61 g/kg_{fuel} (average 1.04 g/kg_{fuel}) is lower than results from earlier studies. Part of the reason may be that the ships in the previous studies were running on higher FSC (1 %) than in the present study (0.1 %). This is consistent with experimental studies (Winnes and Fridell, 2012) showing a correlation between FSC and particle emission. The PM2.5 emission factors can be compared to the port inventory values of 1.3 g/kg_{fuel} and they appear to be on the low side; on the other hand given the measurements uncertainty the emission values agreement is reasonably good. As discussed in section 2.2 it is difficult to obtain the mass of particles using the measured number size distribution due to the fact that uncertain assumptions about geometry and composition has to be made which in turn causes uncertainties in the estimated emissions.

The emission factor for BC corresponds to a median value of 0.49 (0.75 g/kg_{fuel}). A large fraction of the measured PM2.5 mass hence appears to consist of soot. There exists relatively few measurement studies on emission factors of BC from shipping but as can be seen in Table 6 the obtained BC emission factor is comparable to measurements by Lack (2008) conducted in the Gulf of Mexico.

There appears to be an increased variability when vessels that are maneuvering together with tugs at lower speeds below 4 knots. Lack and Corbett (2012) also describe higher BC emissions for engines on low load, which would be the case for the main ship that is being tugged.
The obtained emission factors for particle numbers have a median value of $0.47 \cdot 10^{16}$ particles/kg_{fuel} (average $0.6 \cdot 10^{16}$ particles/kg_{fuel}) and this is in the order of those found by Alföldy (2013) and Pirjola (2013) for measurements in harbor areas. This may indicate that the difference of fuel type has small influence on the number of the emitted particles as compared to the mass of the emitted particles. This is in accordance to the findings of Winnes and Fridell (2012). However, the obtained emission factors are significantly below those found by Jonsson (2011), conducted also in harbor area, and the studies of Pirjola (2013) and Beecken (2014, 2015b) conducted at open sea.

6 References

Alföldy B., ..., Mellqvist J., et al., Measurements of air pollution emission factors for marine transportation, Atmos. Meas. Tech., 6, 1777–1791, 2013

Balzani Lööv J M…. J. Mellqvist, et al., Field test of available methods to measure remotely SOx and NOx emissions from ships, Atmos. Meas. Tech. Discuss., 6, 9735-9782, 2013, www.atmos-meas-tech-discuss.net/6/9735/2013/doi:10.5194/amtd-6-9735-2013.

Beecken, J., Mellqvist, J., Salo, K., Ekholm, J., and Jalkanen, J.-P (2014). Airborne emission measurements of SO2, NOx and particles from individual ships using sniffer technique, Atmos. Meas. Tech., 7, 1957–1968, , www.atmos-meas-tech.net/7/1957/2014/doi:10.5194/amt-7-1957-2014.

Beecken, Jörg (2015a), Remote Measurements of Gas and Particulate Matter Emissions from Individual Ships Göteborg : dissertation, Chalmers University of Technology. ISBN: 978-91-7597-141-4, 2015b. http://publications.lib.chalmers.se/publication/212515-remote-measurements-of-gas-and-particulate-matter-emissions-from-individual-ships, 2015.

Beecken J. et al. (2015b), Emission Factors of SO2, NOx and Particles from Ships in Neva Bay from Ground-Based and Helicopter-Borne Measurements and AIS-Based Model, Atmos. Chem. Phys., 15, 5229-5241, 2015a , www.atmos-chem-phys.net/15/5229/2015/doi:10.5194/acp-15-5229-2015, 2015.

Berg, N., Mellqvist, J. et al., Ship emissions of SO2 and NO2: DOAS measurements from airborne platforms, Atmos. Meas. Tech., 5, 1–14, doi:10.5194/amt-5-1-2012, 2012.

Burtscher, H. (2005). Physical characterization of particulate emissions from diesel engines: a review. J. Aerosol Sci. 36:896–932.

Cooper D. A., Exhaust emissions from ships at berth, Atmospheric Environment 37, 3817–3830, 2003

Corbett, J., Winebrake, J., et al., e. (2007). Mortality from ship emissions: A global assessment. Published online in the American Chemical Society journal Environmental Science and Technology on 7 November.

EMEP. (2002). Effects of international shipping on European pollution levels.
http://www.emp.int/reports/dnmi_note_5_2000.pdf

Furusho-Percot et al. (2016), Improved soot measurements with an engine exhaust particle sizer, 5th International exhaust emission symposium, Bielsko-Biala, Poland, May 19

IHS Global: IHS Maritime, Chemin de la Mairie, Perly, Geneva, Switzerland, 2016.

Jalkanen, J.-P. (2009). A modeling system for the exhaust emissions of marine traffic and its application in the Baltic Sea area. Atmospheric Chemistry and Physics (9), 9209-9223.

Jonsson, A. M., Westerlund, J., and Hallquist, M.: Size-resolved particle emission factors for individual ships, 48 Geophys Res Lett, 38, 2011.

Lack, D. A., B. Lerner, C. Granier, T. Baynard, E. R. Lovejoy, P. Massoli, A. R. Ravishankara, and E. Williams, Light absorbing carbon emissions from commercial shipping, Geophys. Res. Lett., 35, L13815, doi:10.1029/2008GL033906, 2008.

Lack, D. A., Corbett J. J., Black carbon from ships: a review of the effects of ship speed, fuel quality and exhaust gas scrubbing, Atmos. Chem. Phys., 12, 3985–4000, 2012, doi:10.5194/acp-12-3985-2012.

Mellqvist, J and Berg N., Final report to Vinnova: IDENTIFICATION OF GROSS POLLUTING SHIPS RG Report (Göteborg) No. 4, ISSN 1653 333X, Chalmers University of Technology, 2010a.

Mellqvist, J., J. Samuelsson, J. K. E. Johansson, C. Rivera, B. Lefer, S. Alvarez, and J. Jolly Measurements of industrial emissions of alkenes in Texas using the solar occultation flux method, Journal of Geophysical Research: Atmospheres, 115(D7), doi:10.1029/2008JD011682, 2010b

Mellqvist, J., Ekholm, J., Salo, K. and Jörg Beecken, IDENTIFICATION OF GROSS POLLUTING SHIPS TO PROMOTE A LEVEL PLAYING FIELD WITHIN THE SHIPPING SECTOR, FINAL REPORT TO VINNOVA (2008-03884). Technical Report, Earth and Space Sciences, Chalmers University of Technology, No. 11, 2014.

Mellqvist, J., et al., Remote Quantification of Stack Emissions from Marine Vessels, A&WMA's 109th Annual Conference & Exhibition, New Orleans, Louisiana, June 20-23, 2016a, Extended Abstract # 944.

Mellqvist, J., Samuelsson, J., Andersson, P., Brohede, S., Isoz, O. and Marianne Ericsson., Emission Measurements of VOCs, NO2 and SO2 from the refineries in the South Coast Air Basin using Solar Occultation Flux and other Optical Remote Sensing Methods, FluxSense Report to SCAQMD, August, 2016b .

Mellqvist, J., Samuelsson, J., Andersson, P., Brohede, S., Isoz, O. and Marianne Ericsson, Using Solar Occultation Flux and other Optical Remote Sensing Methods to measure VOC emissions from a variety of stationary sources in the South Coast Air Basin, Report to SCAQMD, August, 2016c.

Park, K., Cao, F., Kittelson, D. B., &Mc Murry, P.M. (2003). Relationship between particle mass and mobility for diesel exhaust particles. Environmental Science and Technology, 37, 577–583.

Park, K., Kittelson, D. B., & McMurry, P. H. (2004). Structural properties of diesel exhaust particles measured by transmission electron microscopy (TEM): relationships to particle mass and mobility. Aerosol Science and Technology, 38, 881–889.

Platt, U., and J. Stutz (2008), Differential Absorption Spectroscopy, 597 pp., Springer Berlin Heidelberg, doi:10.1007/978-3-540-75776-4.

Pirjola, L., Pajunoja, A., Walden, J., Jalkanen, J. P., Rönkkö, T., Kousa, A., and Koskentalo, T.: Mobile 44 measurements of ship emissions in two harbor areas in Finland, Atmos. Meas. Tech., 7, 149-161, 10.5194/amt-45 7-149-2014, 2014.

Port of Los Angeles, Port of Los Angeles Inventory of Air emissions-2014, Technical Report ADP# 141007-514, prep by Starcrest consulting group, Sep, 2015.

Port of Long Beach, Port of Long Beach Inventory of Air emissions-2014, Technical Report prep by Starcrest consulting group, Sep, 2015.

Rivera, C., Mellqvist J. et al. (2010), Quantification of NO2 and SO2 emissions from the Houston Ship Channel and Texas City industrial areas during the 2006 Texas Air Quality Study, Journal of Geophysical Research - Atmospheres (0148-0227). Vol. 115.

Vandaele, A. C., C. Hermans, P. C. Simon, M. Carleer, R. Colin, S. Fally, M. F. Mérienne, A. Jenouvrier, and B. Coquart (1998), Measurements of the NO2 absorption cross-section from 42 000 cm -1 to 10 000 cm -1 (238-1000 nm) at 220 K and 294 K, Journal of Quantitative Spectroscopy and Radiative Transfer, 59(3-5), 171-184.

Williams, E. J., Lerrier, B. M., Murphy, P. C., Herndon, S. C., and Zahniser, M. S.: Emissions of NOx, SO2, 11 CO, and HCHO from commercial marine shipping during Texas Air Quality Study (TexAQS) 2006, J Geophys 12 Res D Atmos, 114, Artn D21306, Doi10.1029/2009JD012094, 2009.

Winnes H., Fridell E., Emissions of NOx and particles from maneuvering ships, Transportation Research Part D 15, 204–211, 2010.

Winnes H., Fridell E., Particle Emissions from Ships: Dependence on Fuel Type, Journal of the Air & Waste Management Association, 59:12, 1391-1398, DOI: 10.3155/1047-3289.59.12.1391, 2009.

7 Acknowledgment

This work was funded by the South Coast Air Quality Management District (SCAQMD). We would like to acknowledge the important contributi by SQAQMD, including Dr. Laki Tisopulos, Dr. Andrea Polidori, Dr. Olga Pikelnaya and Mike Hamdan. We also acknowledge the collaboration of Southern California University providing assistance with the Yellow fin. We acknowledge the US Coast Guard and Southern California University providing locations for the site in Port of LA. The Port of Long Beach is acknowledged for proving a location for the fixed site measurements at port of Long Beach. We thank Armin Kleinboehl for assistance with the flight campaign.

8 Appendix I: Chase studies

Here the data of chase studies with several plume traverses are presented in detail.

8.1 Cargo vessels

8.1.1 CHICAGO BRIDGE (23 Oct 2015, 22:17)

Table A. 1. Detailed vessel information from Sea-web on CHICAGO BRIDGE (IHS, 2016).

IMO	MMSI	Flag	GT	DWT	YoB	MEng	Tot. power	RPM	Stroke
9247558	352018000	Panama	66,332	67,170	2001	Oil	57,201 kW	94	2

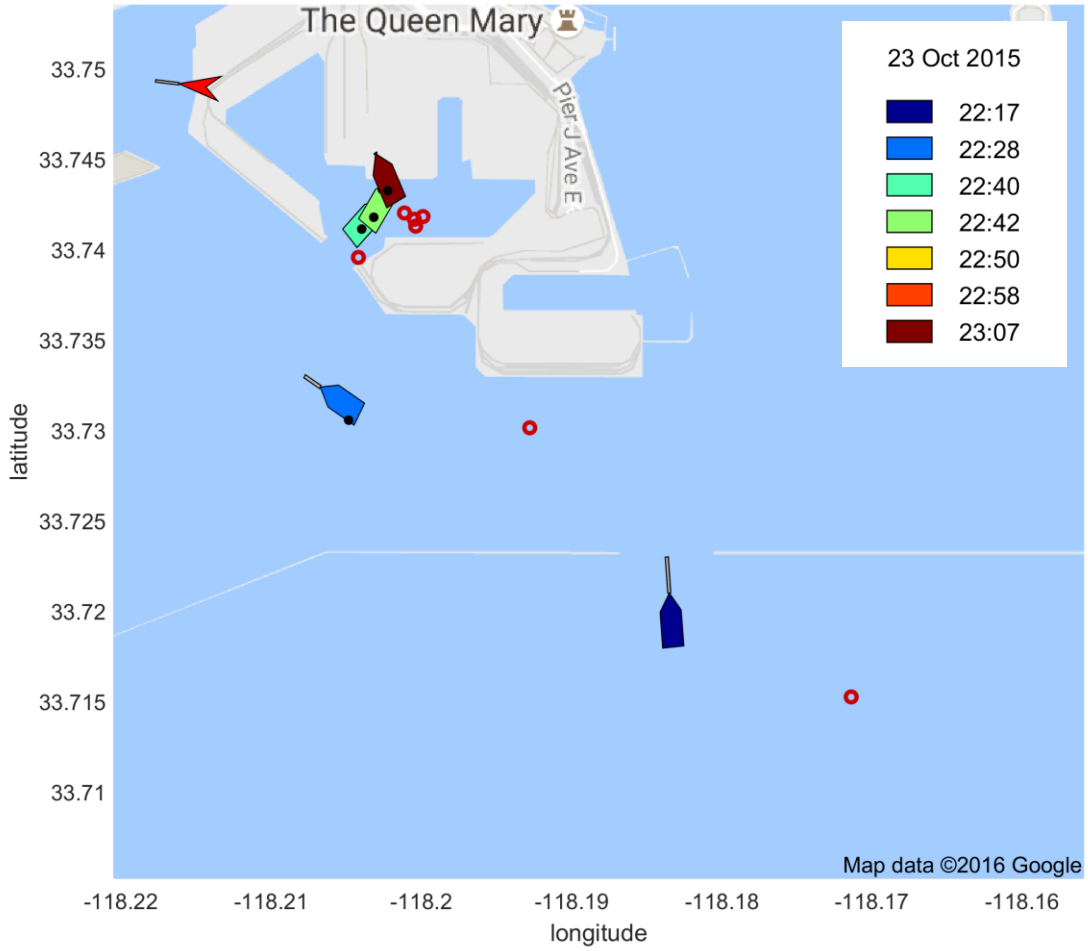

Figure A. 1. An illustration of a chase study of the cargo vessel CHICAGO BRIDGE.

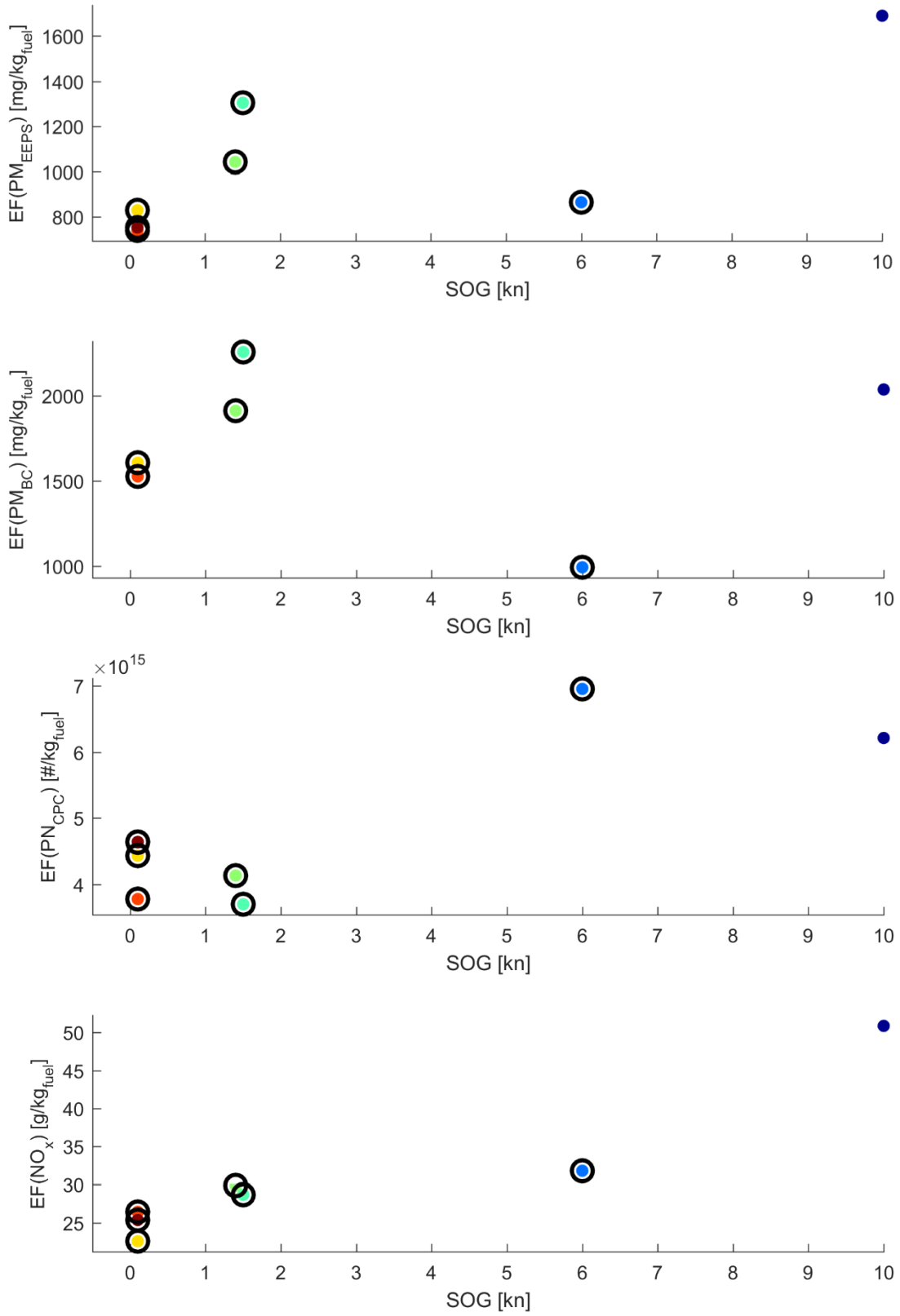

Figure A. 2. Specific emissions factors versus speed for CHICAGO BRIDGE. Different colours correspond to different times as shown in the legend in the corresponding map.

8.1.2 CMA CGM GEMINI (14 Oct 2015, 21:17)

Table A. 2. Detailed vessel information from Sea-web on CMA CGM GEMINI (IHS, 2016).

IMO	MMSI	Flag	GT	DWT	YoB	MEng	Tot. Power	RPM	Stroke
9410791	235078078	United Kingdom	131,332	131,236	2011	Oil	72,240 kW	104	2

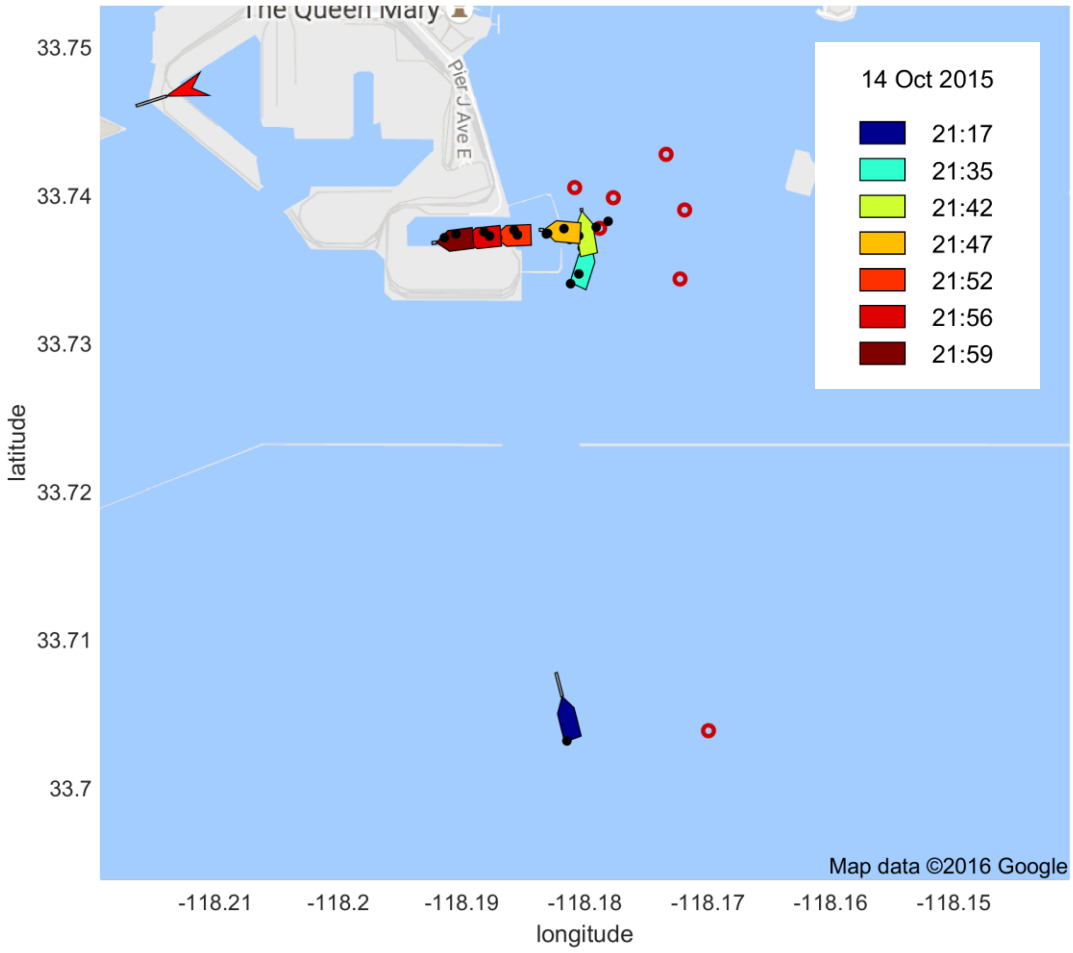

Figure A. 3. An illustration of a chase study of the cargo vessel CMA CGM GEMINI.

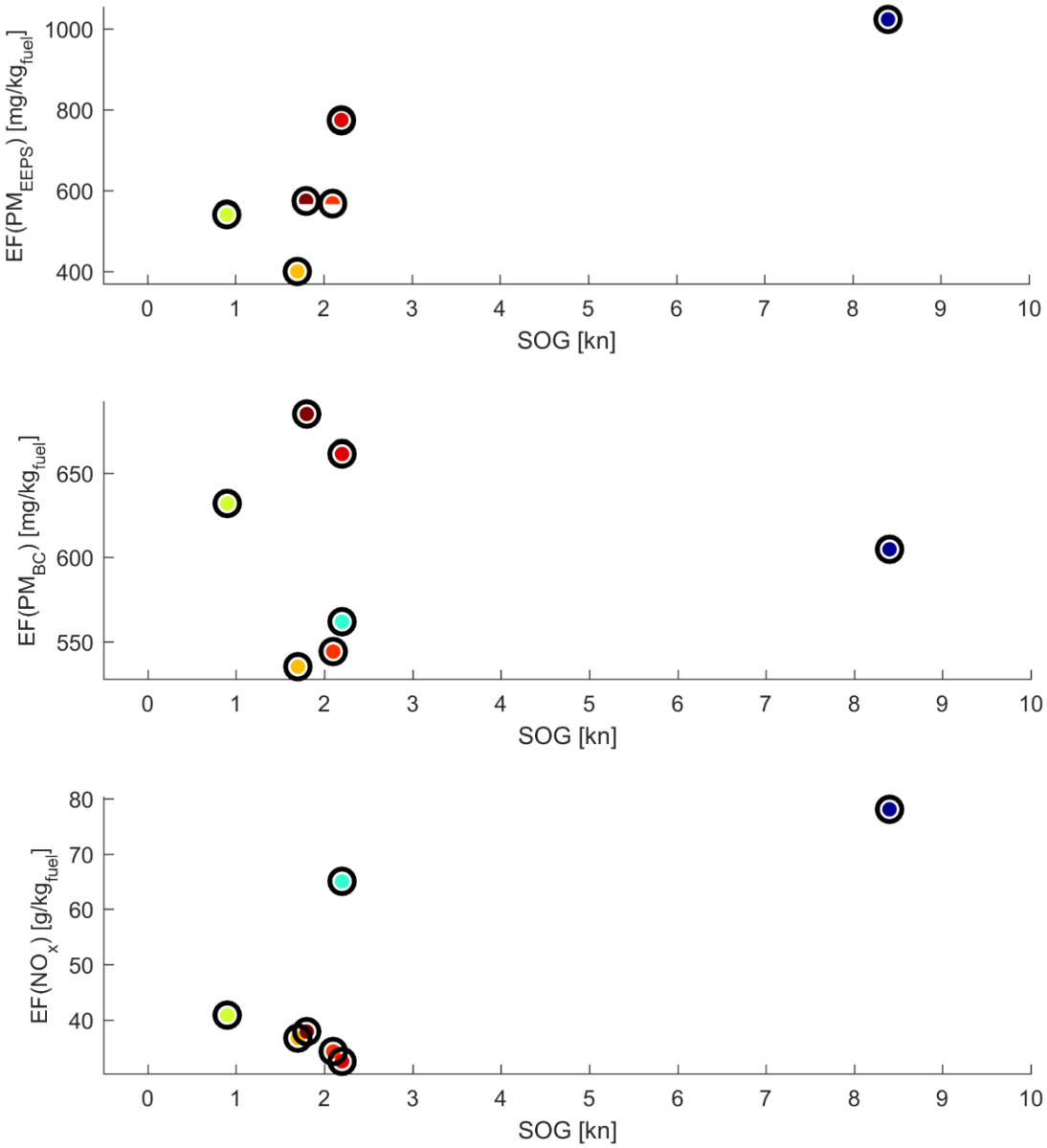

Figure A. 4. Specific emissions factors versus speed for CMA CMG GEMINI. Different colours correspond to different times as shown in the legend in the corresponding map.

8.1.3 EVER LEADING (19 Oct 2015, 21:06)

Table A. 3. Detailed vessel information from Sea-web on EVER LEADING (IHS, 2016).

IMO	MMSI	Flag	GT	DWT	YoB	MEng	Tot. Power	RPM	Stroke
9595462	235093619	United Kingdom	98,882	104,409	2012	Oil	56,070 kW	97	2

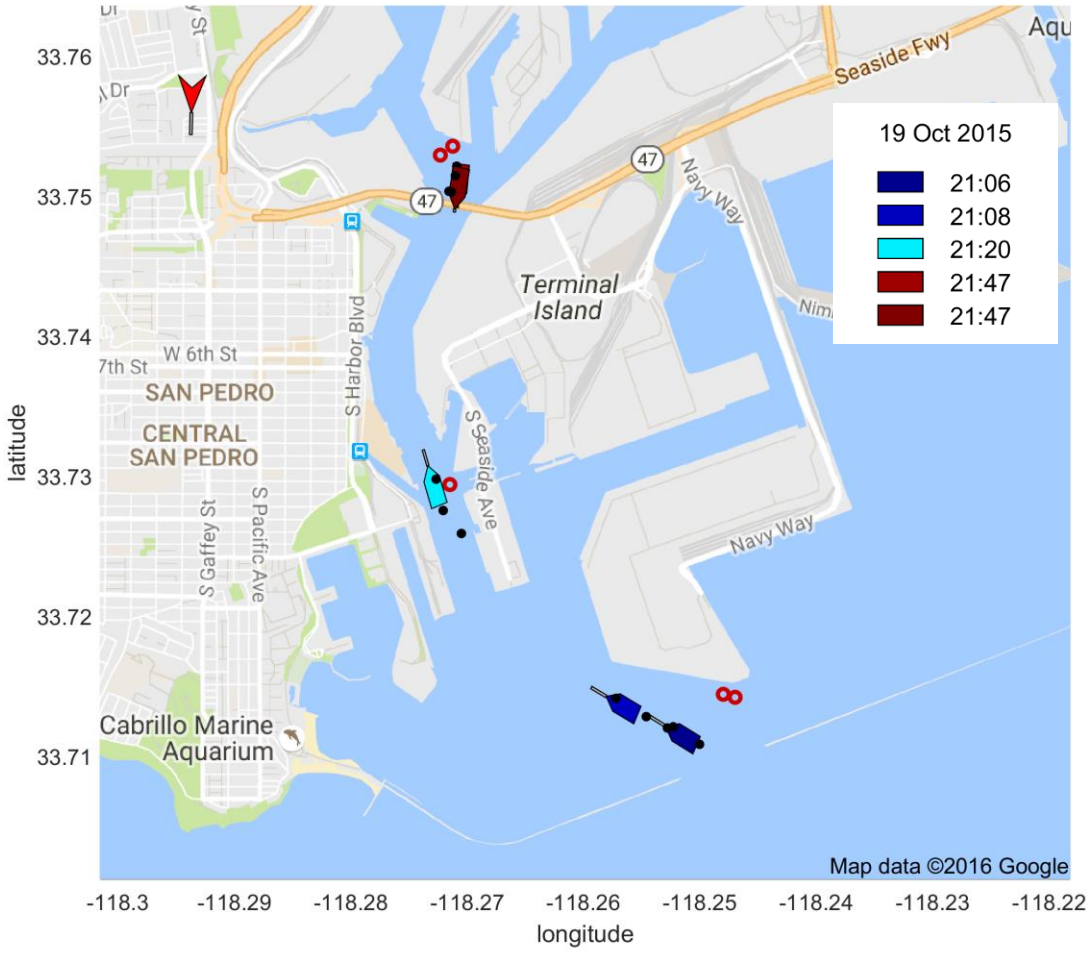

Figure A. 5. An illustration of a chase study of the cargo vessel EVER LEADING.

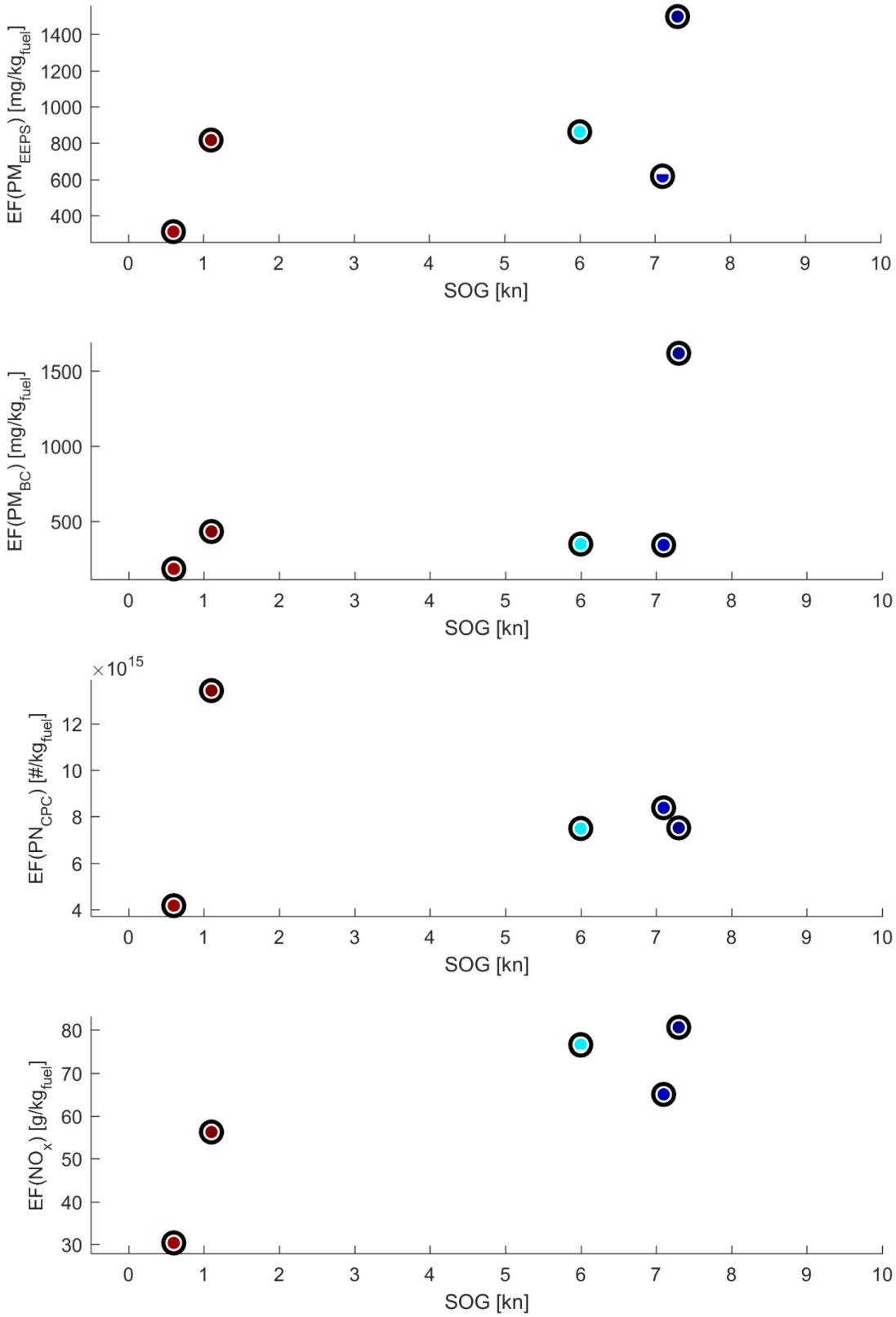

Figure A. 6. Specific emissions factors versus speed for EVER LEADING. Different colours correspond to different times as shown in the legend in the corresponding map.

8.1.4 GERD MAERSK (14 Oct 2015, 22:55)

Table A. 4. Detailed vessel information from Sea-web on GERD MAERSK (IHS, 2016).

IMO	MMSI	Flag	GT	DWT	YoB	MEng	Tot. Power	RPM	Stroke
9320245	220415000	Denmark	98,648	115,700	2006	Oil	68,658 kW	100	2

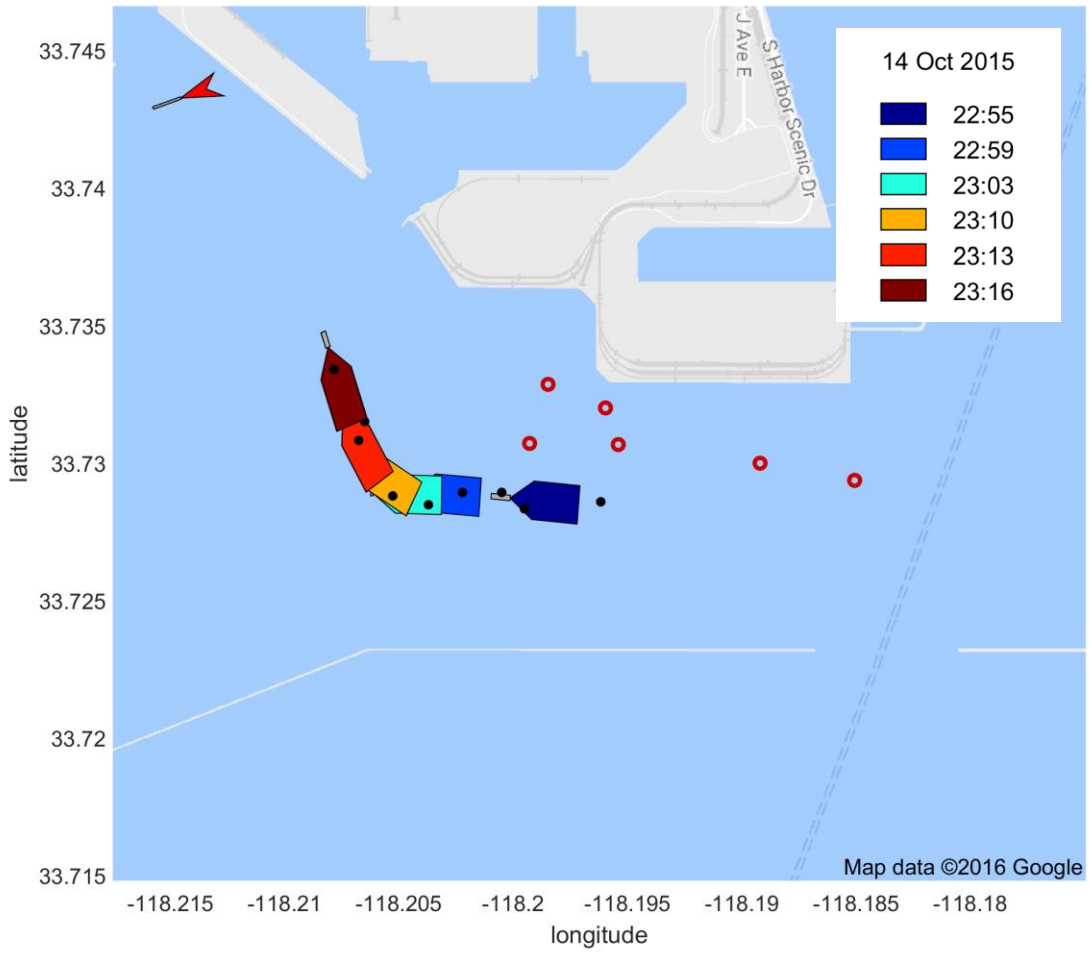

Figure A. 7. An illustration of a chase study of the cargo vessel GERD MAERSK.

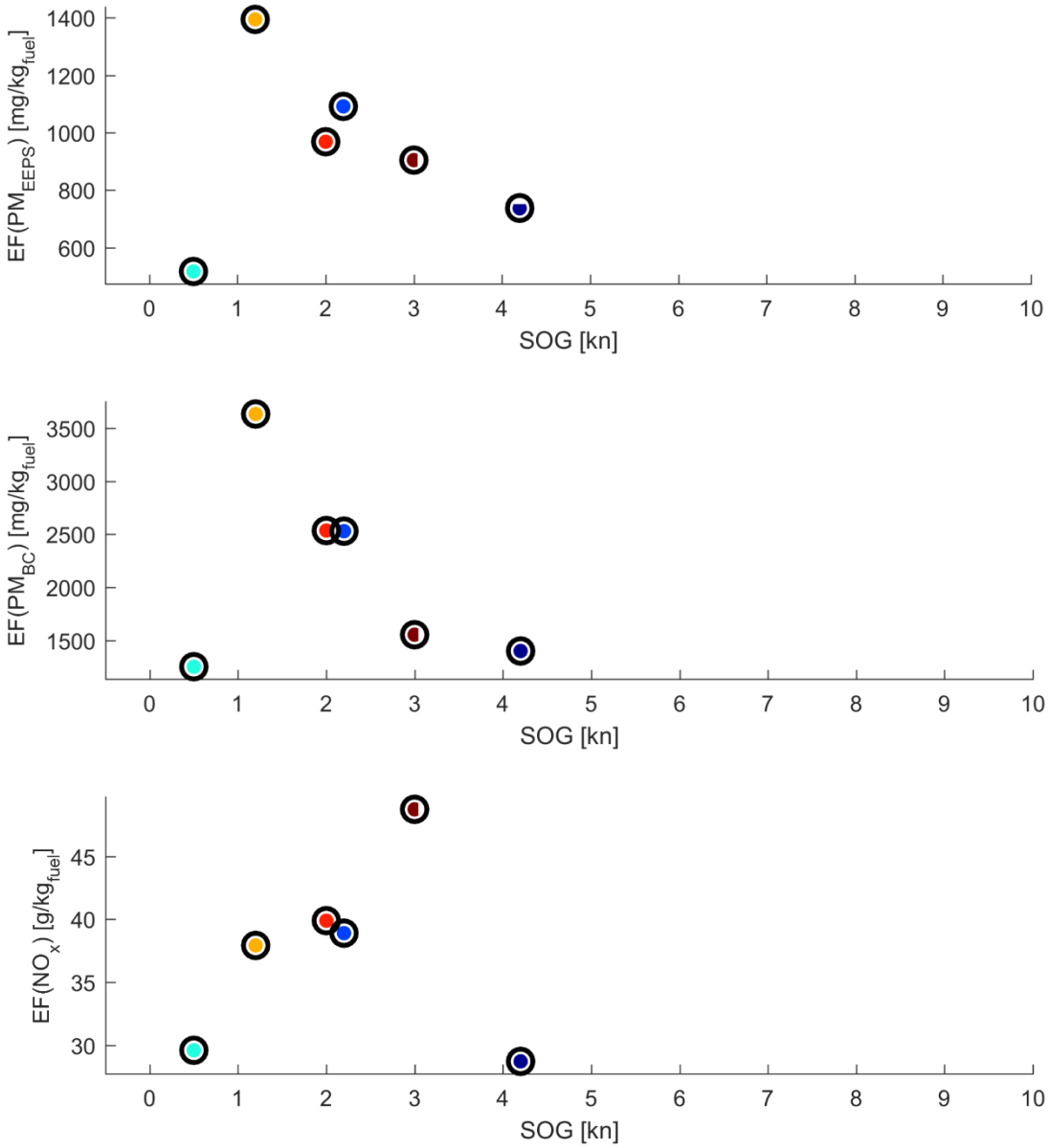

Figure A. 8. Specific emissions factors versus speed for GERD MAERSK. Different colours correspond to different times as shown in the legend in the corresponding map.

8.1.5 HORIZON NAVIGATOR (16 Oct 2015, 00:09)

Table A. 5. Detailed vessel information from Sea-web on HORIZON NAVIGATOR (IHS, 2016).

IMO	MMSI	Flag	GT	DWT	YoB	MEng	Tot. Power	RPM	Stroke
7116315	366792000	United States	28,212	31,203	1972	Turbo electric steam turbine	20,962 kW	NA	NA

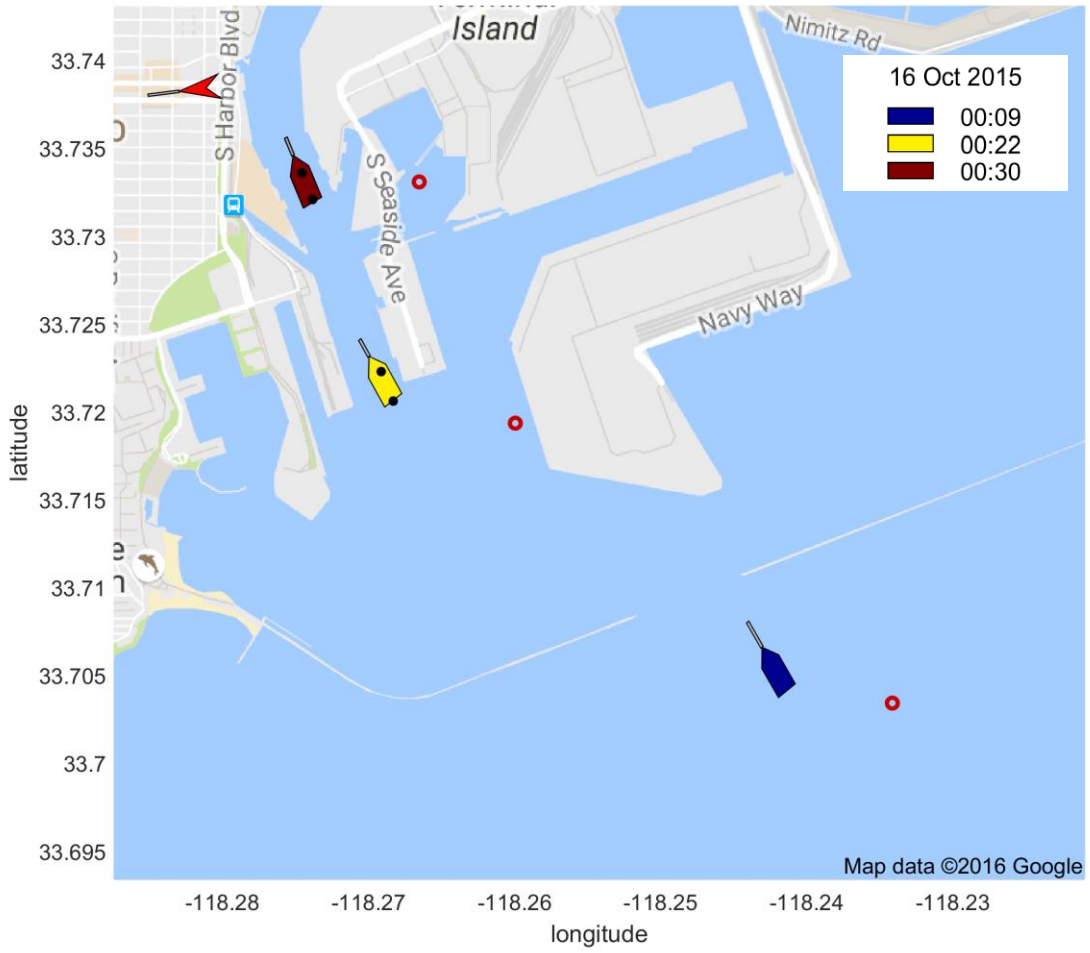

Figure A. 9. An illustration of a chase study of the cargo vessel HORIZON NAVIGATOR.

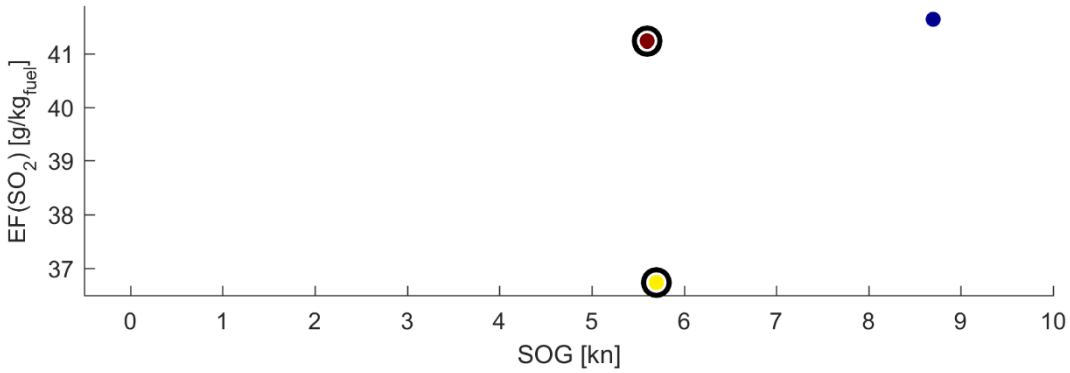
EF(SO2) [g/kgfuel]
41
40
39
38
37
0
1
2
3
4
5
6
7
8
9
10
SOG [kn]

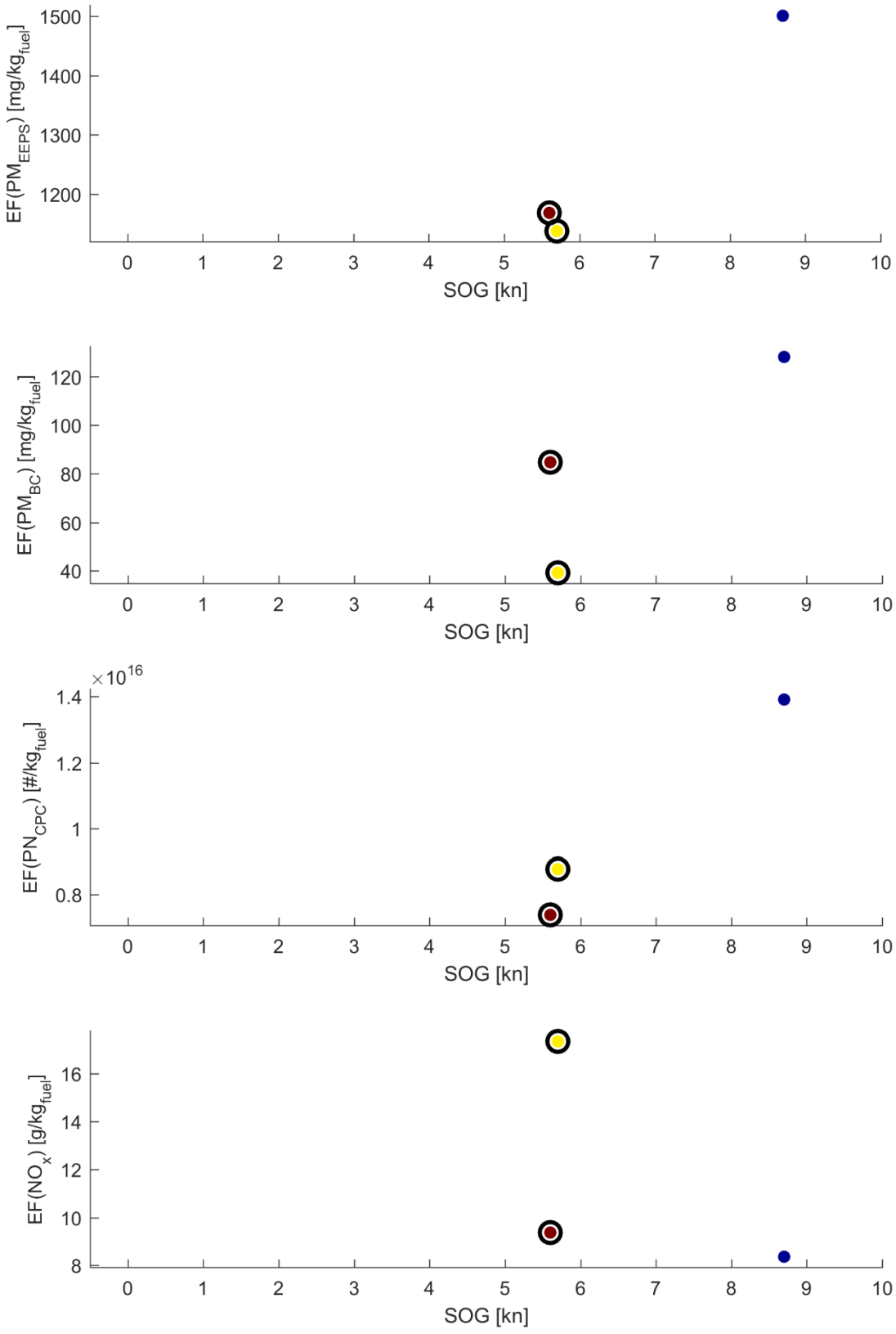

Figure A. 10. Specific emissions factors versus speed for HORIZON NAVIGATOR. Different colours correspond to different times as shown in the legend in the corresponding map.

8.1.6 HYUNDAI NEW YORK (25 Oct 2015, 23:51)

Table A. 6. Detailed vessel information from Sea-web on HYUNDAI NEW YORK (IHS, 2016).

IMO	MMSI	Flag	GT	DWT	YoB	MEng	Tot. Power	RPM	Stroke
9385025	566999000	Singapore	71,786	72,982	2009	Oil	62,920 kW	94	2

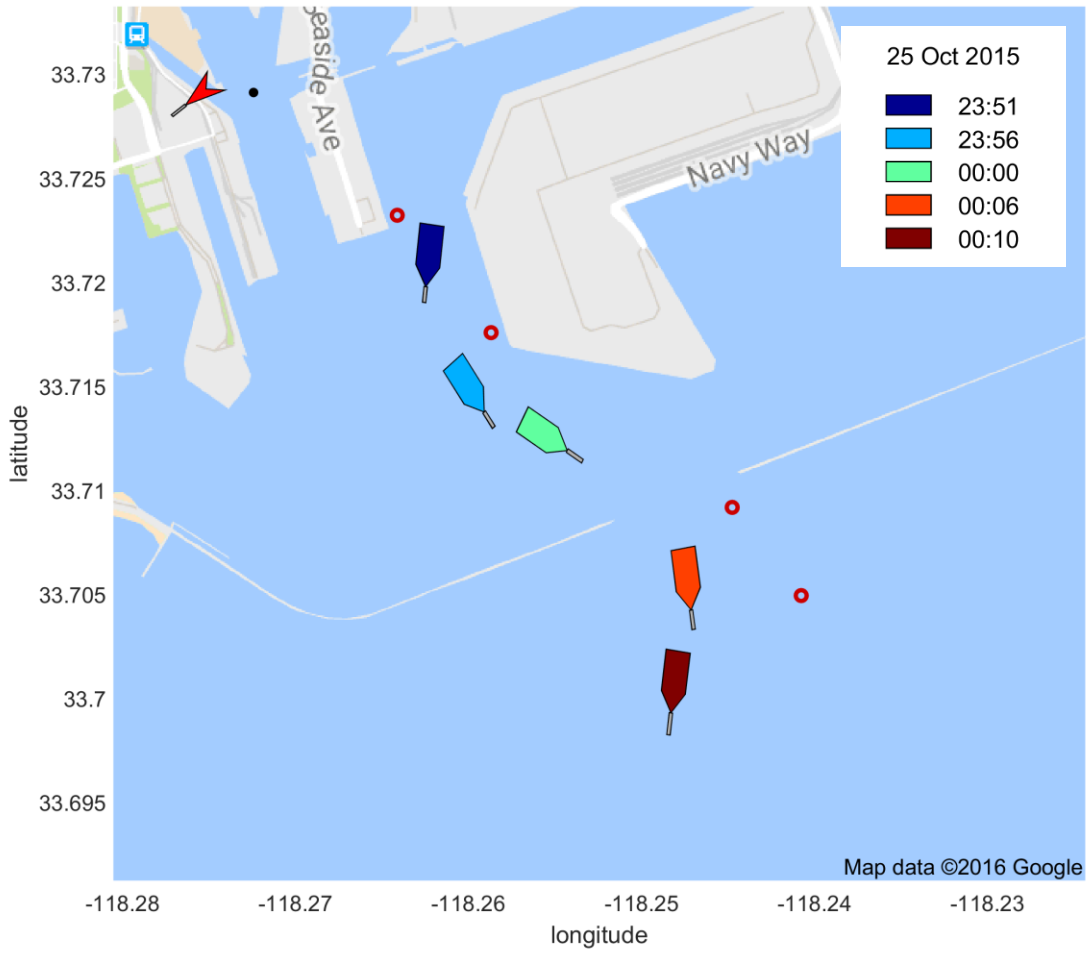

Figure A. 11. An illustration of a chase study of the cargo vessel HYUNDAI NEW YORK.

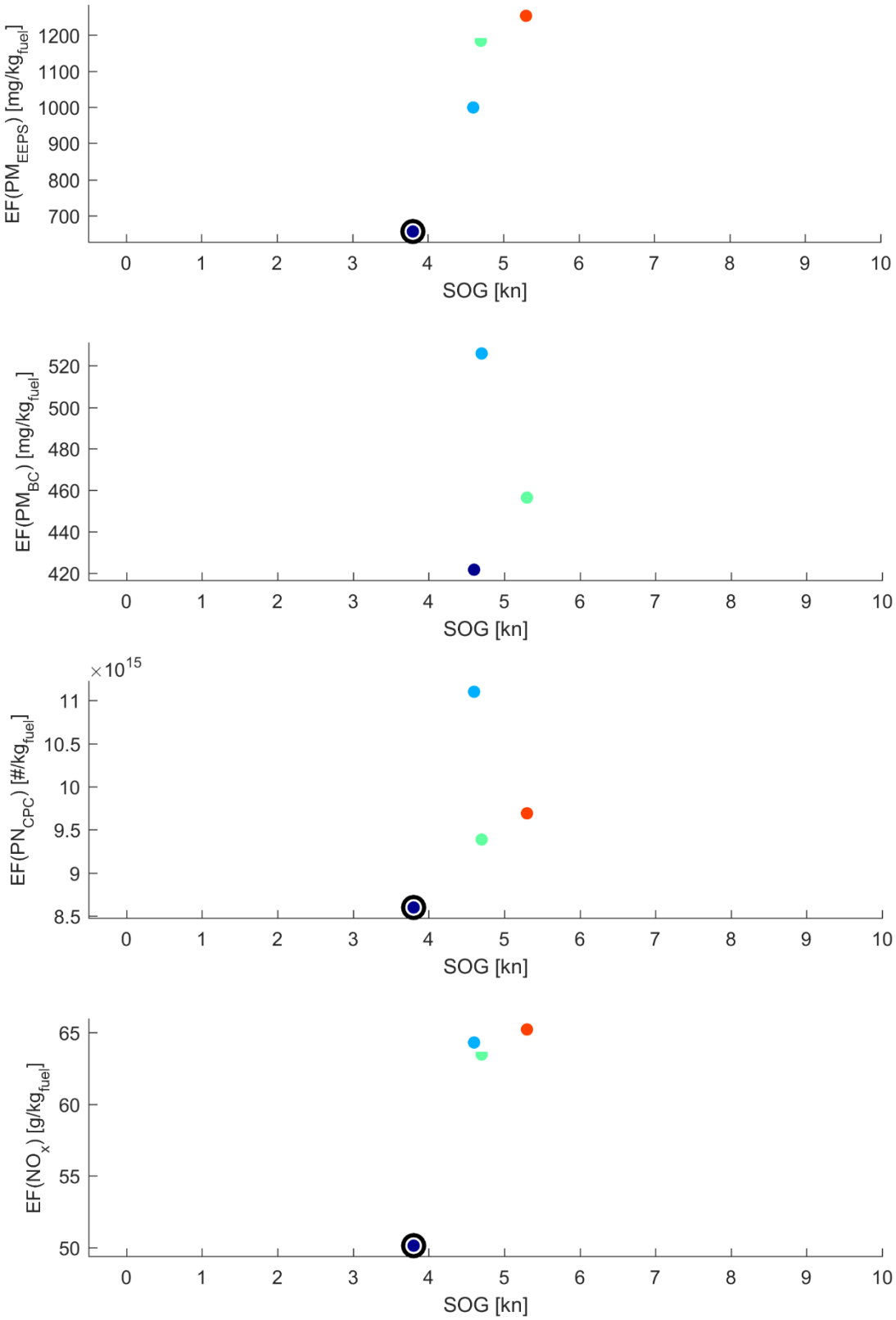

Figure A. 12. Specific emissions factors versus speed for HYUNDAI NEW YORK. Different colours correspond to different times as shown in the legend in the corresponding map.

8.1.7 MOLLY MANX (16 Oct 2015, 23:17)

Table A. 7. Detailed vessel information from Sea-web on MOLLY MANX (IHS, 2016).

IMO	MMSI	Flag	GT	DWT	YoB	MEng	Tot. Power	RPM	Stroke
9425863	235105197	Isle of Man	32,296	57,982	2010	Oil	8,400 kW	113	2

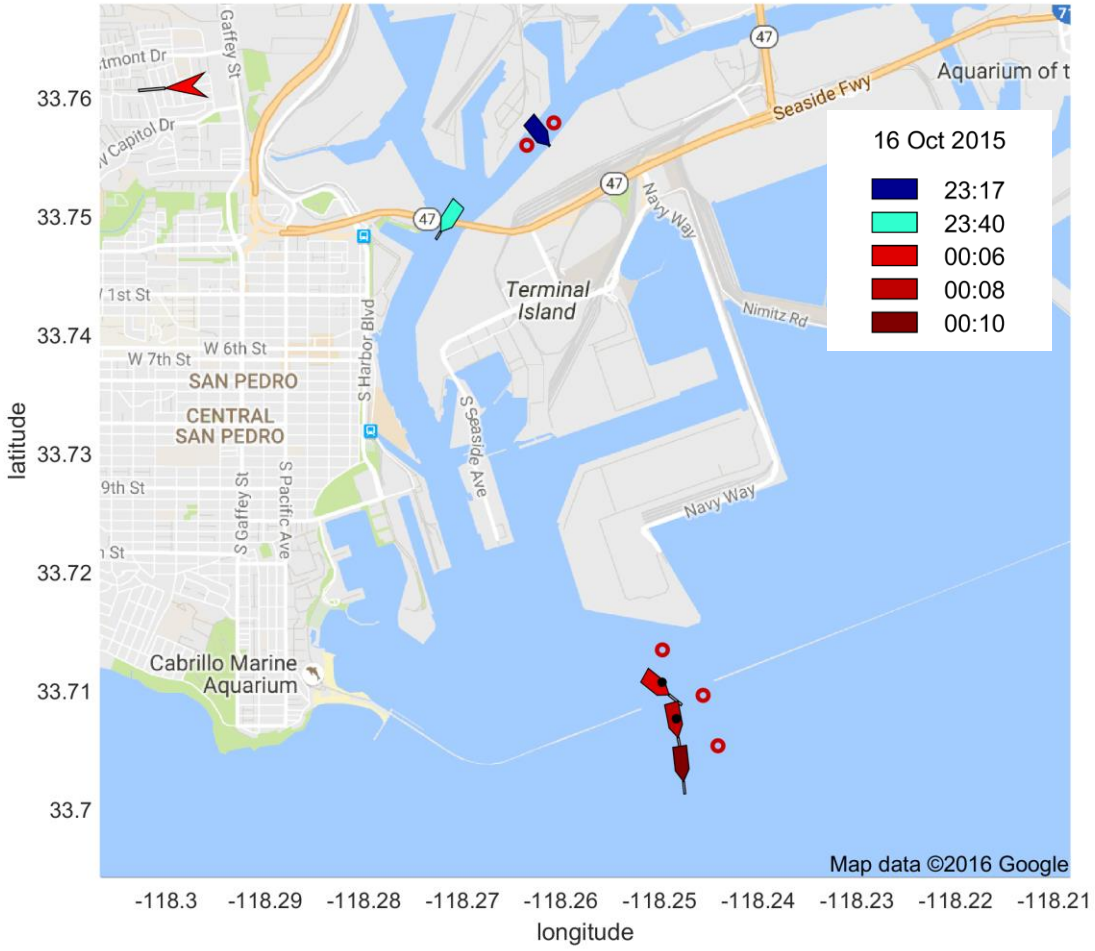

Figure A. 13. An illustration of a chase study of the cargo vessel MOLLY MANX.

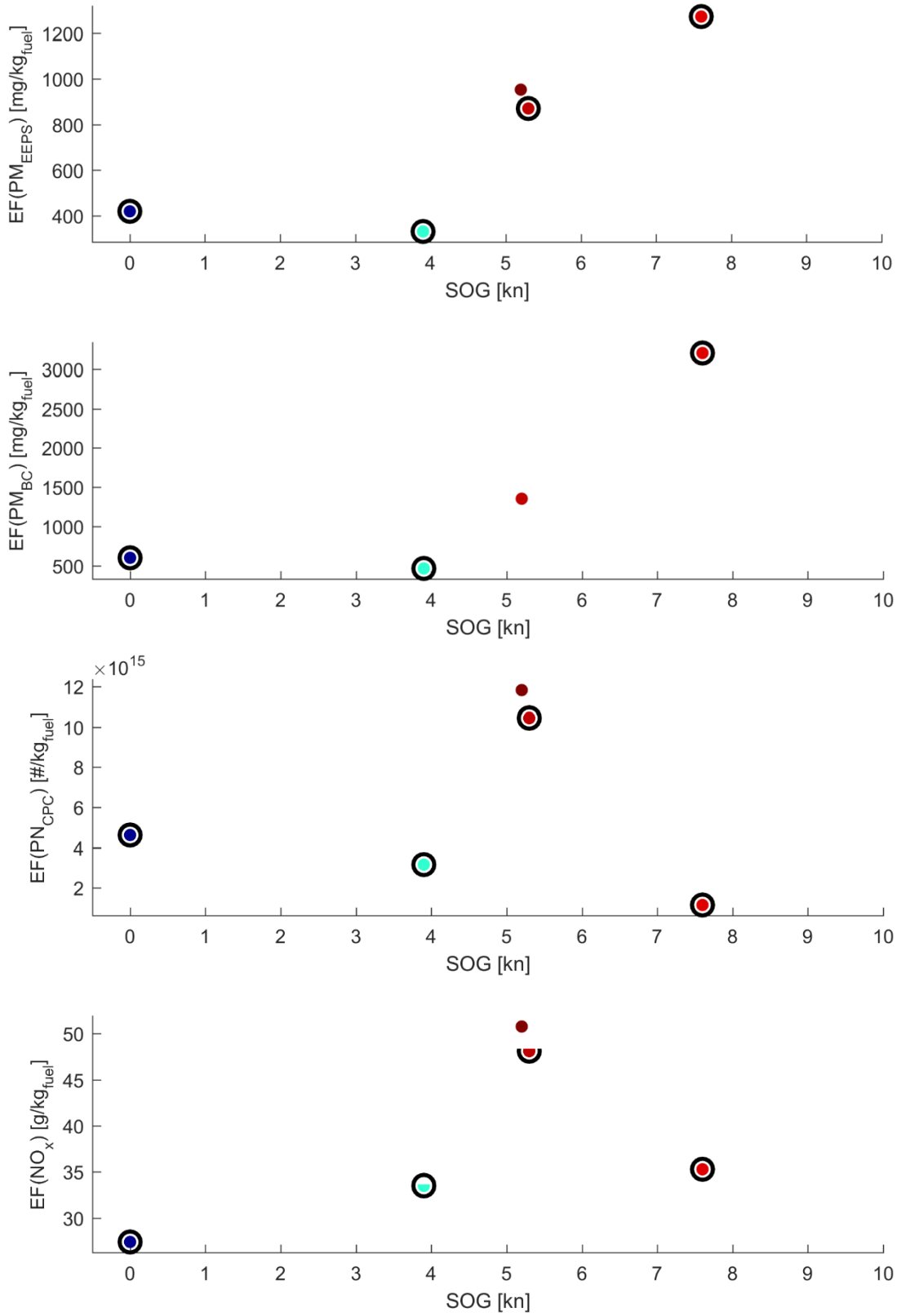

Figure A. 14. Specific emissions factors versus speed for MOLLY MANX. Different colours correspond to different times as shown in the legend in the corresponding map.

8.1.8 NYK DIANA (19 Oct 2015, 22:05)

Table A. 8. Detailed vessel information from Sea-web on NYK DIANA (IHS, 2016).

IMO	MMSI	Flag	GT	DWT	YoB	MEng	Tot. Power	RPM	Stroke
9337688	372319000	Panama	55,487	65,976	2008	Oil	51,390 kW	104	2

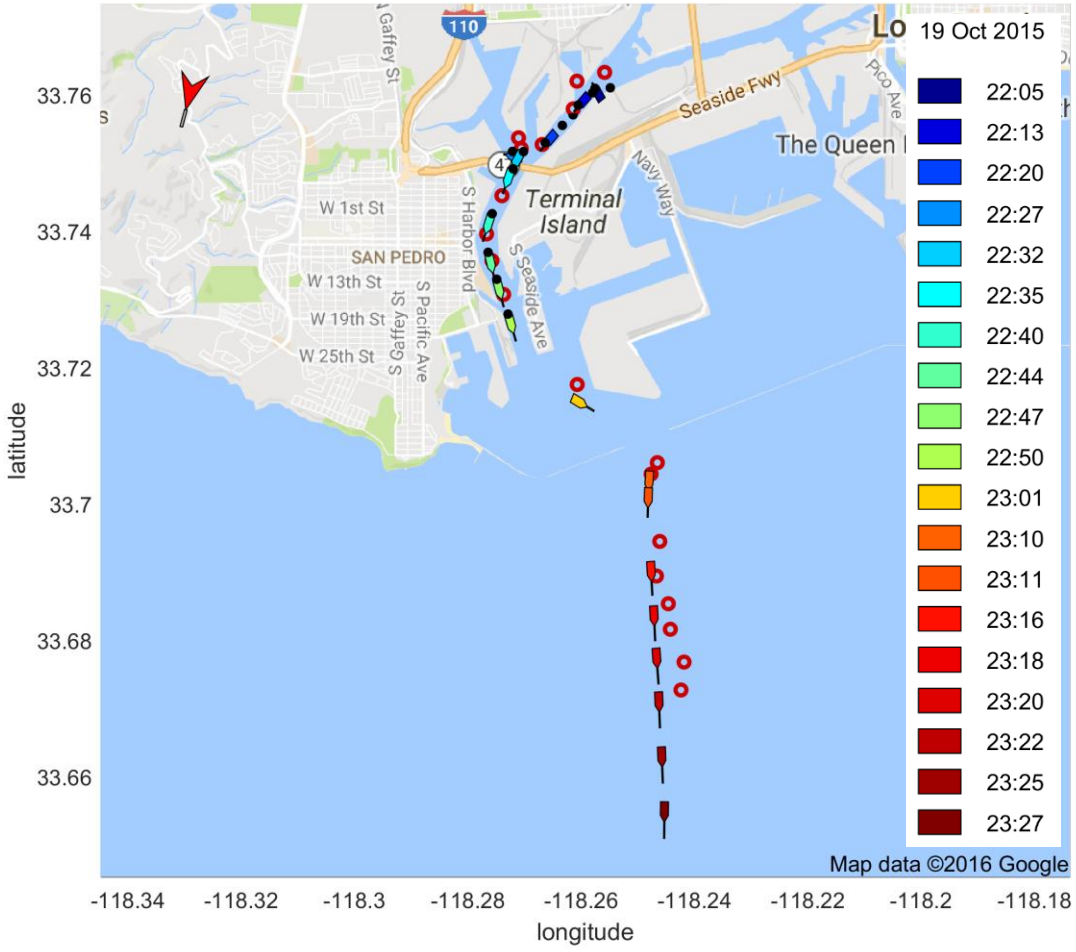

Figure A. 15. An illustration of a chase study of the cargo vessel NYK DIANA.

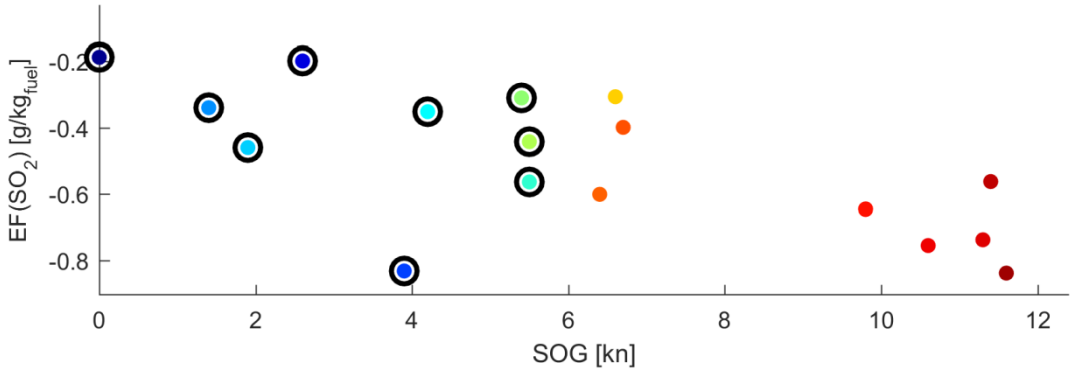

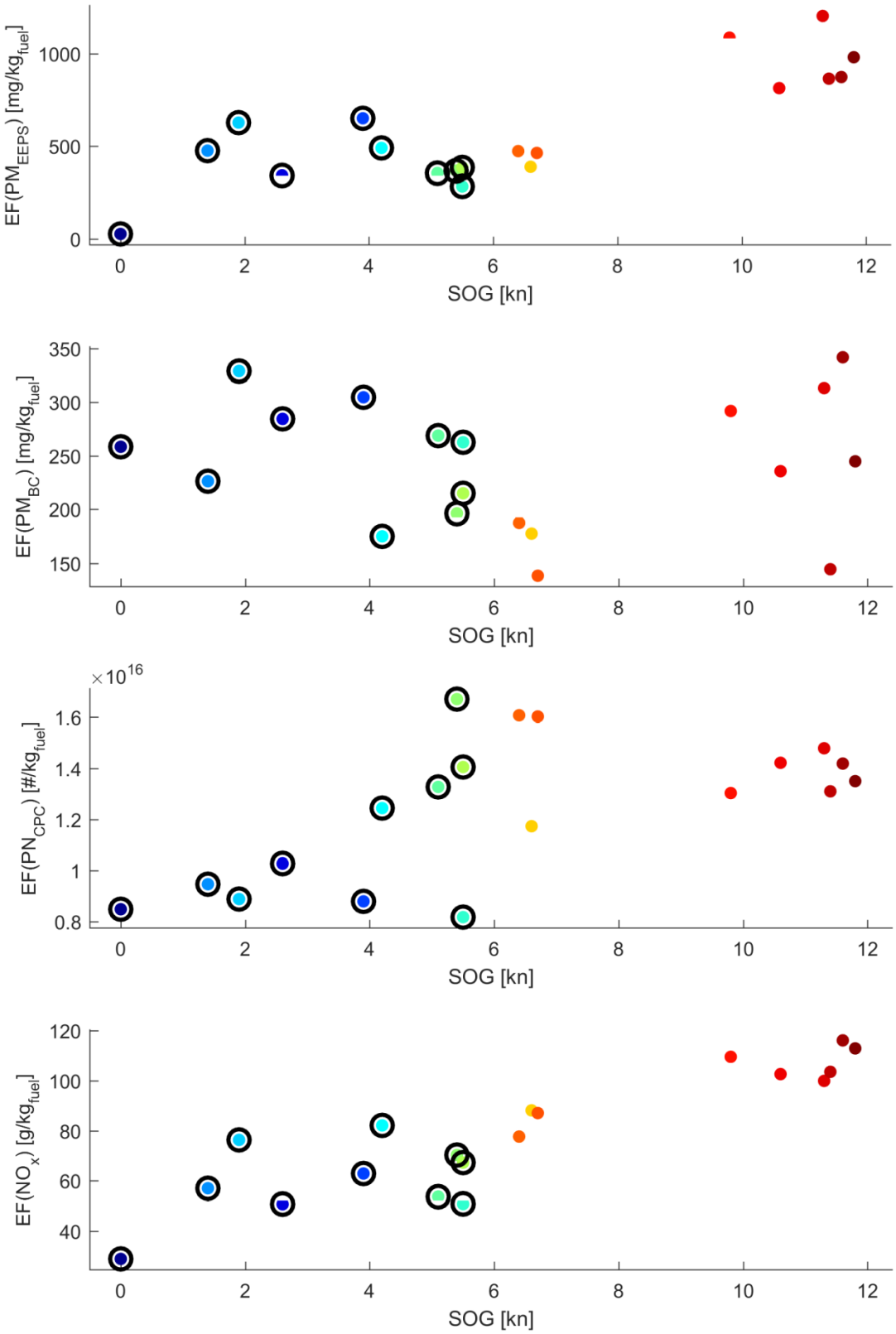

Figure A. 16. Specific emissions factors versus speed for NYK DIANA. Different colours correspond to different times as shown in the legend in the corresponding map.

8.1.9 OOCL LONG BEACH (22 Oct 2015, 22:09)

Table A. 9. Detailed vessel information from Sea-web on OOCL LONG BEACH (IHS, 2016).

IMO	MMSI	Flag	GT	DWT	YoB	MEng	Tot. Power	RPM	Stroke
9243409	477316000	Hong Kong	89,097	99,508	2003	Oil	68,495 kW	104	2

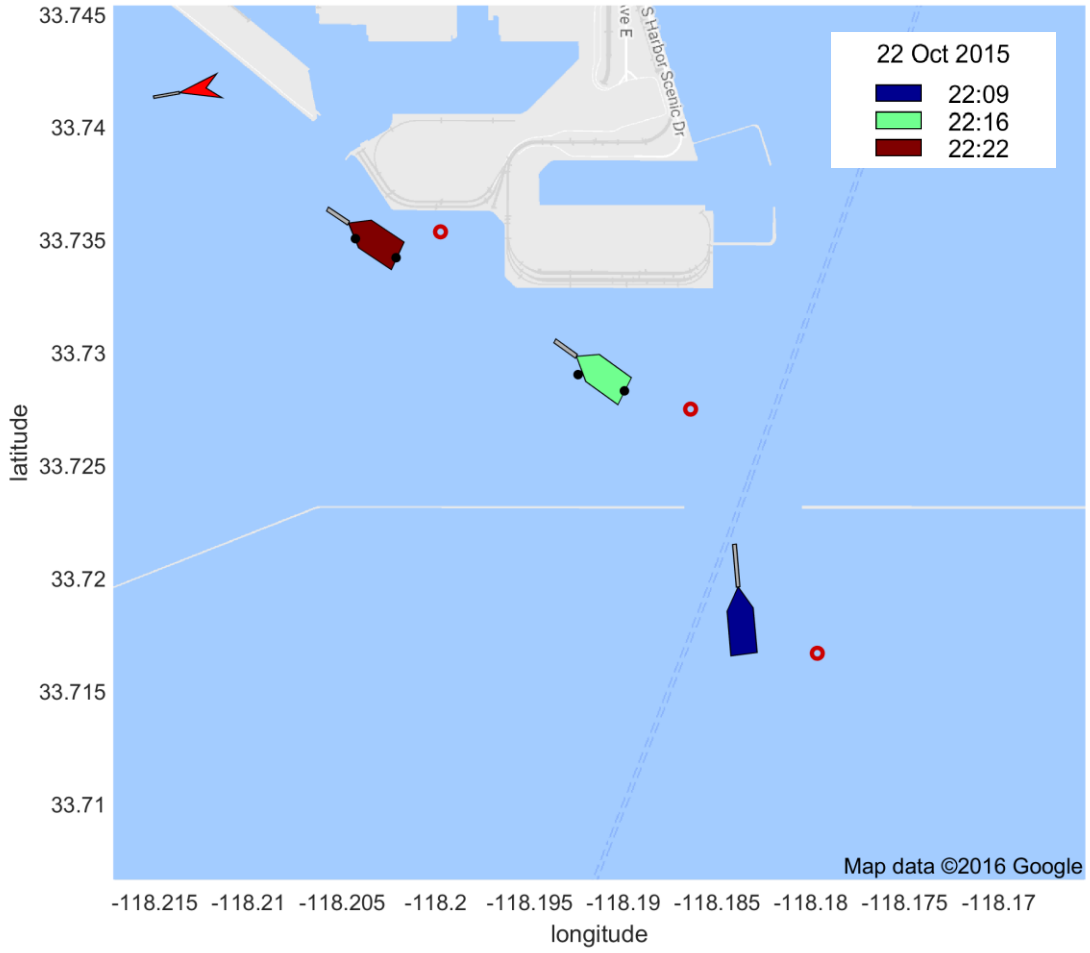

Figure A. 17. OOCL LONG BEACH.

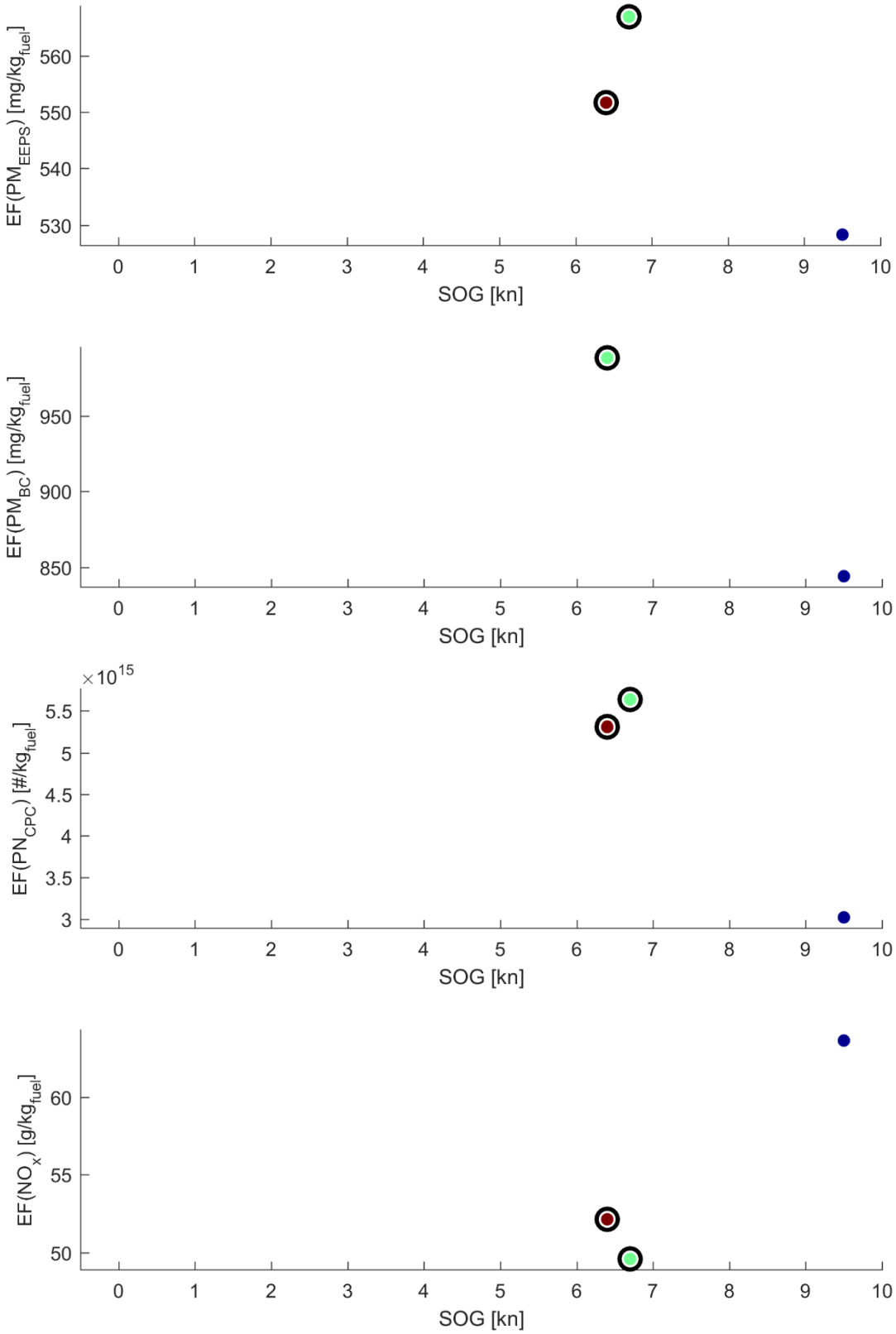

Figure A. 18. Specific emissions factors versus speed for OOCL LONG BEACH. Different colours correspond to different times as shown in the legend in the corresponding map.

8.1.10 SWAN ARROW (14 Oct 2015, 19:04)

Table A. 10. Detailed vessel information from Sea-web on SWAN ARROW (IHS, 2016).

IMO	MMSI	Flag	GT	DWT	YoB	MEng	Tot. Power	RPM	Stroke
8512970	311682000	Bahamas	28,805	45,295	1987	Oil	8,076 kW	100	2

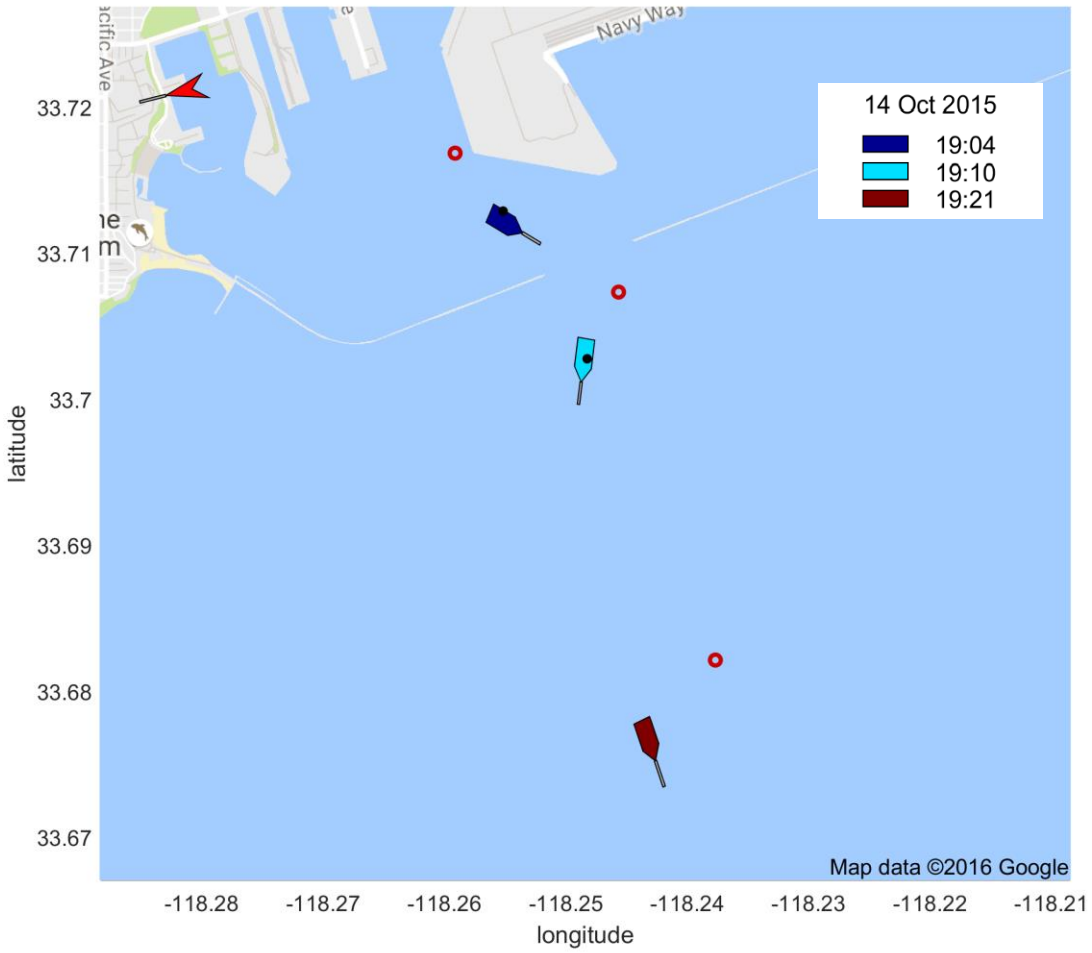

Figure A. 19. An illustration of a chase study of the cargo vessel SWAN ARROW.

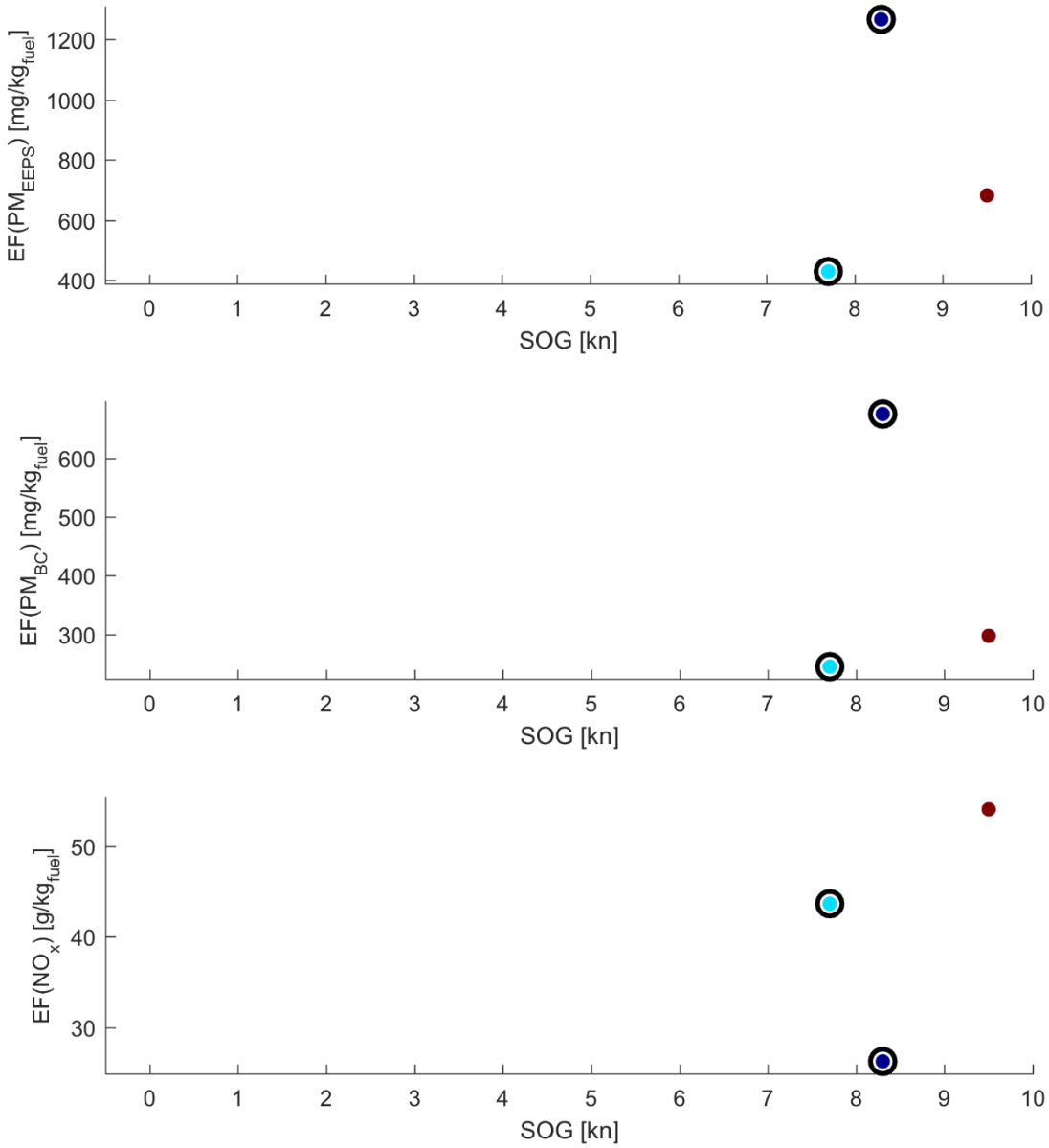

Figure A. 20. Specific emissions factors versus speed for SWAN ARROW. Different colours correspond to different times as shown in the legend in the corresponding map.

8.2 Tanker vessels

8.2.1 AQUALEGEND (13 Oct 2015, 18:48)

Table A. 11. Detailed vessel information from Sea-web on AQUALEGEND (IHS, 2016).

IMO	MMSI	Flag	GT	DWT	YoB	MEng	Tot. Power	RPM	Stroke
9592240	636015176	Liberia	61,237	115,571	2012	Oil	13,560 kW	105	2

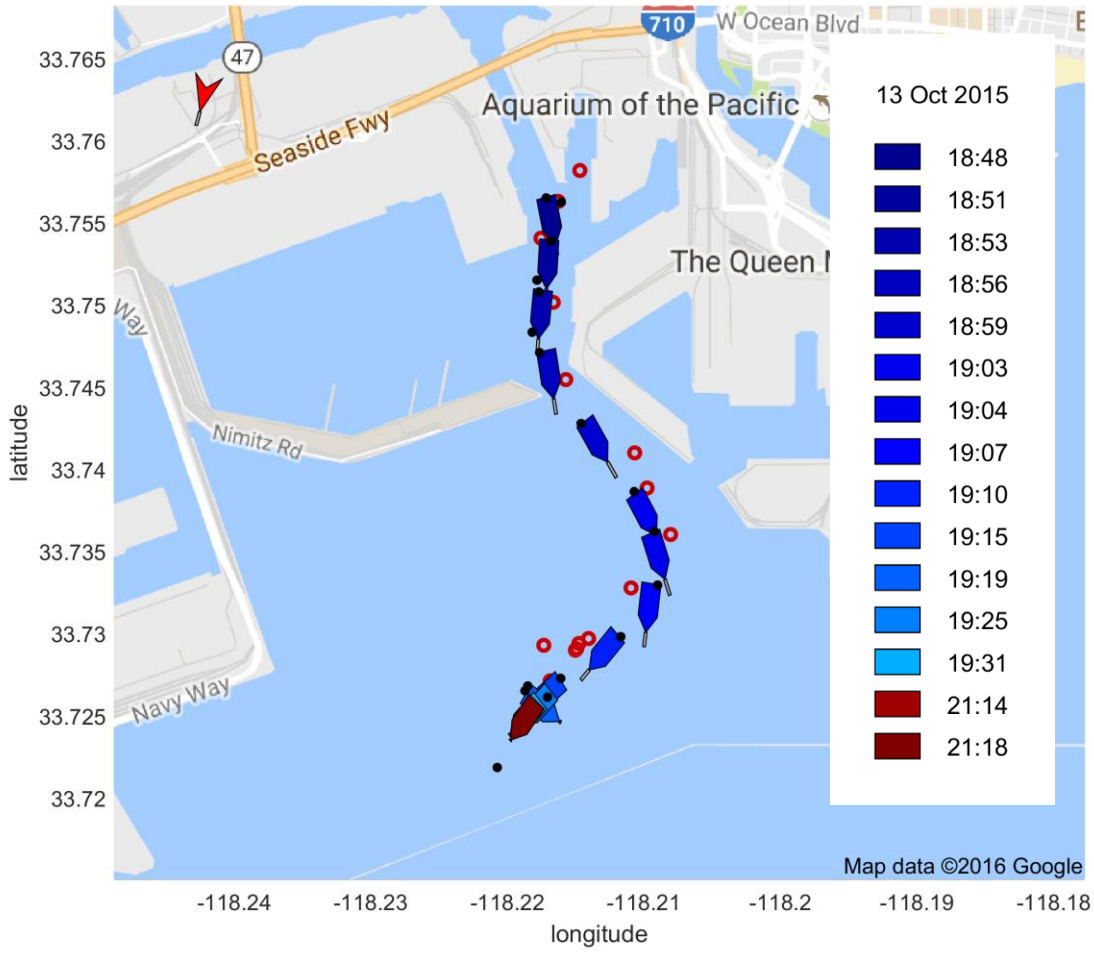

Figure A. 21. An illustration of a chase study of the tanker vessel AQUALEGEND.

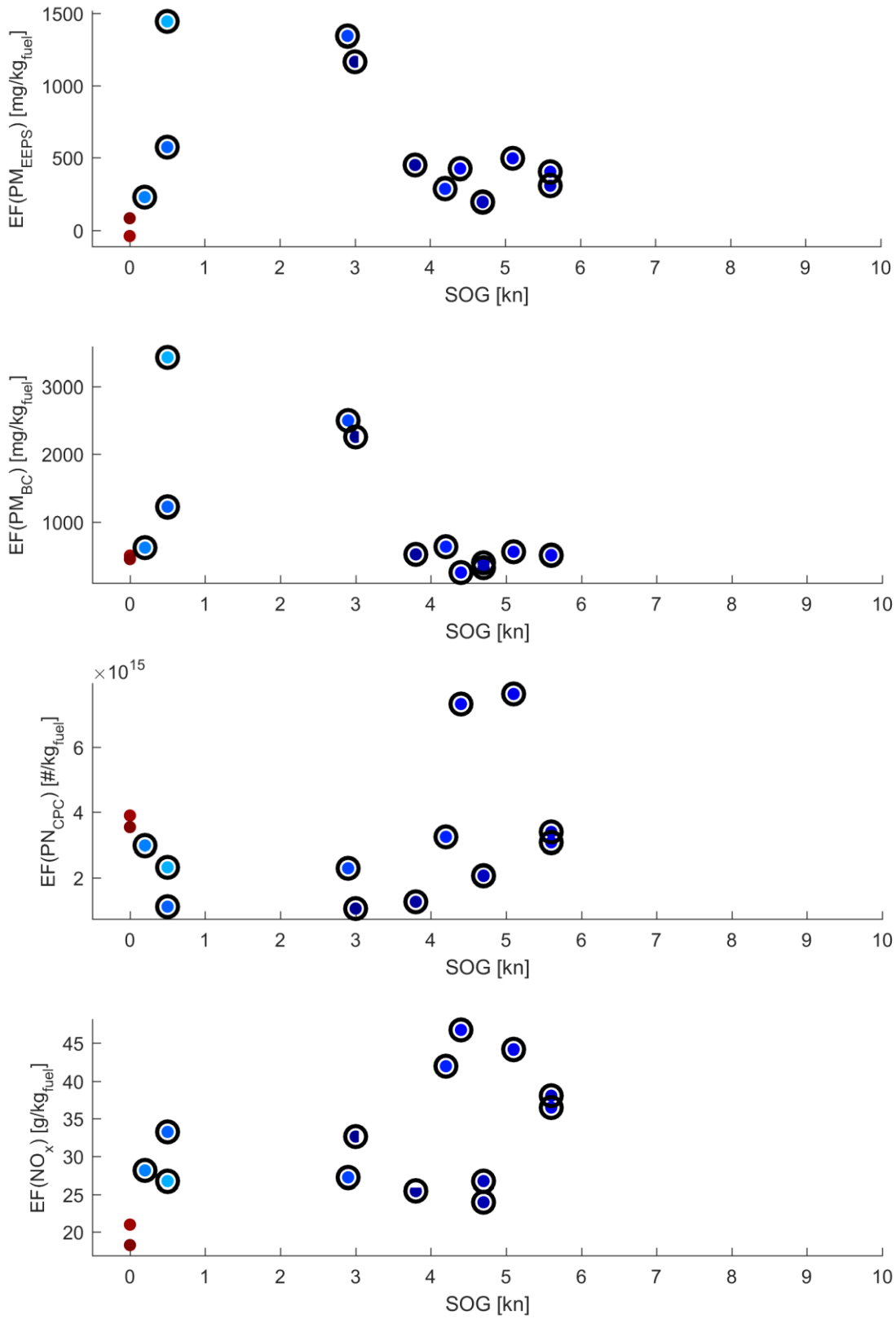

Figure A. 22. Specific emissions factors versus speed for AQUALEGEND. Different colours correspond to different times as shown in the legend in the corresponding map.

8.2.2 CHEMICAL AQUARIUS (25 Oct 2015, 22:37

Table A. 12. Detailed vessel information from Sea-web on CHEMICAL AQUARIUS (IHS, 2016).

IMO	MMSI	Flag	GT	DWT	YoB	MEng	Tot. Power	RPM	Stroke
9576820	477211400	Hong Kong	11,383	18,045	2012	Oil	5,180 kW	173	2

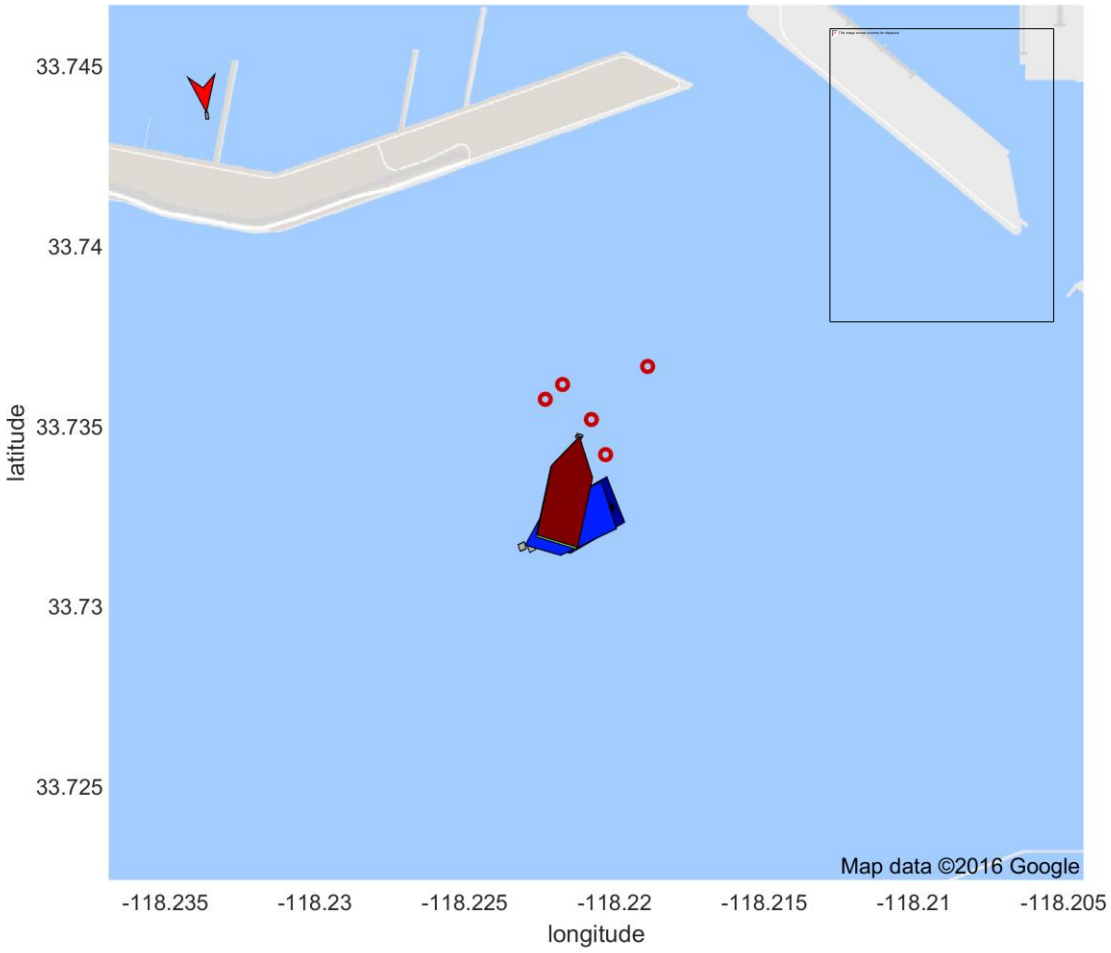

Figure A. 23. An illustration of a chase study of the tanker vessel CHEMICAL AQUARIUS.

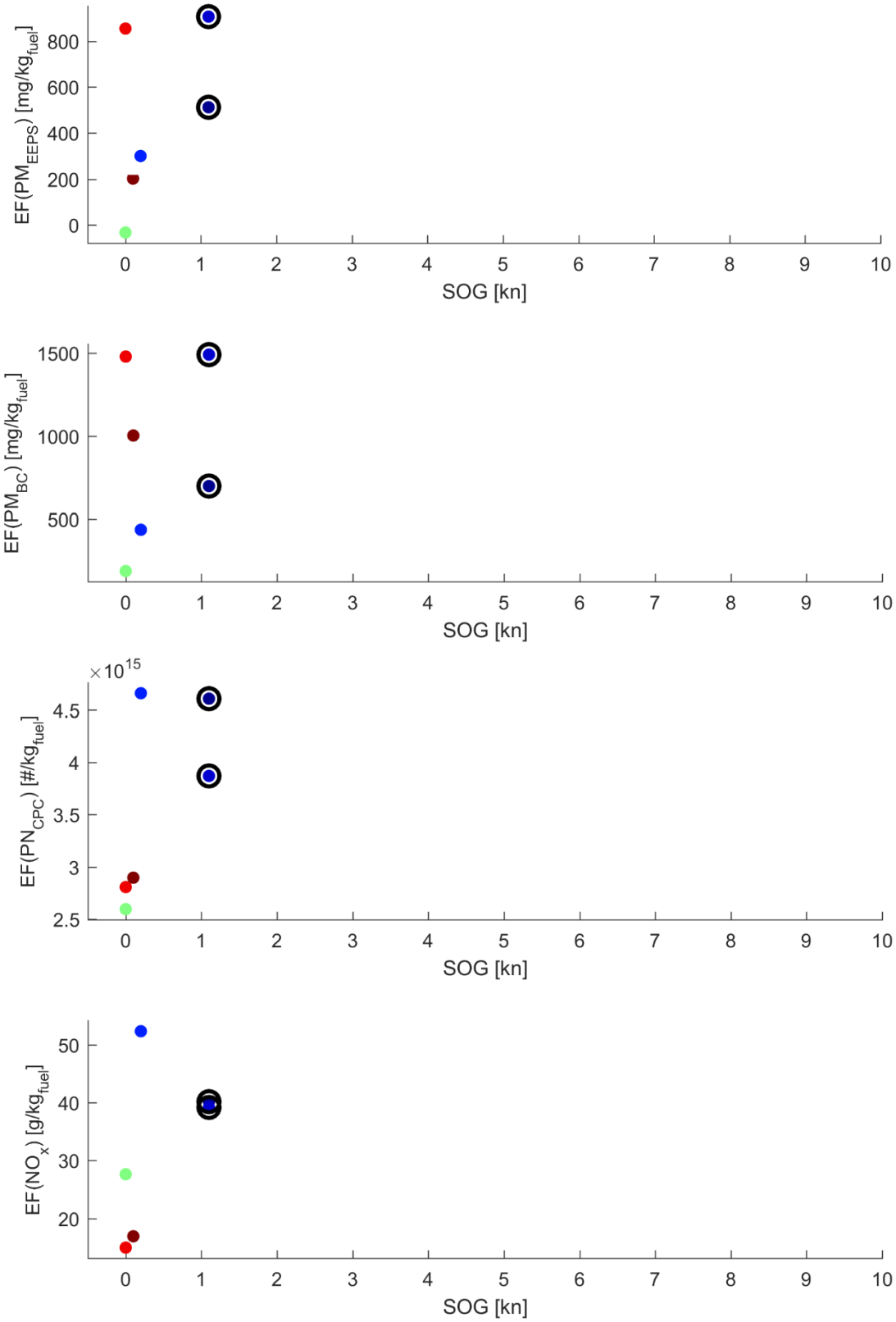

Figure A. 24. Specific emissions factors versus speed for CHEMICAL AQUARIUS. Different colours correspond to different times as shown in the legend in the corresponding map.

8.2.3 GULF STREAM (15 Oct 2015, 18:08)

Table A. 13. Detailed vessel information from Sea-web on GULF STREAM (IHS, 2016).

IMO	MMSI	Flag	GT	DWT	YoB	MEng	Tot. Power	RPM	Stroke
9298662	309038000	Bahamas	42,443	74,999	2005	Oil	13,539 kW	105	2

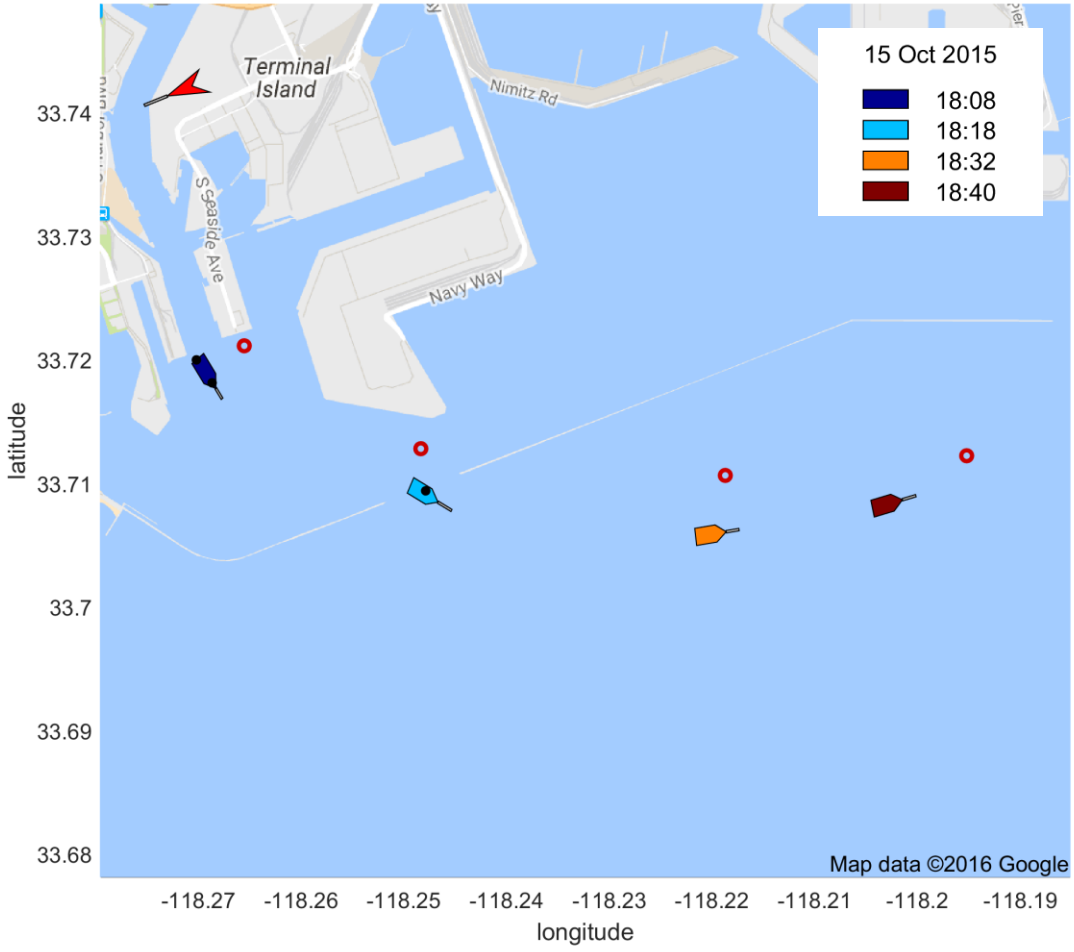

Figure A. 25. An illustration of a chase study of the tanker vessel GULF STREAM.

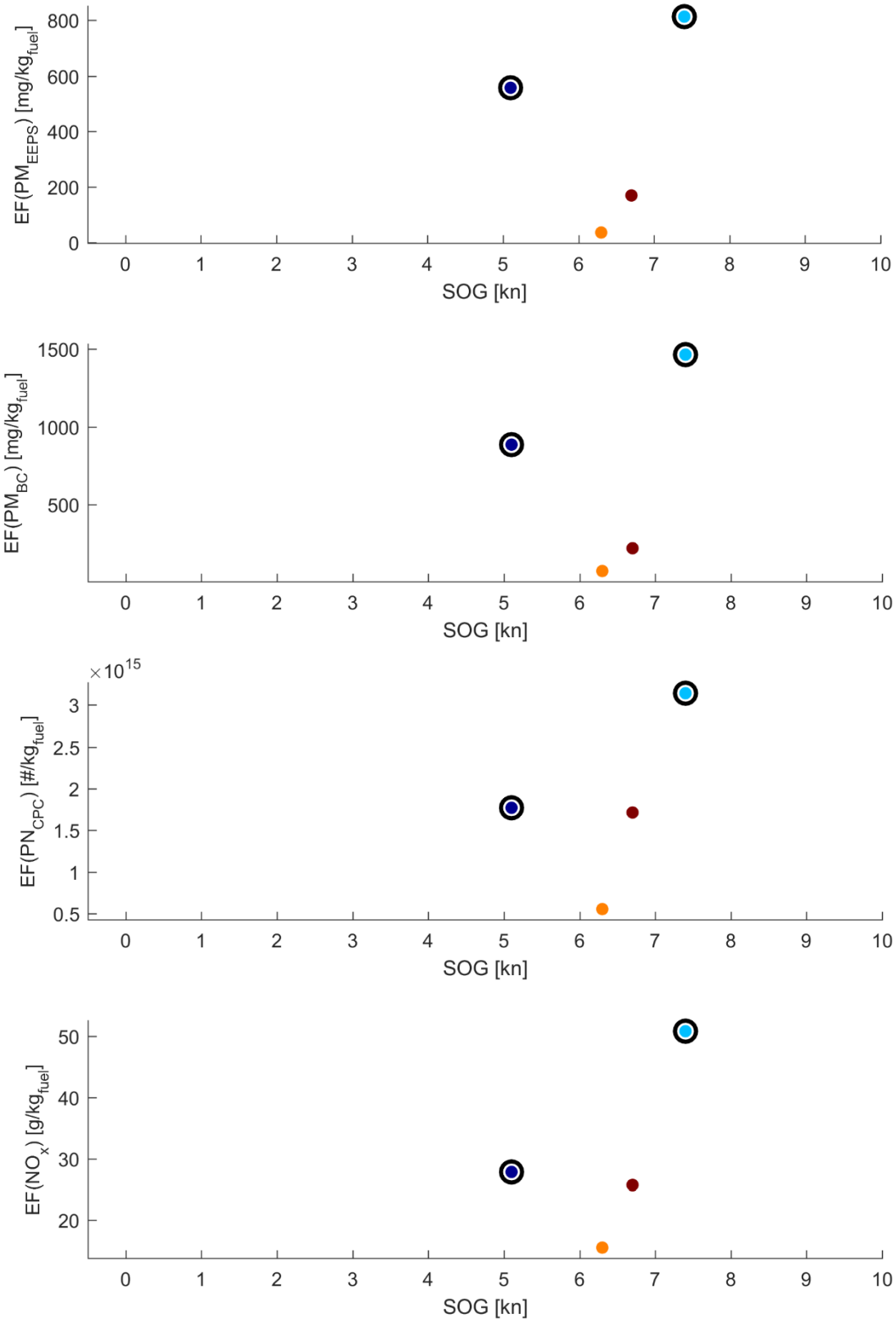

Figure A. 26. Specific emissions factors versus speed for GULF STREAM. Different colours correspond to different times as shown in the legend in the corresponding map.

8.2.4 KALAMAS (16 Oct 2015, 20:07)

Table A. 14. Detailed vessel information from Sea-web on KALAMAS (IHS, 2016).

IMO	MMSI	Flag	GT	DWT	YoB	MEng	Tot. Power	RPM	Stroke
9460564	636014807	Liberia	55,909	105,391	2011	Oil	13,560 kW	105	2

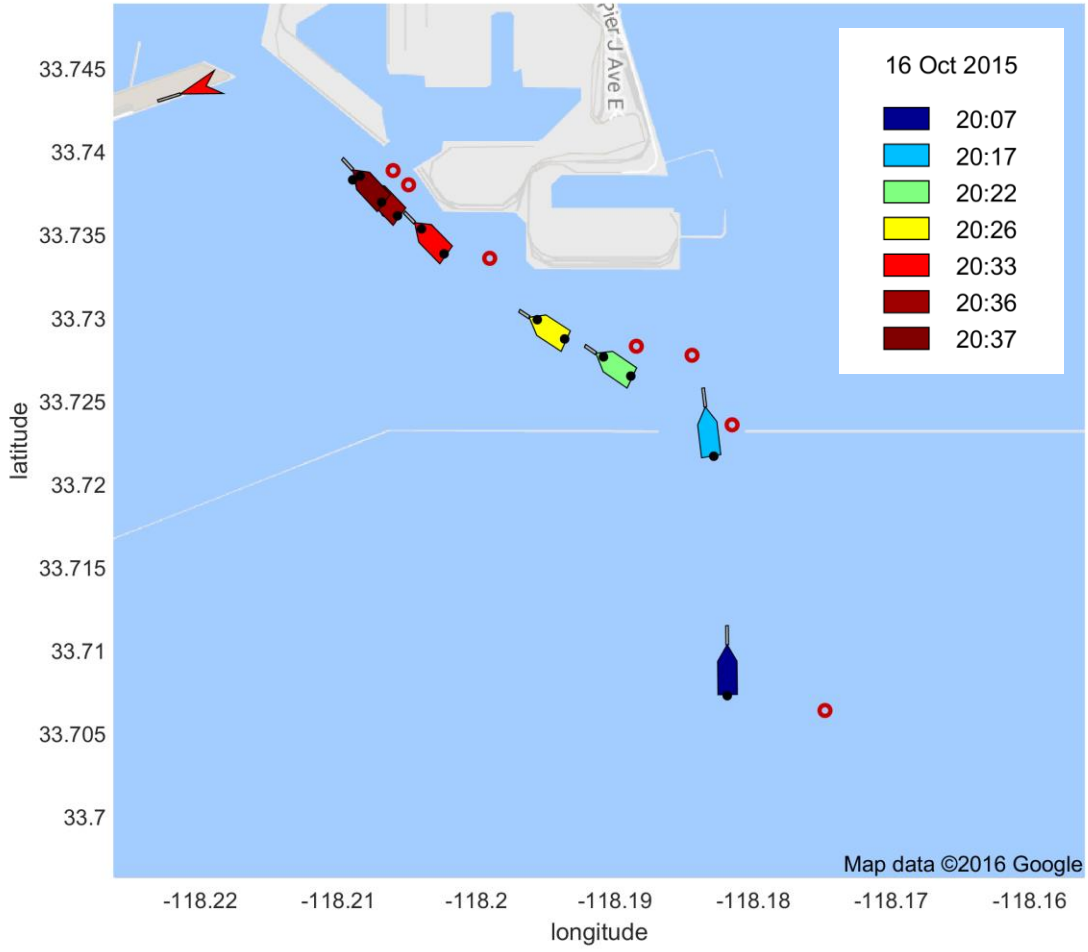

Figure A. 27. An illustration of a chase study of the tanker vessel KALAMAS.

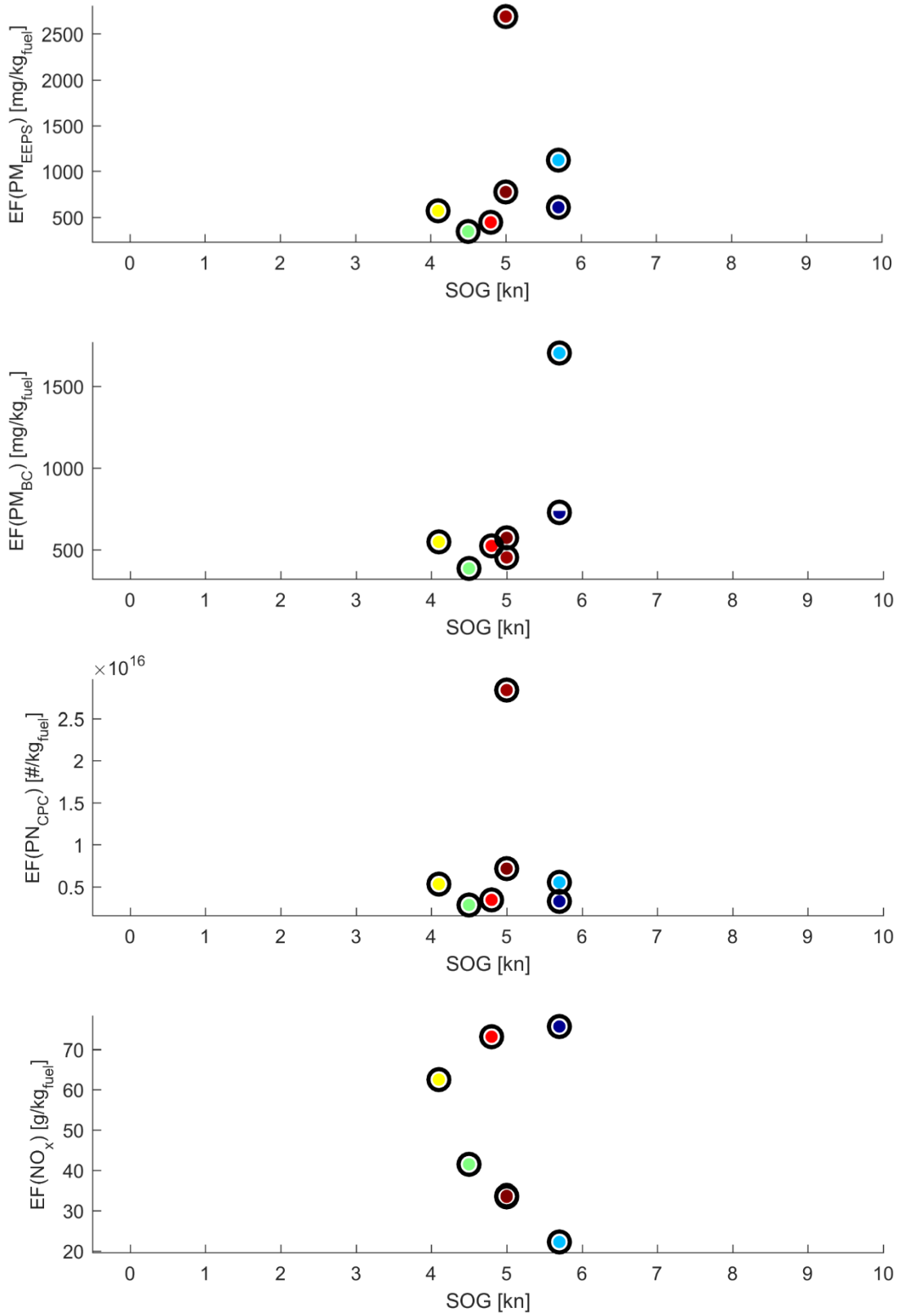

Figure A. 28. Specific emissions factors versus speed for KALAMAS. Different colours correspond to different times as shown in the legend in the corresponding map.

8.2.5 NORD GAINER (15 Oct 2015, 19:05)

Table A. 15. Detailed vessel information from Sea-web on NORD GAINER (IHS, 2016).

IMO	MMSI	Flag	GT	DWT	YoB	MEng	Tot. Power	RPM	Stroke
9448724	219290000	Denmark	30,241	50,281	2011	Oil	9,480 kW	127	2

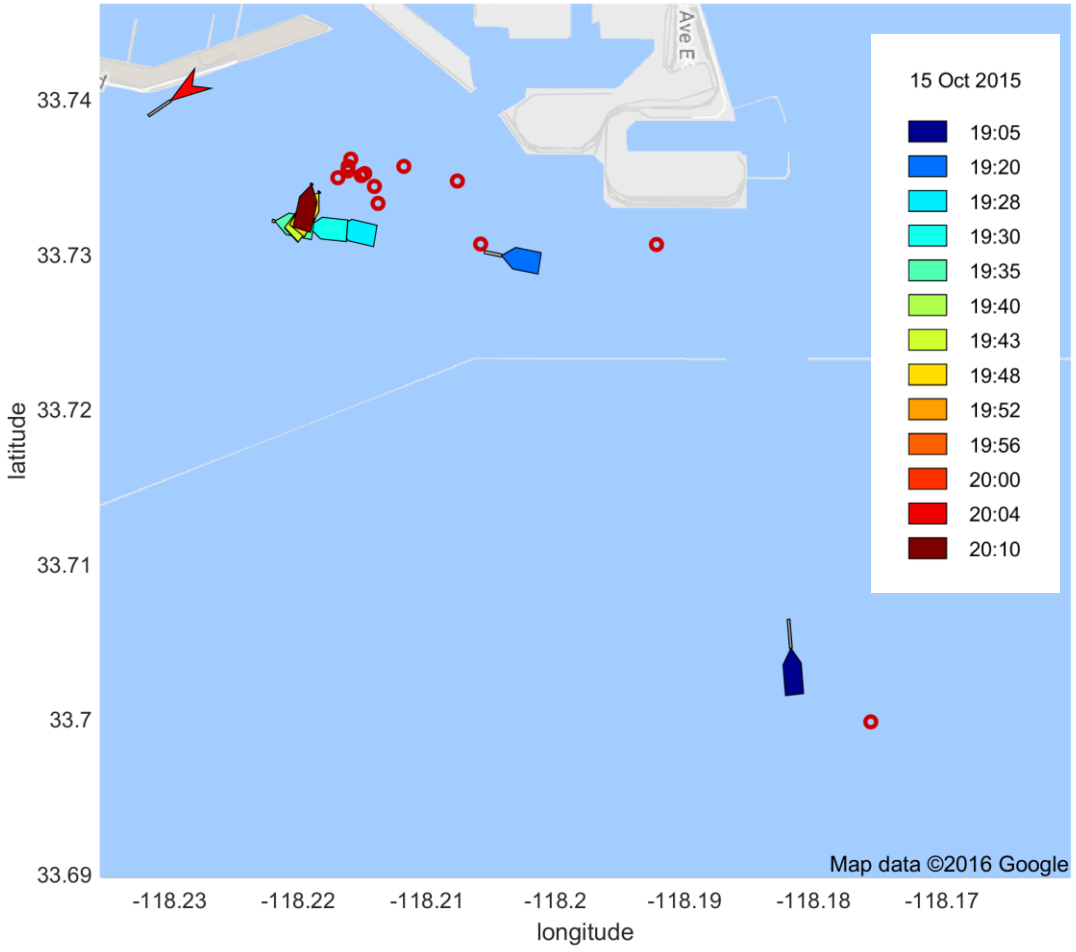

Figure A. 29. An illustration of a chase study of the tanker vessel NORD GAINER.

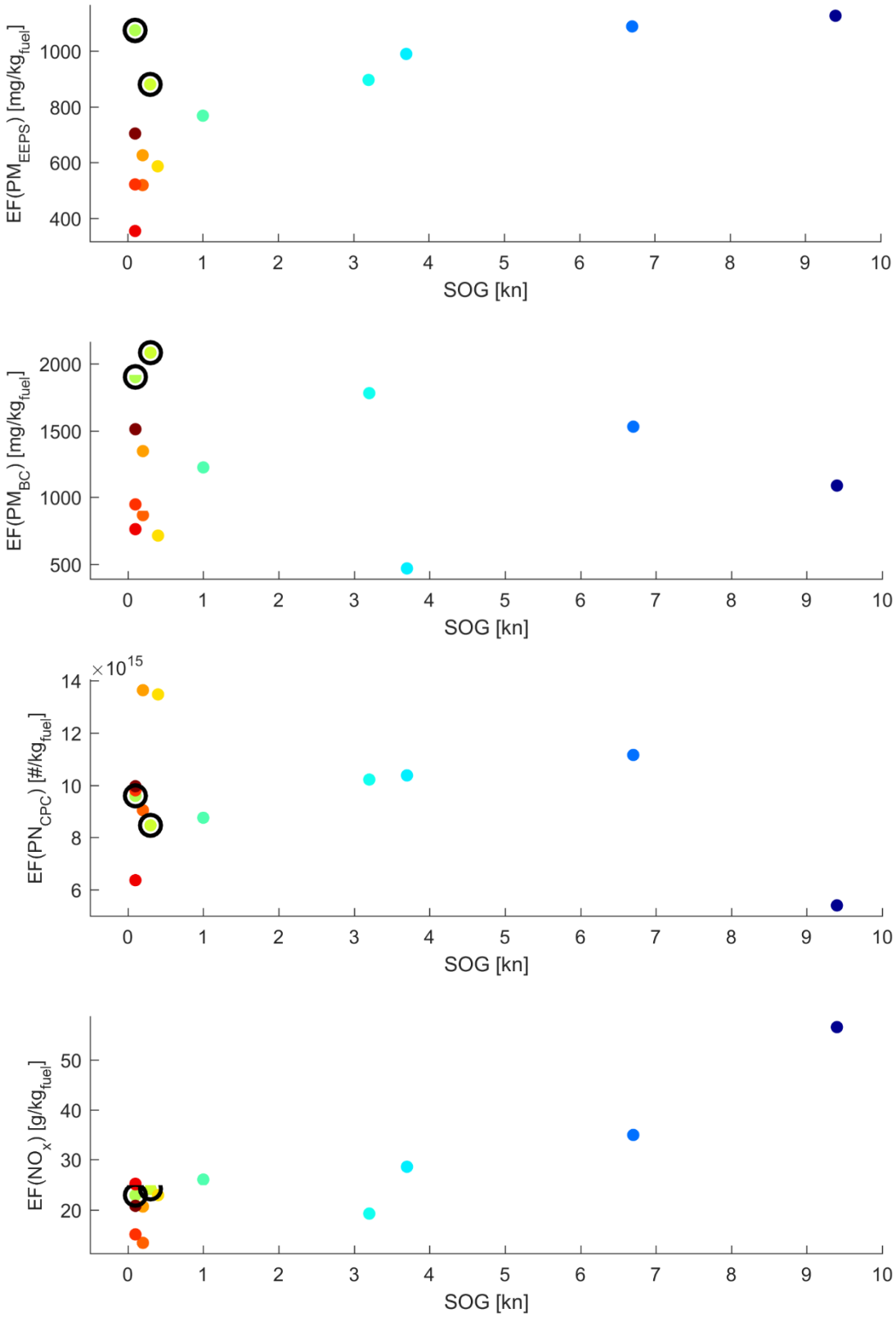

Figure A. 30. Specific emissions factors versus speed for NORD GAINER. Different colours correspond to different times as shown in the legend in the corresponding map.

8.2.6 NORD GOODWILL (15 Oct 2015, 20:15)

Table A. 16. Detailed vessel information from Sea-web on NORD GOODWILL (IHS, 2016).

IMO	MMSI	Flag	GT	DWT	YoB	MEng	Tot. Power	RPM	Stroke
9448334	219011000	Denmark	30,241	50,326	2009	Oil	9,960 kW	127	2

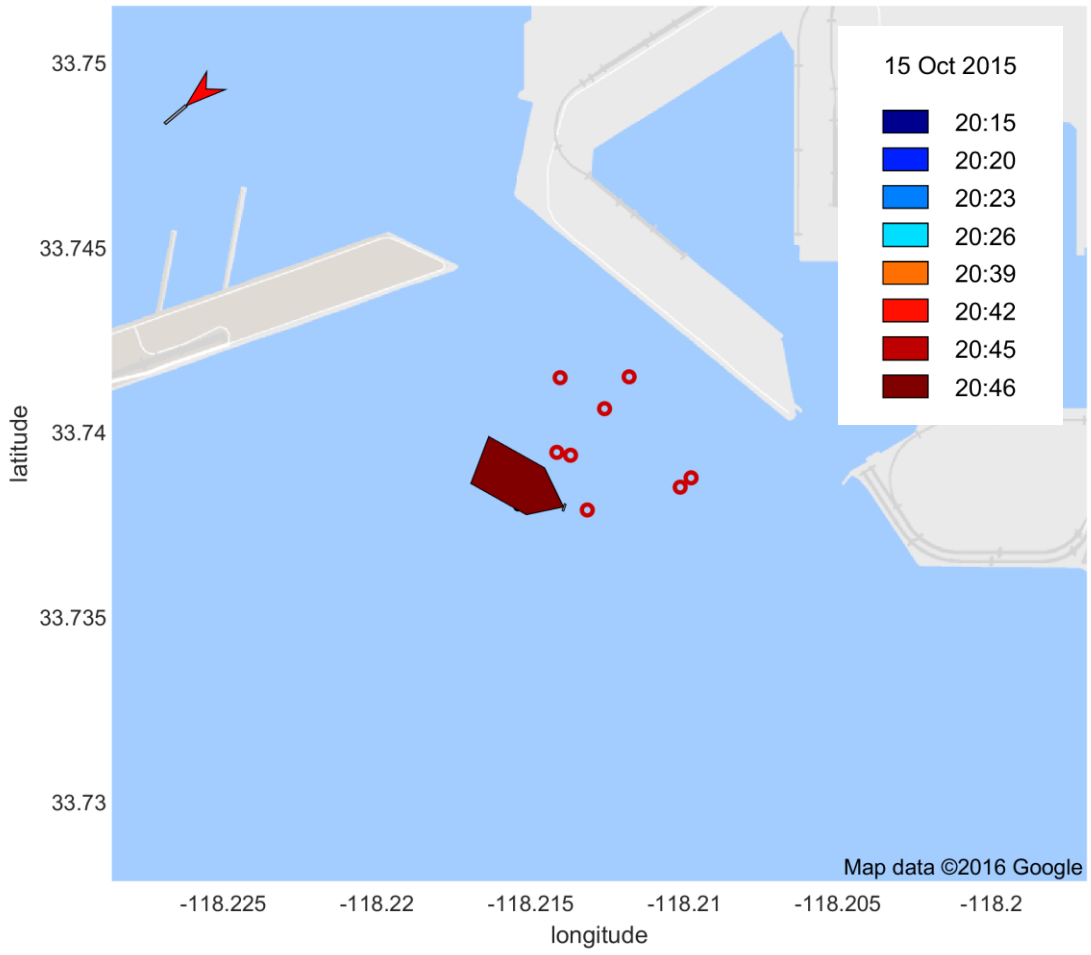

Figure A. 31. An illustration of a chase study of the tanker vessel NORD GOODWILL.

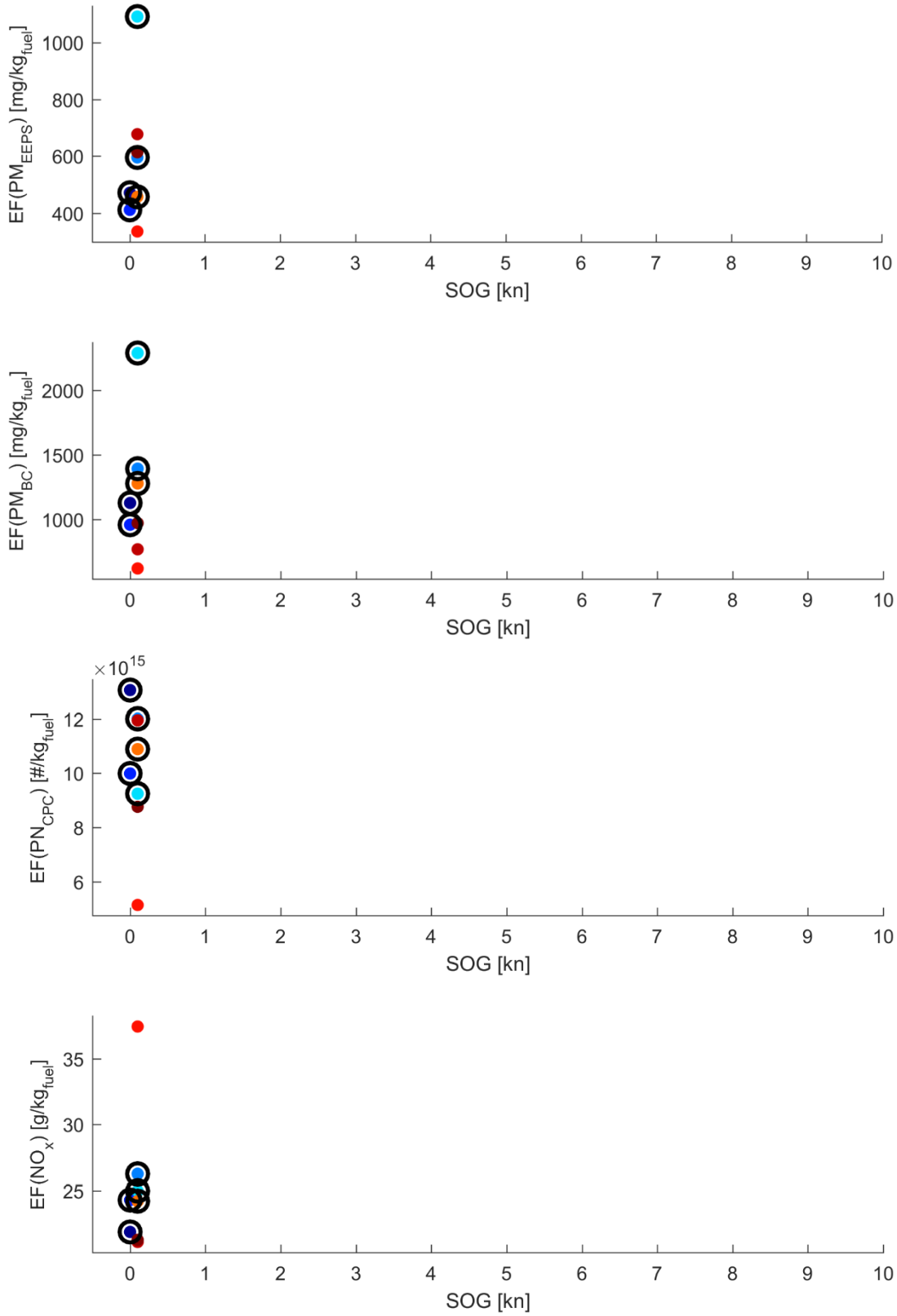

Figure A. 32. Specific emissions factors versus speed for NORD GOODWILL. Different colours correspond to different times as shown in the legend in the corresponding map.

8.2.7 STELLAR LILAC (25 Oct 2015, 19:18)

Table A. 17. Detailed vessel information from Sea-web on STELLAR LILAC (IHS, 2016).

IMO	MMSI	Flag	GT	DWT	YoB	MEng	Tot. Power	RPM	Stroke
9499943	370731000	Panama	7,522	12,601	2008	Oil	4,200 kW	170	2

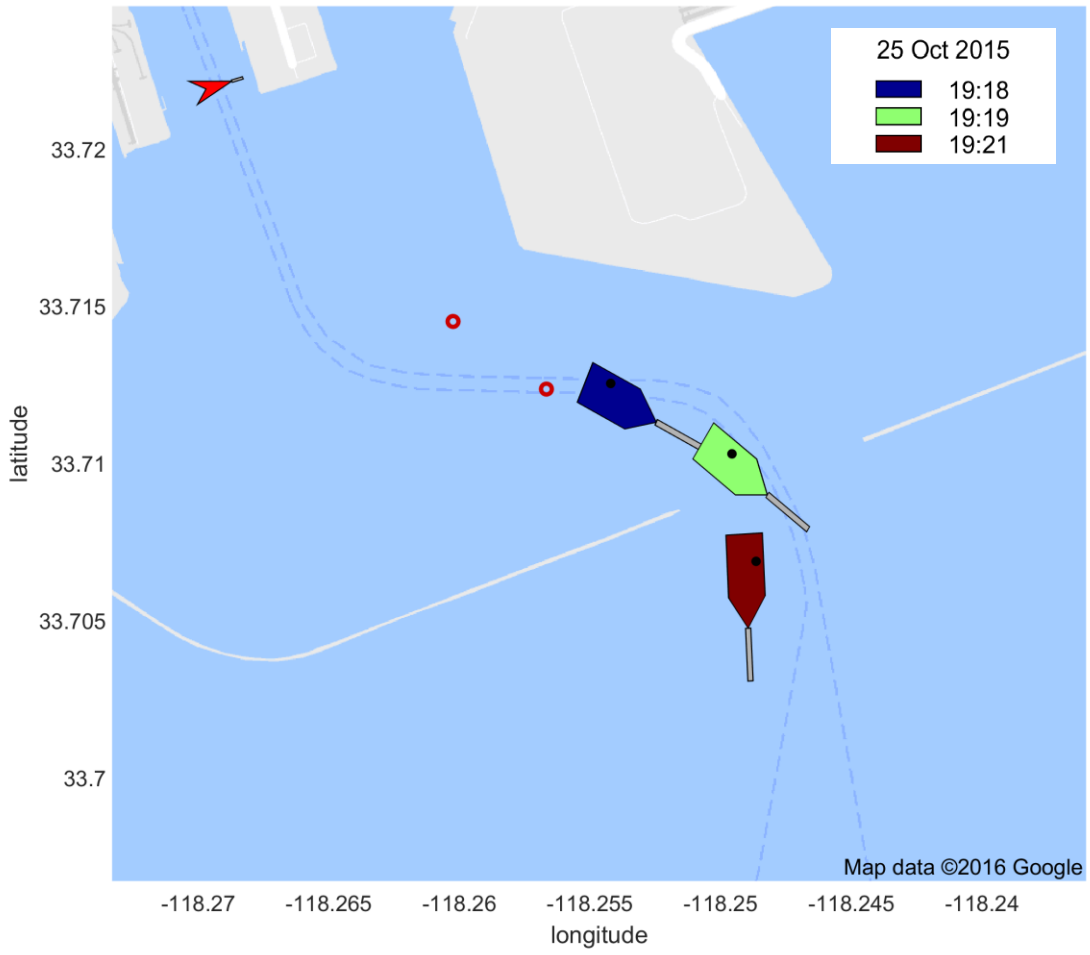

Figure A. 33. An illustration of a chase study of the tanker vessel STELLAR LILAC.

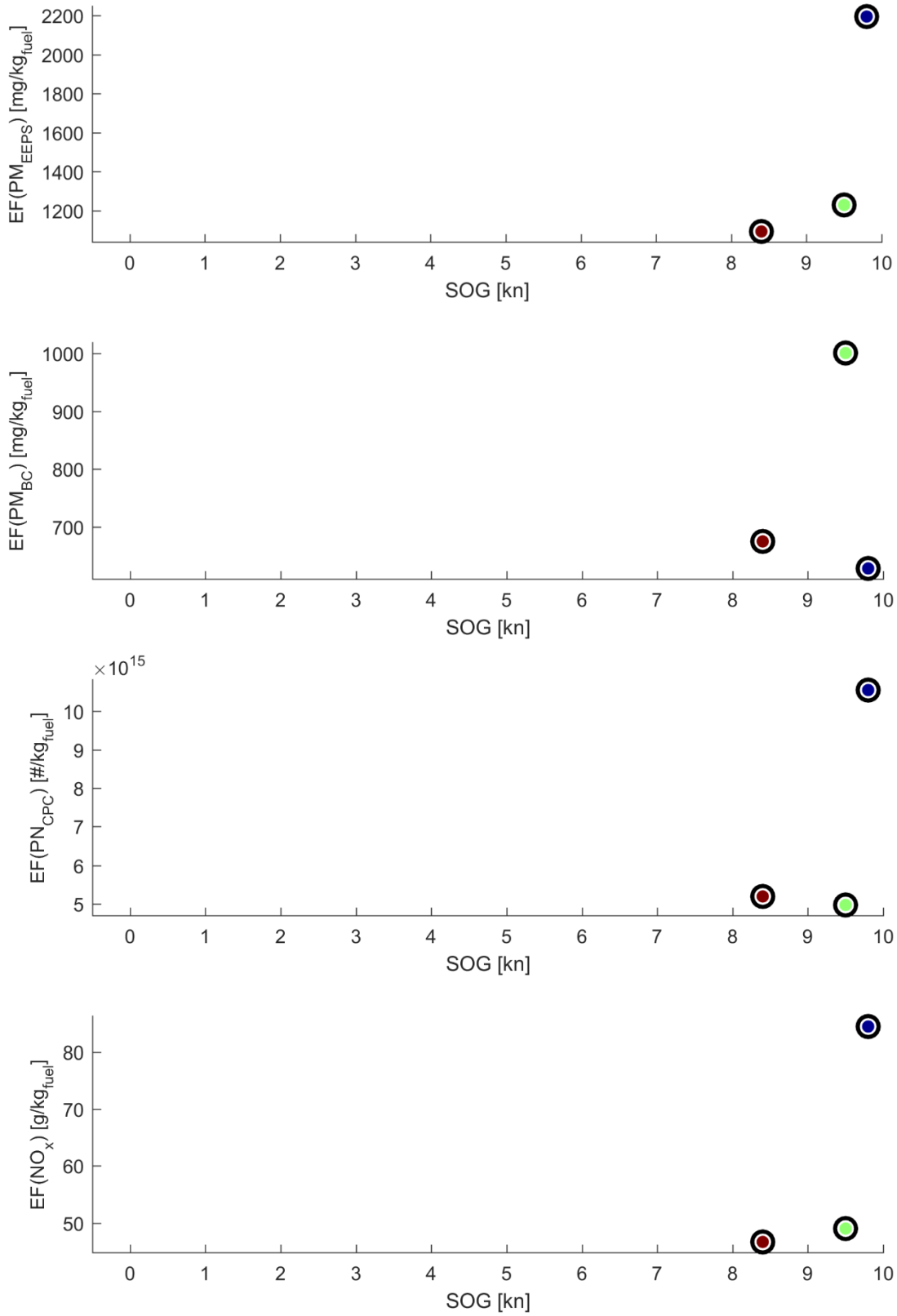

Figure A. 34. Specific emissions factors versus speed for STELLAR LILAC. Different colours correspond to different times as shown in the legend in the corresponding map.

8.2.8 TAQAH (16 Oct 2015, 18:37)

Table A. 18. Detailed vessel information from Sea-web on TAQAH (IHS, 2016).

IMO	MMSI	Flag	GT	DWT	YoB	MEng	Tot. Power	RPM	Stroke
9501174	538004833	Marshall Islands	162,960	316,373	2012	Oil	31,640 kW	80	2

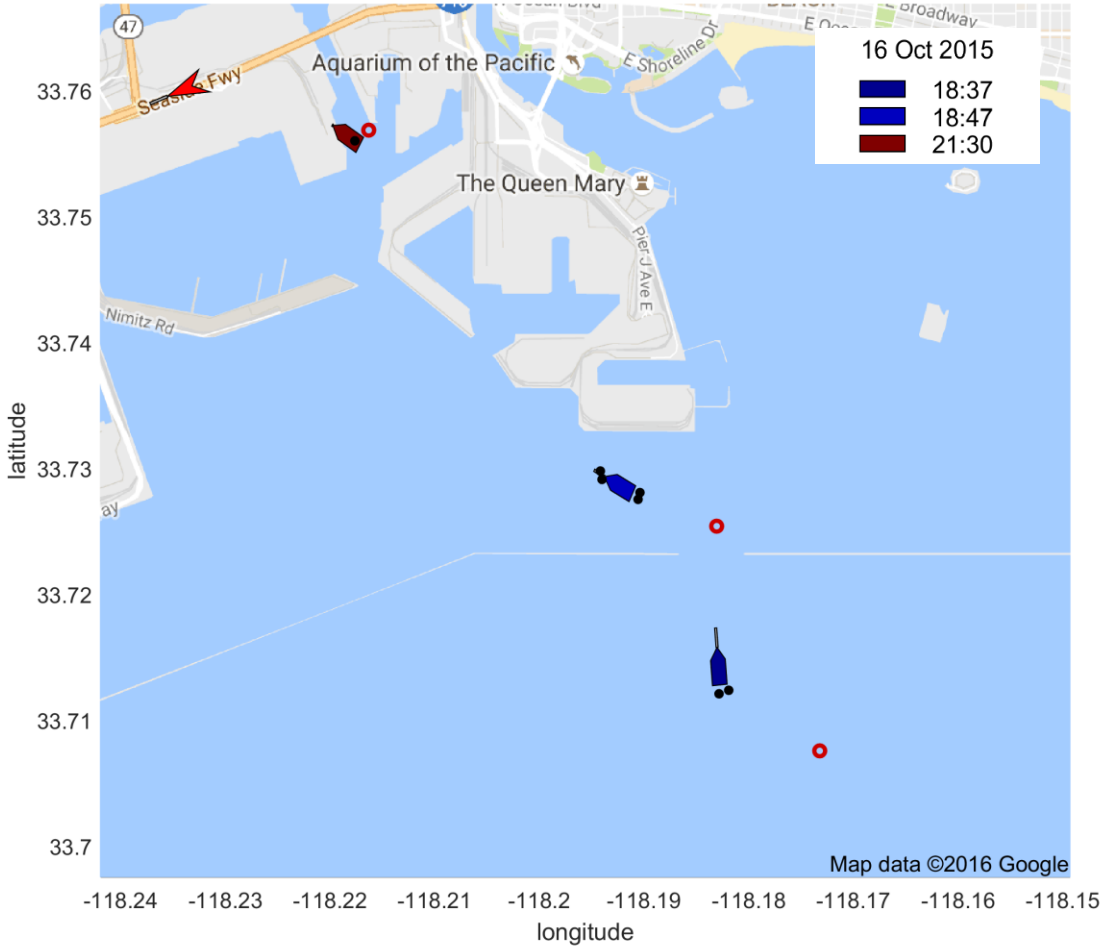

Figure A. 35. An illustration of a chase study of the tanker vessel TAQAH.

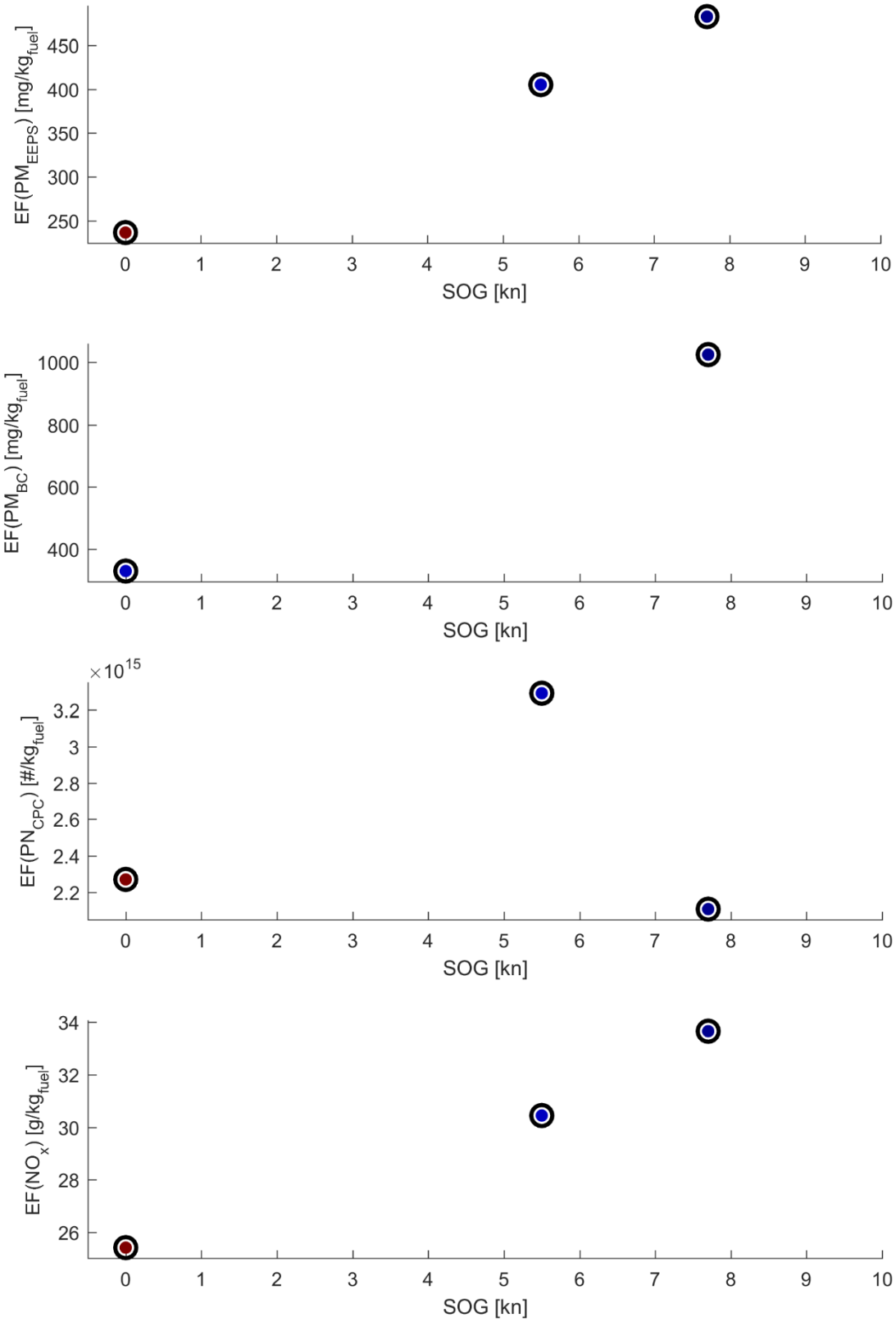

Figure A. 36. Specific emissions factors versus speed for TAQAH. Different colours correspond to different times as shown in the legend in the corresponding map.

8.3 Passenger vessels

8.3.1 CARNIVAL IMAGINATION (22 Oct 2015, 23:19)

Table A. 19. Detailed vessel information from Sea-web on CARNIVAL IMAGINATION (IHS, 2016).

IMO	MMSI	Flag	GT	DWT	YoB	MEng	Tot. Power	RPM	Stroke
9053878	309933000	Bahamas	70,367	7,180	1995	Diesel-electric	42,240 kW	140	4

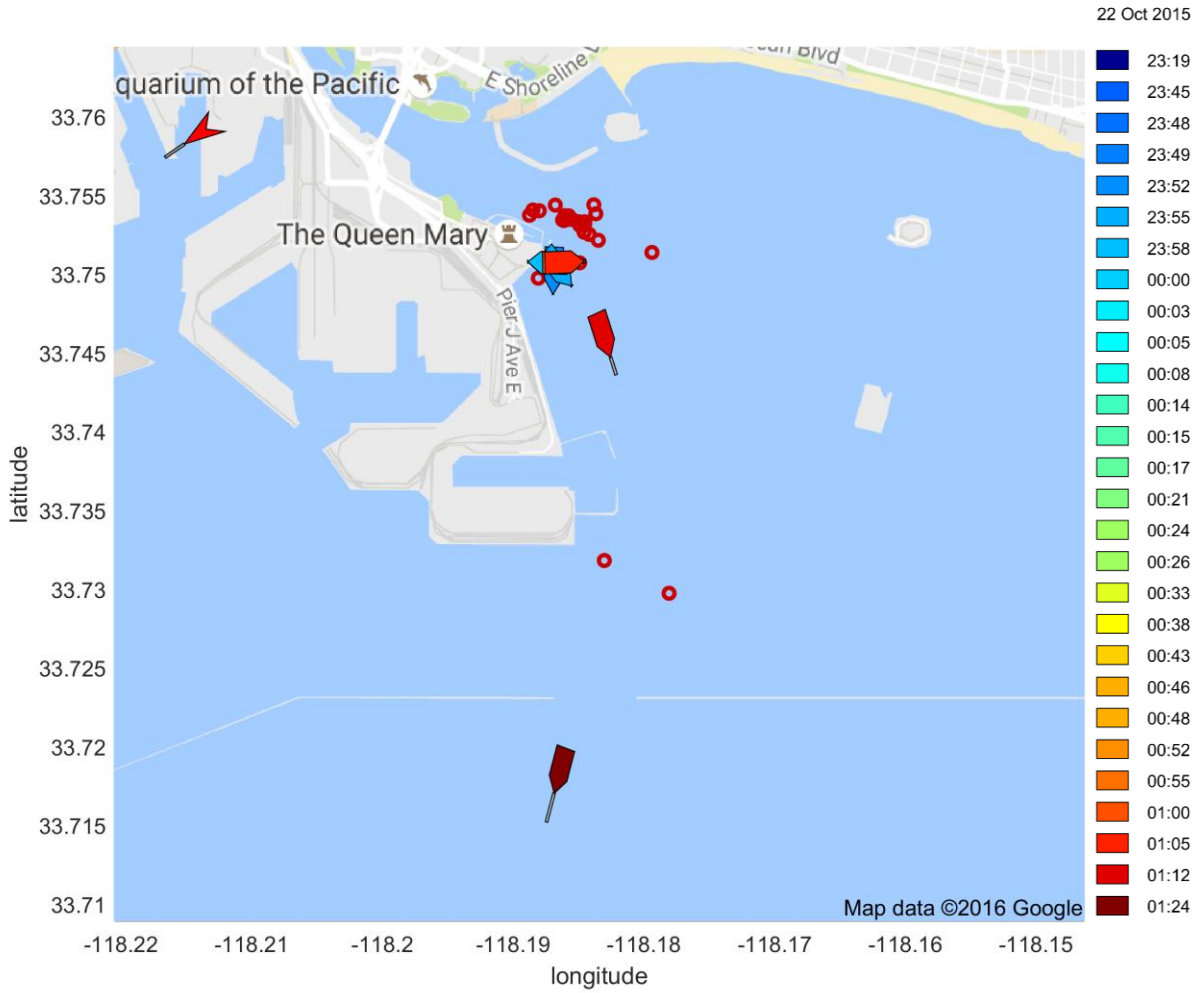

Figure A. 37. An illustration of a chase study of the passenger vessel CARNIVAL IMAGINATION.

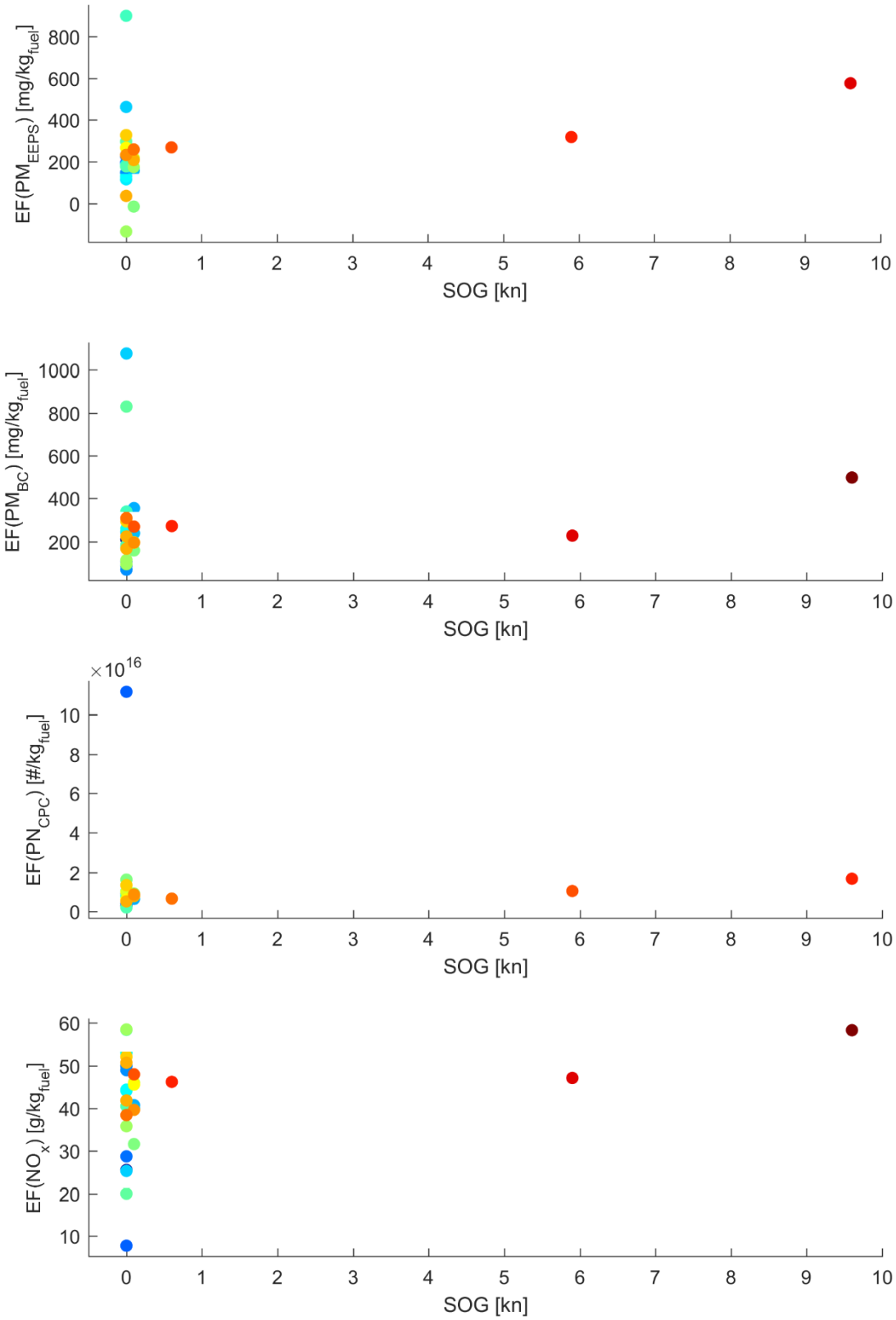

Figure A. 38. Specific emissions factors versus speed for CARNIVAL IMAGINATION. Different colours correspond to different times as shown in the legend in the corresponding map.

8.4 Harbor craft

8.4.1 ARTHUR FOSS (23 Oct 2015, 18:21)

Table A. 20. Detailed vessel information from Sea-web on ARTHUR FOSS (IHS, 2016).

IMO	MMSI	Flag	GT	DWT	YoB	MEng	Tot. Power	RPM	Stroke
8219011	366979360	United States	372	0	1982	Oil	2,868 kW	NA	2

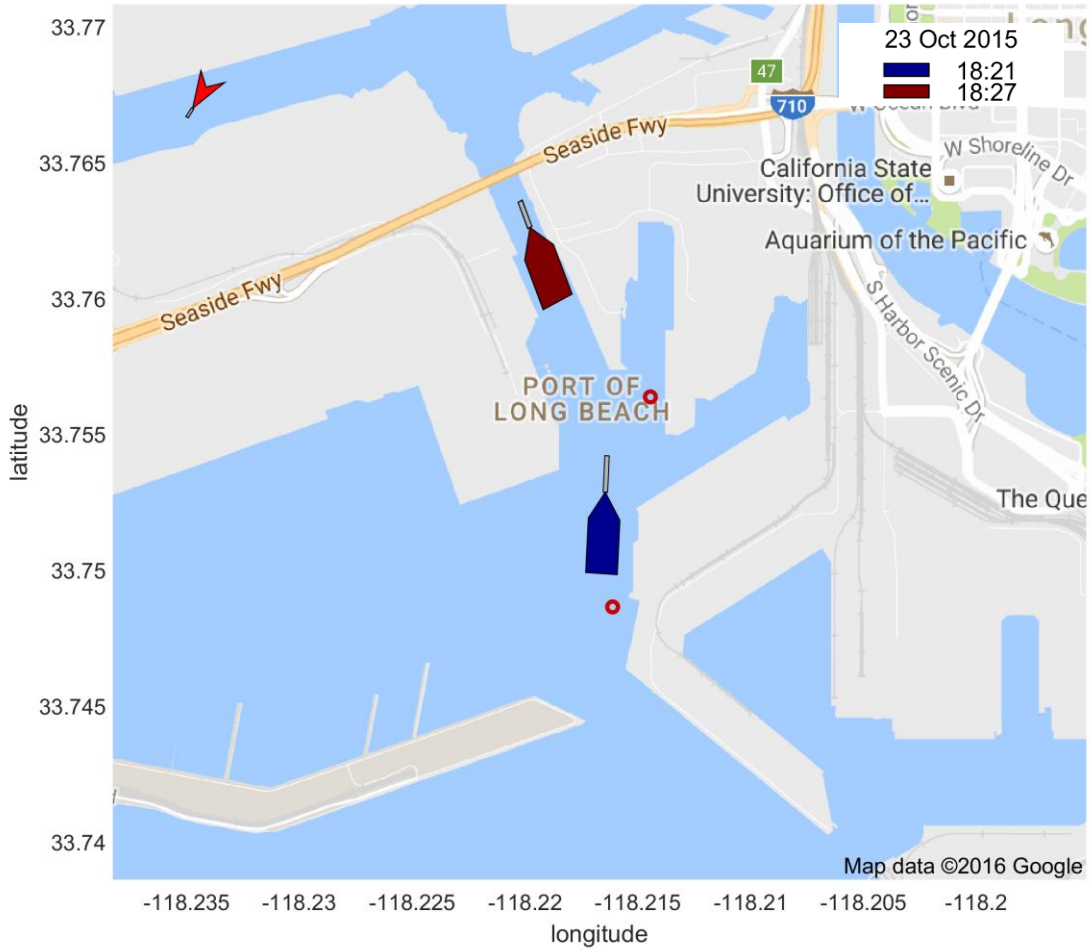

Figure A. 39. An illustration of a chase study of the harbor craft ARTHUR FOSS.

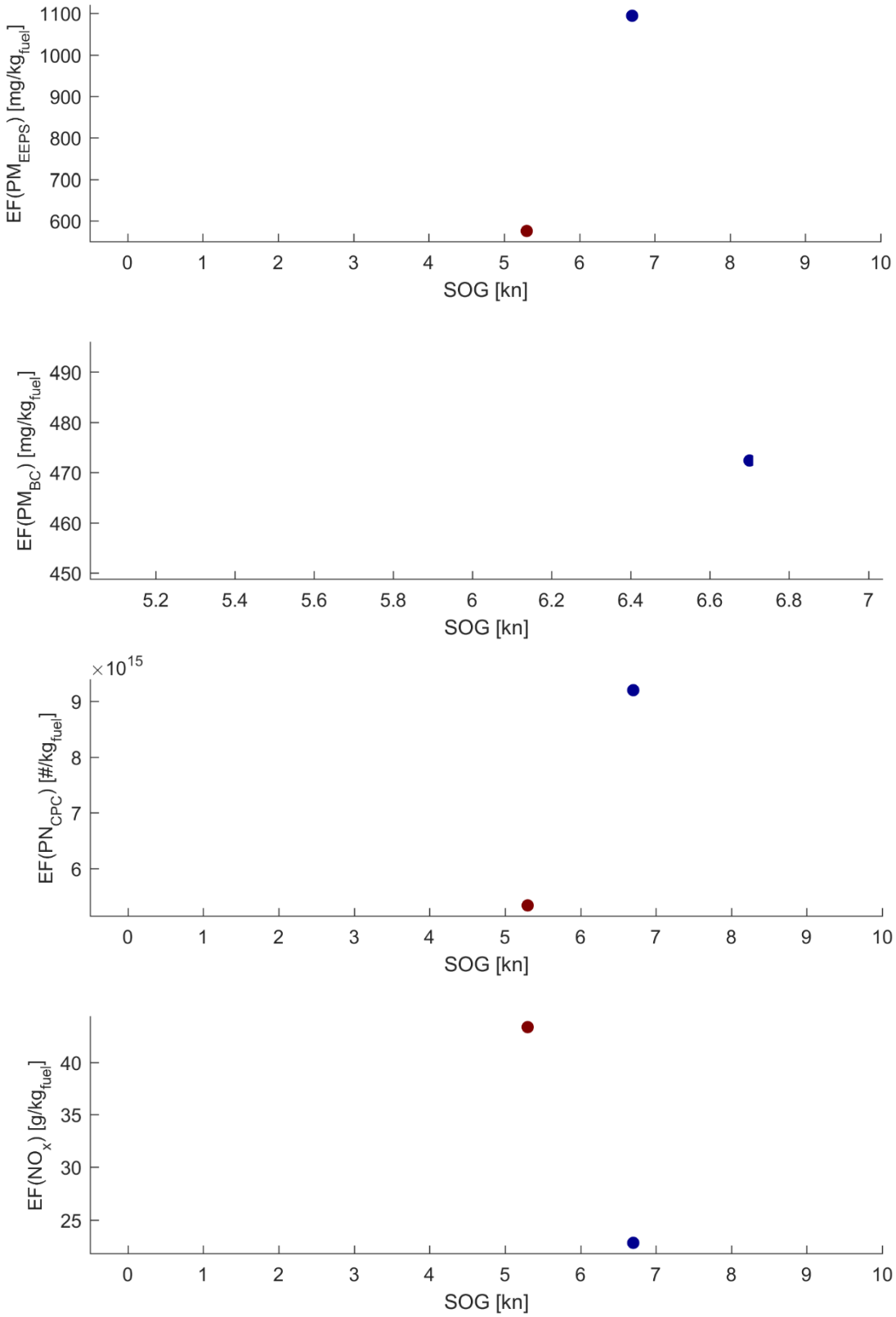

Figure A. 40. Specific emissions factors versus speed for ARTHUR FOSS. Different colours correspond to different times as shown in the legend in the corresponding map.

8.4.2 CAROLYN DOROTHY (19 Oct 2015, 20:53)

Table A. 21. Detailed vessel information from Sea-web on CAROLYN DOROTHY (IHS, 2016).

IMO	MMSI	Flag	GT	DWT	YoB	MEng	Tot. Power	RPM	Stroke
9552288	367384780	United States	144	0	2009	Oil + electric	2,648 kW	1800	4

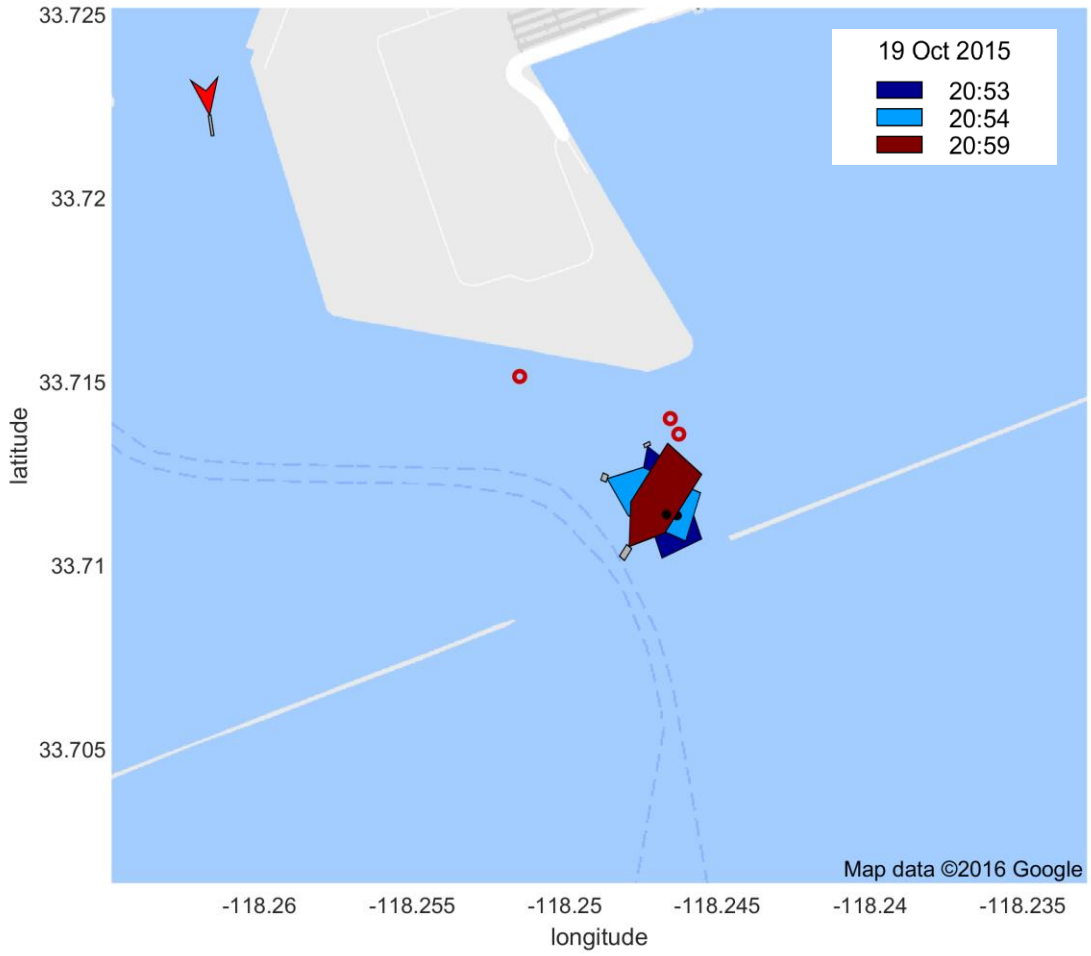

Figure A. 41. An illustration of a chase study of the harbor craft CAROLYN DOROTHY.

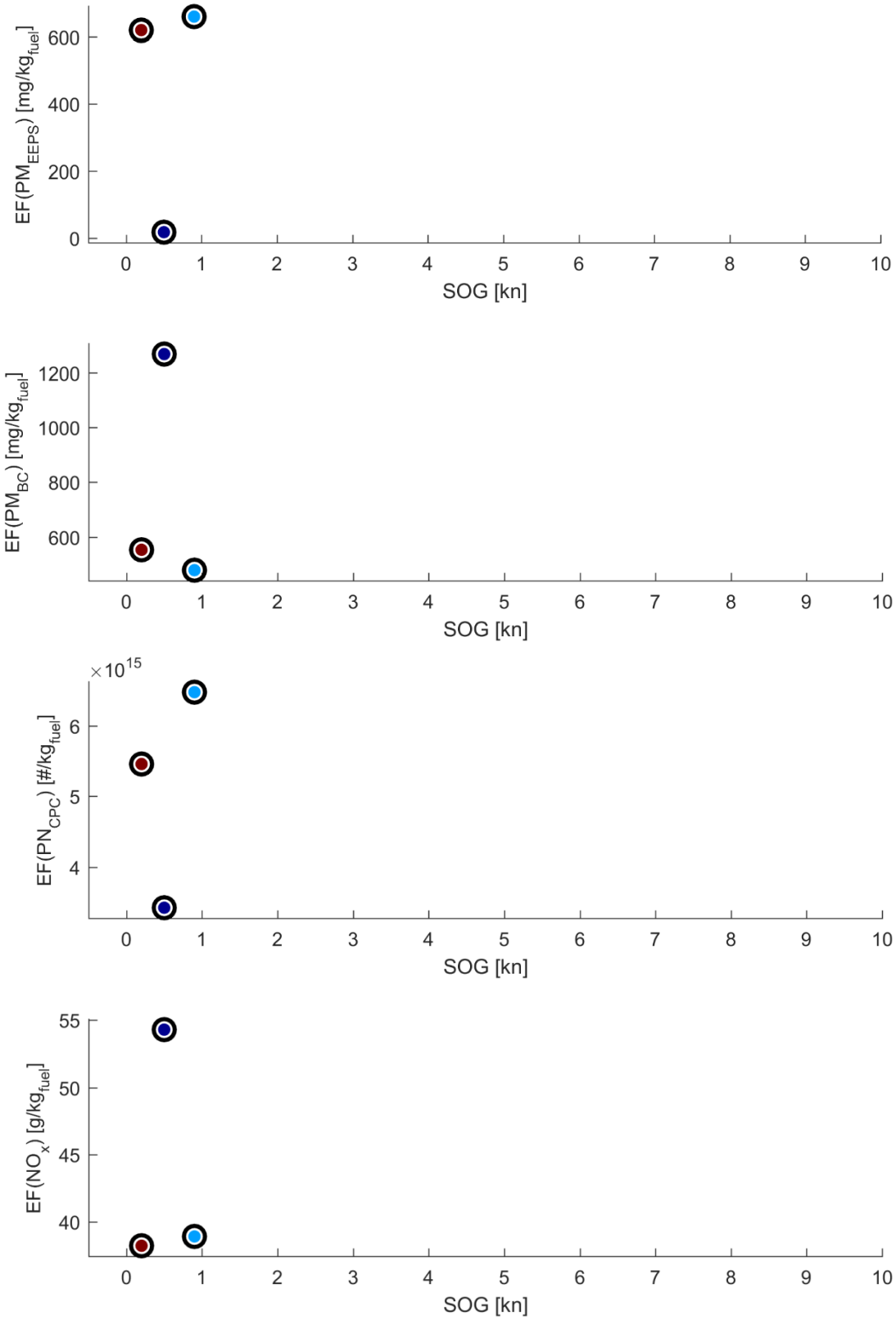

Figure A. 42. Specific emissions factors versus speed for CAROLYN DOROTHY. Different colours correspond to different times as shown in the legend in the corresponding map.

8.4.3 LELA FRANCO (22 Oct 2015 18:57)

Table A. 22. Detailed vessel information from Sea-web on LELA FRANCO (IHS, 2016).

IMO	MMSI	Flag	GT	DWT	YoB	MEng	Tot. Power	RPM	Stroke
9747821	367678850	United States	175	0	2015	Oil	3,788 kW	1600	4

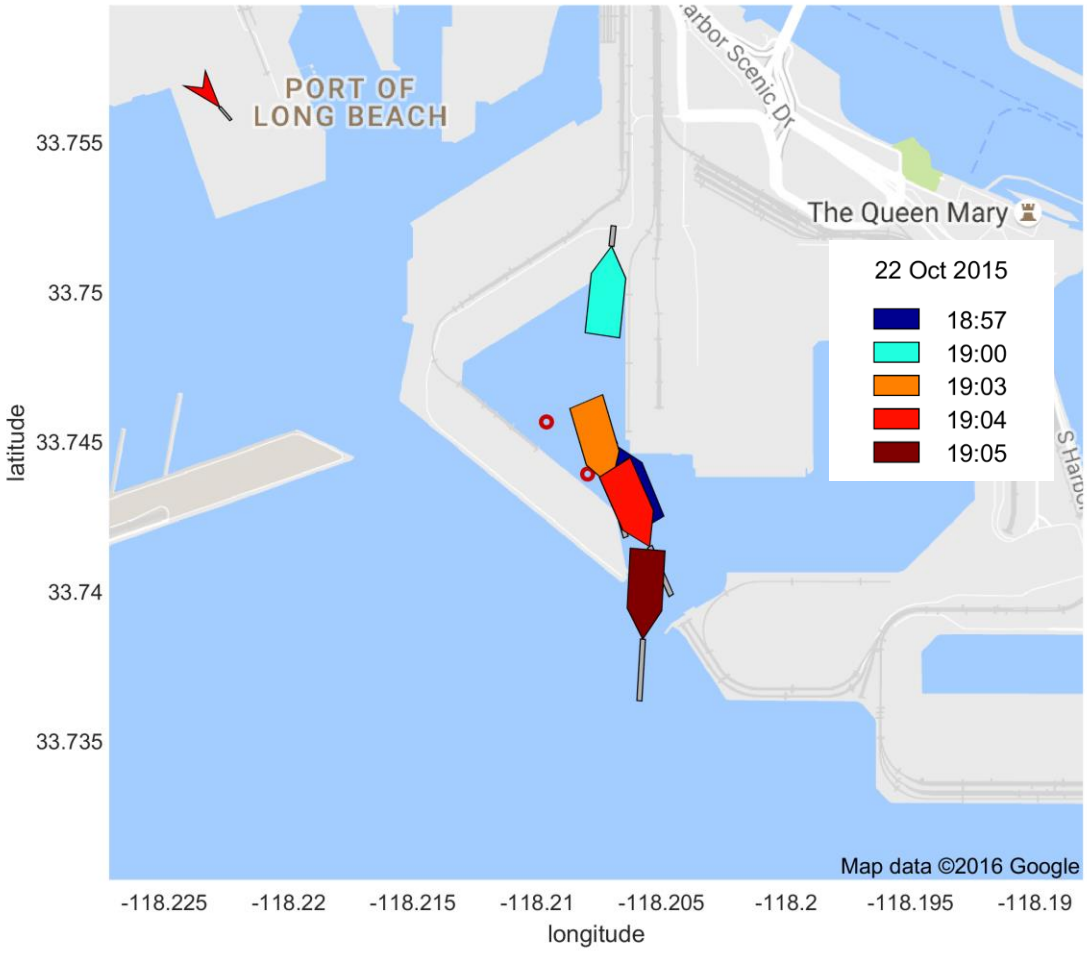

Figure A. 43. An illustration of a chase study of the harbor craft LELA FRANCO.

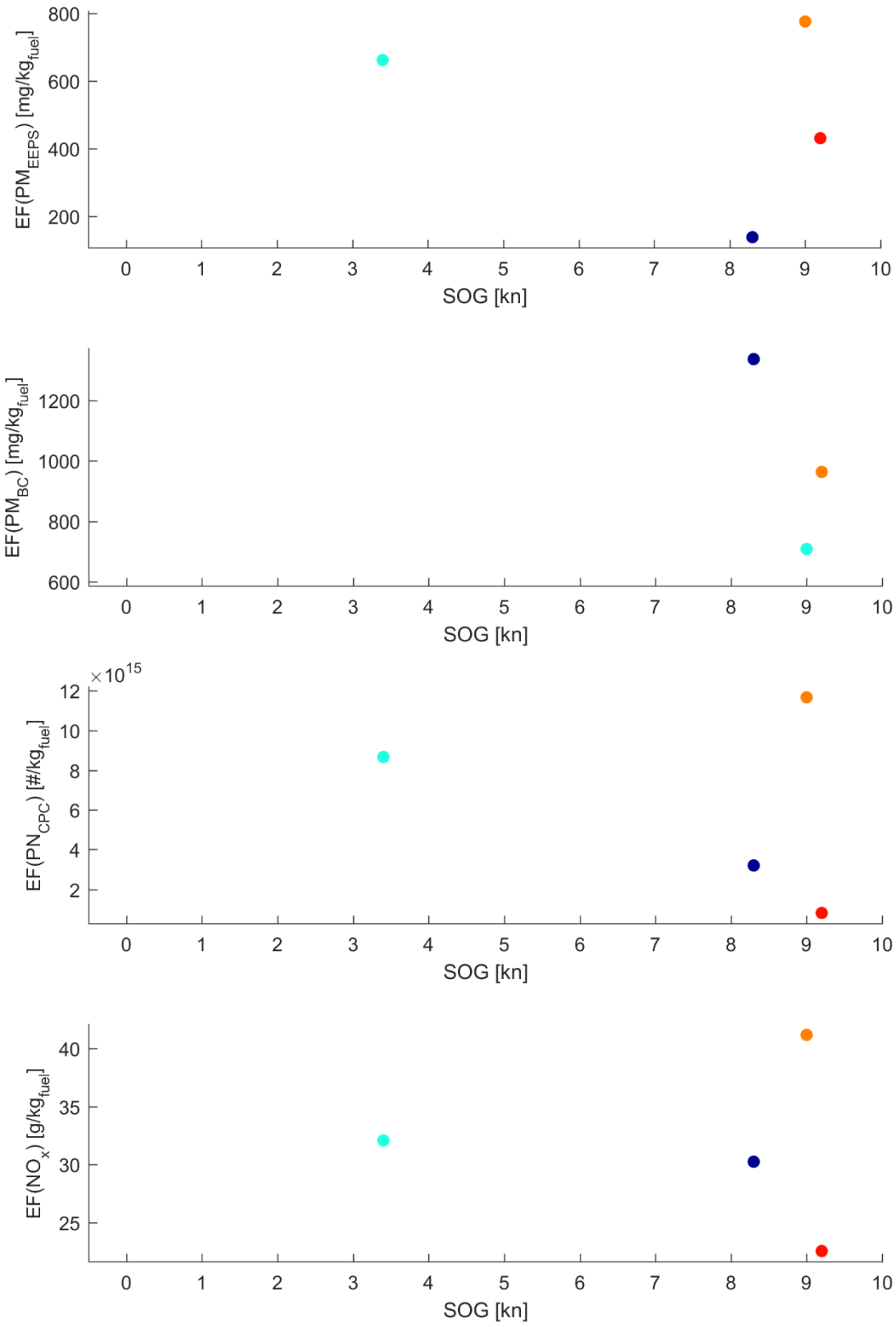

Figure A. 44. Specific emissions factors versus speed for LELA FRANCO. Different colours correspond to different times as shown in the legend in the corresponding map.

8.4.4 LELA FRANCO (27 Oct 2015 18:06)

Table A. 23. Detailed vessel information from Sea-web on LELA FRANCO (IHS, 2016).

IMO	MMSI	Flag	GT	DWT	YoB	MEng	Tot. Power	RPM	Stroke
9747821	367678850	United States	175	0	2015	Oil	3,788 kW	1600	4

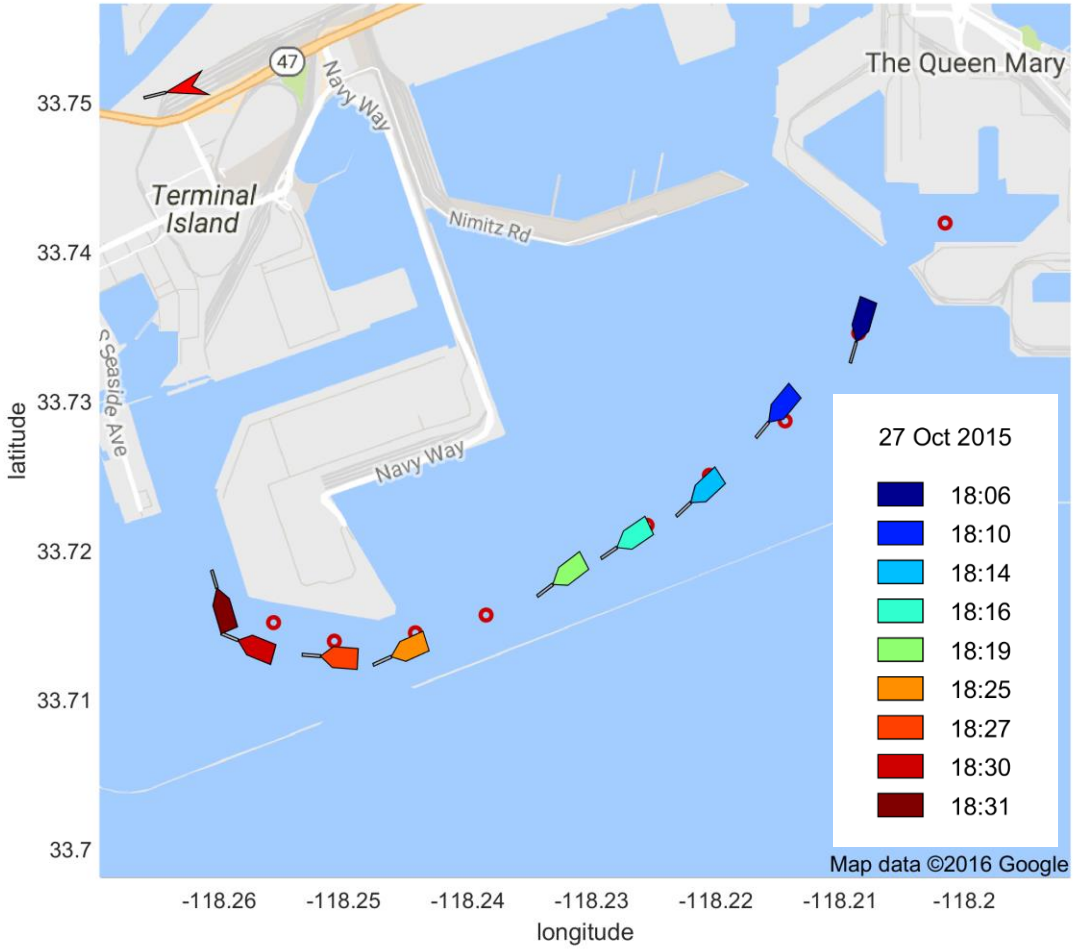

Figure A. 45. An illustration of a chase study of the harbor craft LELA FRANCO.

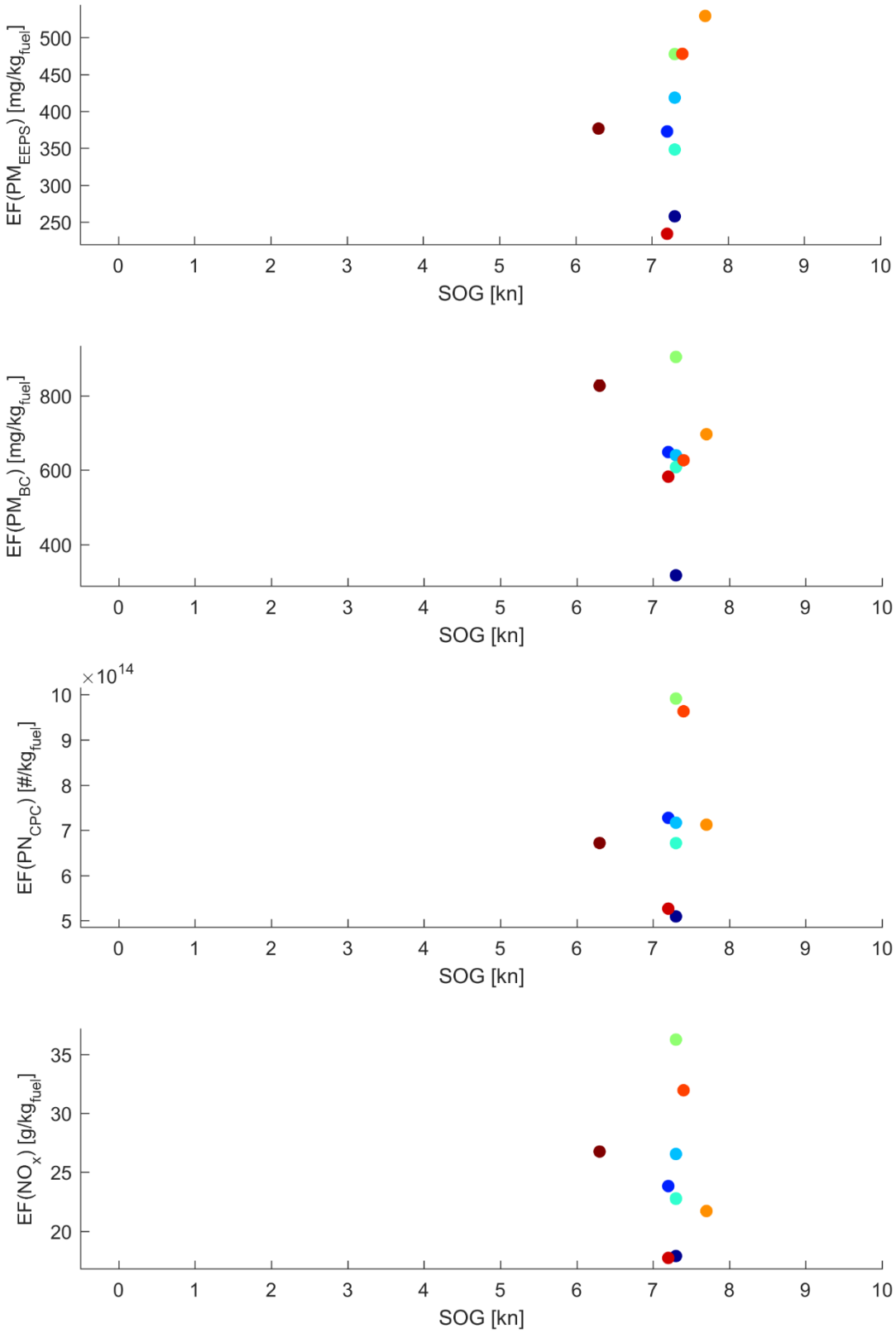

Figure A. 46. Specific emissions factors versus speed for LELA FRANCO. Different colors correspond to different times as shown in the legend in the corresponding map.

8.4.5 VICKI ANN (22 Oct 2015, 20:06)

Table A. 24. Detailed vessel information from Sea-web on VICKI ANN (IHS, 2016).

IMO	MMSI	Flag	GT	DWT	YoB	MEng	Tot. Power	RPM	Stroke
NA	367006790	United States	NA	NA	NA	NA	NA	NA	NA

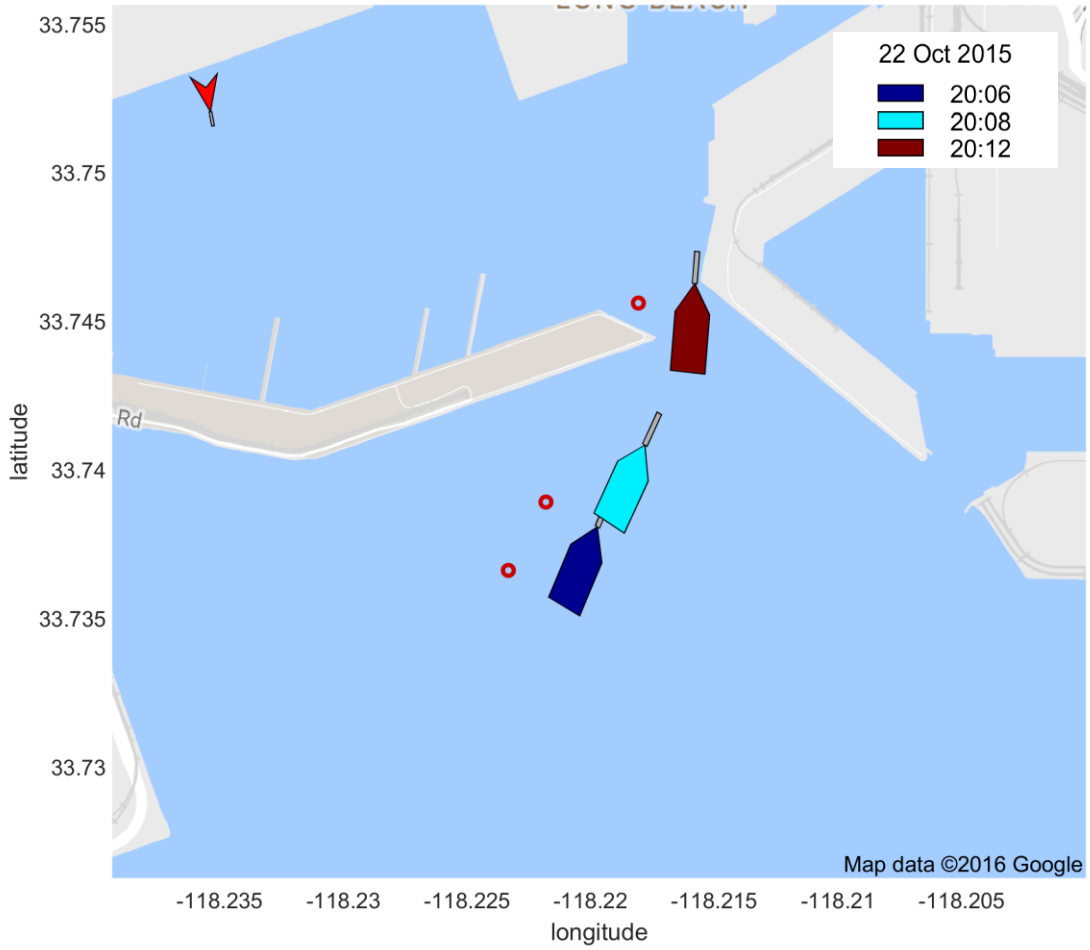

Figure A. 47. An illustration of a chase study of the harbor craft VICKI ANN.

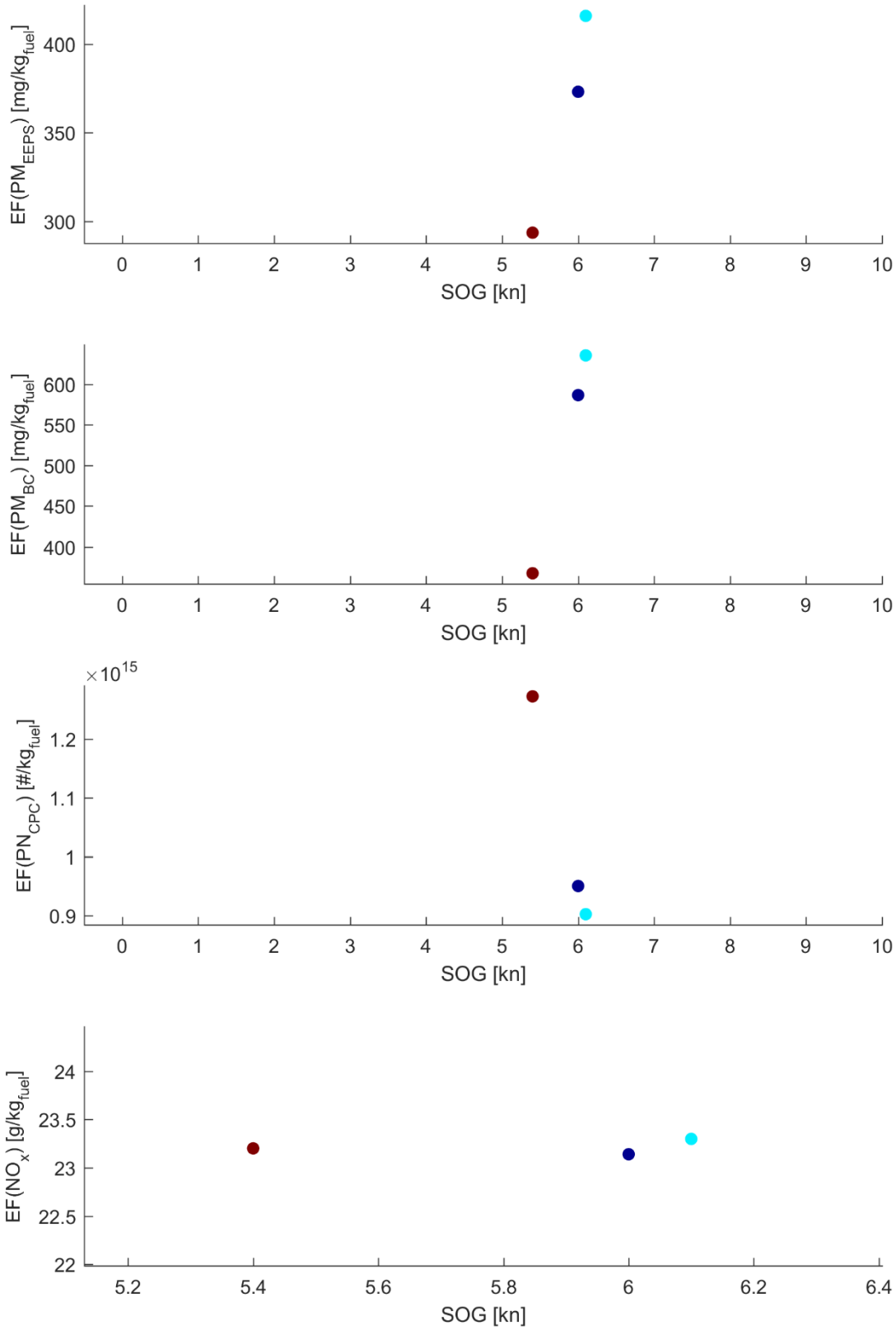

Figure A. 48. Specific emissions factors versus speed for VICKI ANN. Different colours correspond to different times as shown in the legend in the corresponding map.

Appendix II: Overall emissions for single ships

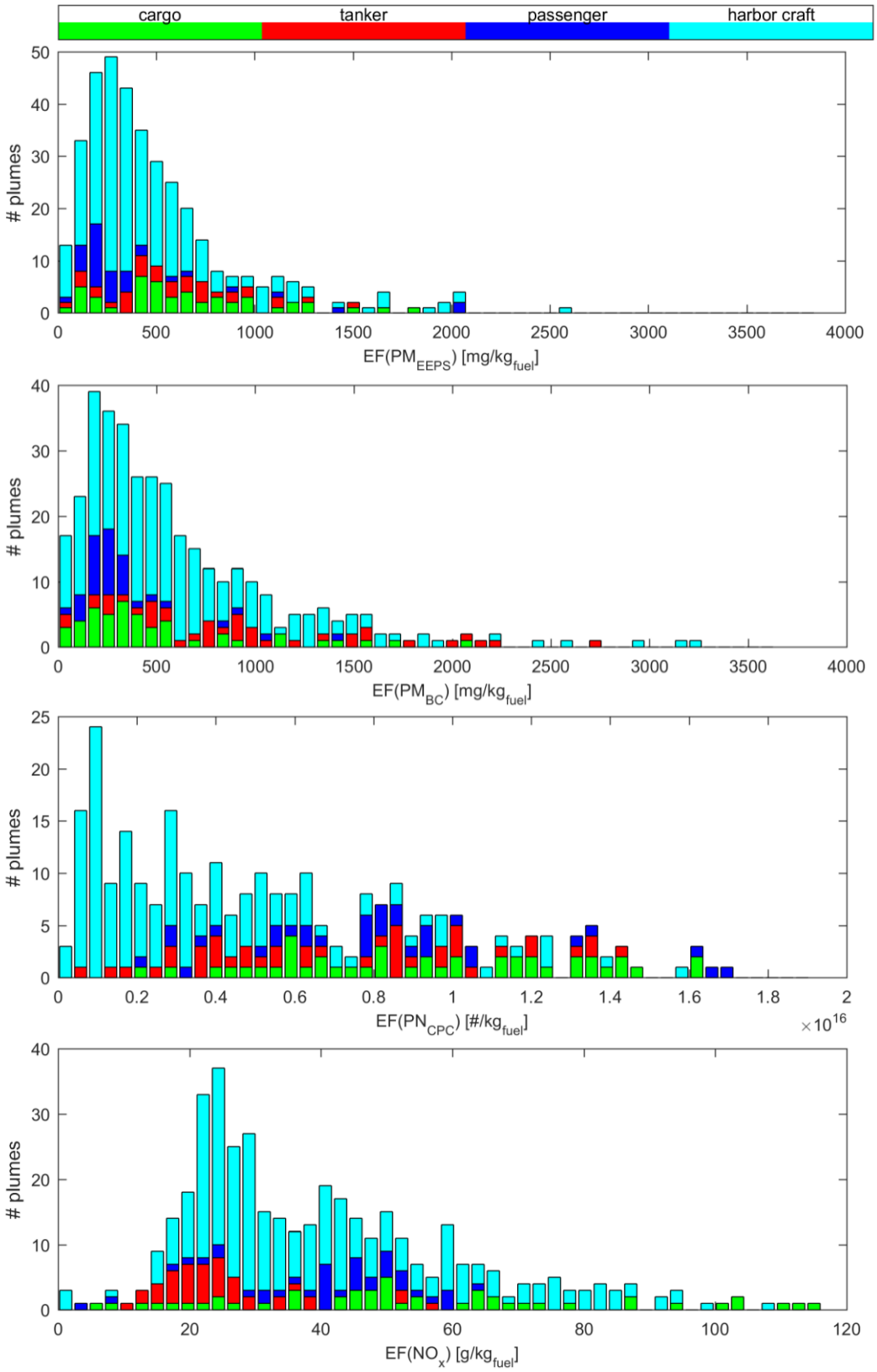

Figure A2 1. Frequency distributions for particulate matter and NO_x emissions from measurements with only one ship involved. The results for particulate matter are shown as particulate mass between 5.6 to 560 nm, as measured

by EEPS, and BC and particle number between 5 nm to 1 µm, as measured by CPC. The colours indicate the types of the main contributing vessel as assumed from its size.